An Evaluation of the Feasibility of Disposal of Nuclear Waste in Very Deep Boreholes

by

Victoria Katherine Anderson

S.B., Nuclear Engineering (2002)
S.B., Political Science (2002)

Massachusetts Institute of Technology

Submitted to the Department of Nuclear Engineering
in Partial Fulfillment of the Requirements for the Degree of
Master of Science in Nuclear Engineering

at the

Massachusetts Institute of Technology

September 2004

MASSACHUSETTS INSTITUTE OF TECHNOLOGY
OCT 11 2005
LIBRARIES

© Massachusetts Institute of Technology
All rights reserved

Signature of Author.....
Department of Nuclear Engineering
August 11, 2004

Certified by.....
Michael J. Driscoll
Professor Emeritus of Nuclear Engineering

Certified by.....
Karen L. Noyes, Sc.D.
Postdoctoral Associate, Department of Nuclear Engineering

Accepted by.....
Jeffrey A. Coderre
Chairman, Department Committee on Graduate Students

ARCHIVES

An Evaluation of the Feasibility of Disposal of Nuclear Waste in Very Deep Boreholes

by

Victoria Katherine Anderson

Submitted to the Department of Nuclear Engineering
on August 11, 2004 in Partial Fulfillment of the
Requirements for the Degree of Master of Science in
Nuclear Engineering

ABSTRACT

Deep boreholes, 3 to 5 km into igneous rock, such as granite, are evaluated for next-generation repository use in the disposal of spent nuclear fuel and other high level waste. The primary focus is on the stability and solubility of waste species, waste forms, and canister materials in saline, anoxic water, which is the most severe potential downhole environment given the sparse data available.

Pourbaix (Eh-pH) diagrams and solubility products were calculated for 20 materials of interest. In general, extremely low dissolved concentrations were estimated. Copper was identified as the best canister material. Wall-to-far-field temperature increases were estimated to be about 20° C for canisters containing two PWR assemblies, which is quite tolerable. Aspects requiring further work in the near term are detailed canister interior design to withstand crushing under a 1 km stack of same, and development of a borehole plug concept having a comparable or better impermeability and radionuclide holdup than the surrounding granite bedrock.

Thesis Supervisor: Michael J. Driscoll
Title: Professor Emeritus of Nuclear Engineering

Thesis Reader: Karen L. Noyes, Sc.D.
Title: Postdoctoral Associate, Department of Nuclear Engineering

Acknowledgements

First and foremost, Professor Michael Driscoll provided a great deal of guidance and support in the completion of this thesis as my advisor. His dedication to further exploration of the deep borehole concept for nuclear waste disposal was vital to the completion of this thesis. Dr. Karen Noyes, as the reader for this thesis, also provided a great deal of insightful comments to ensure that the final version of this thesis was of the highest quality possible.

It is also of great note that it would not have been possible for me to embark on a graduate degree without the generous support of the Defense Nuclear Facilities Safety Board. The support that the Board provided me eclipsed their financial support, as the staff at the DNFSB was extremely helpful in assuring my continued academic success during this past year. In particular, my mentor, Dr. Farid Bamdad, continuously checked up on me to ensure that my studies were going well and to offer any help he could.

Along with the support from the DNFSB, the MIT Swimming and Diving and Synchronized Swimming teams provided a great deal of moral support throughout my year of graduate studies. Their antics provided for some outstanding relief from my studies when I needed it the most. My fellow students in the Nuclear Engineering department, particularly Vered Anzenberg, Mark Laughter, and Leigh Outten, provided another incredible support network with their help both academically and personally.

Finally, if it weren't for the family that encouraged me to pursue my interest in nuclear waste management at the relatively early age of 12, I would have never envisioned embarking on such a project.

TABLE OF CONTENTS

1. Introduction.....p. 9
1.1. Current state of research.....p. 9
1.2. Review of recent borehole repository literature.....p. 11
1.3. General concept as a basis for current research efforts.....p. 13
1.4. Topics of research covered.....p. 17
2. Description of Environment.....p. 20
2.1. Kola Borehole data.....p. 20
2.2. Other data.....p. 25
2.3. Description of environmental model.....p. 29
3. Material Suitability for Borehole Environment.....p. 31
3.1. Waste forms.....p. 31
3.1.1. Spent nuclear fuel.....p. 31
3.1.2. Vitrified HWL.....p. 32
3.1.3. Ceramic waste forms.....p. 33
3.1.4. Summary of waste form susceptibility.....p. 35
3.2. Waste package materials.....p. 35
3.2.1. Corrosion mechanisms.....p. 36
3.2.2. Pure metals.....p. 37
3.2.3. Alloys.....p. 39
3.2.4. Summary of waste package material susceptibilities.....p. 41
3.3. Conclusions.....p. 41
4. Thermal Analysis.....p. 43
4.1. Calculation of thermal output of waste.....p. 43
4.2. Temperature gradient in waste package canister wall.....p. 49
4.3. Temperature gradient in gaps.....p. 51
4.4. Temperature gradient in granite.....p. 52
4.5. Summary.....p. 54
5. Chemical Analysis.....p. 56
5.1. Previous data on chemical behavior under reducing conditions.....p. 56
5.2. Probable chemical state of waste components.....p. 59
5.3. Solubilities of chemical species formed.....p. 62
5.4. Summary of chemical model.....p. 64
6. Conclusions.....p. 66
6.1. Summary of results.....p. 66
6.2. Future Work.....p. 68
Appendix 1: Pourbaix Diagrams for potential waste package materials.....p. 73
Appendix 2: Data used in thermal analysis.....p. 81
Appendix 3: Pourbaix Diagrams of radionuclides common in nuclear waste.....p. 97
Appendix 4: Solubilities of common radionuclides in nuclear waste in a deep borehole environment .....p. 111
References.....p. 117

LIST OF FIGURES

Figure 1.1: Schematic of waste emplacement depth and rock types encountered.....p. 15
Figure 1.2: Illustration of a portion of the borehole array viewed from above.....p. 16
Figure 1.3: Illustration of radial profile of the waste in a borehole.....p. 17
Figure 2.1: Illustration of rock types by suite, up to 6840 m, in the Kola Borehole....p. 23
Figure 3.1: Pourbaix diagram for copper in 20 M calcium, 60 M sodium, and 100 M chloride at 122° C.....p. 38
Figure 4.1: Flowchart for calculation of P(t) from radionuclide activities at 23 years as reported by DOE and radionuclide decay energies.....p. 47
Figure 4.2: Log-log plot of thermal output of waste over time.....p. 48
Figure 4.3: Model of thermal resistance circuit for flow of heath through copper waste package canister wall.....p. 49
Figure 4.4: Temperature gradient across copper canister wall with exposure to three different waste types over time.....p. 50
Figure 4.5: Temperature drop across a gap filled with various materials as a function of heat flux.....p. 52
Figure 4.6: Radially-dependent temperature gradient for three different waste types 10 years after emplacement.....p. 54
Figure 5.1: Pourbaix diagram for americium in a 20 M calcium, 60 M sodium, and 100 M chloride solution at 122° C.....p. 60
Figure A1.1: Pourbaix diagram for aluminum in 20 M calcium, 60 M sodium, and 100 Mchloride at 122° C.....p. 73
Figure A1.2: Pourbaix diagram for chromium in 20 M calcium, 60 M sodium, and 100 M chloride at 122° C.....p. 74
Figure A1.3: Pourbaix diagram for copper in 20 M calcium, 60 M sodium, and 100 M chloride at 122° C.....p. 75
Figure A1.4: Pourbaix diagram for iron in 20 M calcium, 60 M sodium, and 100 M chloride at 122° C.....p. 76
Figure A1.5: Pourbaix diagram for nickel in 20 M calcium, 60 M sodium, and 100 M chloride at 122° C.....p. 77
Figure A1.6: Pourbaix diagram for tin in 20 M calcium, 60 M sodium, and 100 M chloride at 122° C.....p. 78
Figure A1.7: Pourbaix diagram for titanium in 20 M calcium, 60 M sodium, and 100 M chloride at 122° C.....p. 79
Figure A1.8: Pourbaix diagram for zinc in 20 M calcium, 60 M sodium, and 100 M chloride at 122° C.....p. 80
Figure A2.1: Radially-dependent temperature gradient for three different waste types 1 year after emplacement.....p. 88
Figure A2.2: Radially-dependent temperature gradient for three different waste types 4 years after emplacement.....p. 89
Figure A2.3: Radially-dependent temperature gradient for three different waste types 10 years after emplacement.....p. 90
Figure A2.4: Radially-dependent temperature gradient for three different waste types 50 years after emplacement.....p. 91

Figure A2.5: Radially-dependent temperature gradient for three different waste types 100 years after emplacement.....p. 92
Figure A2.6: Radially-dependent temperature gradient for three different waste types 250 years after emplacement.....p. 93
Figure A2.7: Radially-dependent temperature gradient for three different waste types 500 years after emplacement.....p. 94
Figure A2.8: Radially-dependent temperature gradient for three different waste types 1000 years after emplacement.....p. 95
Figure A2.9: Radially-dependent temperature gradient for three different waste types 5000 years after emplacement.....p. 96
Figure A3.1 Pourbaix diagram for americium at 122° C with 20 M calcium, 60 M sodium and 100 M chloride.....p. 97
Figure A3.2 Pourbaix diagram for carbon at 122° C with 20 M calcium, 60 M sodium and 100 M chloride.....p. 98
Figure A3.3 Pourbaix diagram for cesium at 122° C with 20 M calcium, 60 M sodium and 100 M chloride.....p. 99
Figure A3.4 Pourbaix diagram for cobalt at 122° C with 20 M calcium, 60 M sodium and 100 M chloride.....p. 100
Figure A3.5 Pourbaix diagram for curium at 122° C with 20 M calcium, 60 M sodium and 100 M chloride.....p. 101
Figure A3.6 Pourbaix diagram for iodine at 122° C with 20 M calcium, 60 M sodium and 100 M chloride.....p. 102
Figure A3.7 Pourbaix diagram for neptunium at 122° C with 20 M calcium, 60 M sodium and 100 M chloride.....p. 103
Figure A3.8 Pourbaix diagram for nickel at 122° C with 20 M calcium, 60 M sodium and 100 M chloride.....p. 104
Figure A3.9 Pourbaix diagram for plutonium at 122° C with 20 M calcium, 60 M sodium and 100 M chloride.....p. 105
Figure A3.10 Pourbaix diagram for strontium at 122° C with 20 M calcium, 60 M sodium and 100 M chloride.....p. 106
Figure A3.11 Pourbaix diagram for technetium at 122° C with 20 M calcium, 60 M sodium and 100 M chloride.....p. 107
Figure A3.12 Pourbaix diagram for thorium at 122° C with 20 M calcium, 60 M sodium and 100 M chloride.....p. 108
Figure A3.13 Pourbaix diagram for uranium at 122° C with 20 M calcium, 60 M sodium and 100 M chloride.....p. 109
Figure A3.14 Pourbaix diagram for zirconium at 122° C with 20 M calcium, 60 M sodium and 100 M chloride.....p. 110

LIST OF TABLES

Table 2.1: Chemical composition of diabases in the Kola Borehole.....p. 24
Table 2.2: Properties of leachates and rocks in a laboratory study of granite-water interactions (50° C with fine grained rock powder for approximately one hour.....p. 27
Table 3.1: Effect of Temperature on HLW Glass Dissolution and Diffusion .....p. 33
Table 3.2: Hypothesized stable states of eight different metals for potential use as a waste package material for very deep borehole disposal of nuclear waste.....p. 39
Table 4.1: Daughter isotopes with parent source material in waste.....p. 45
Table 4.2: Parameters from fitting of time-power output data to power law decay curve.....p. 49
Table 4.3: Thermal conductivities and effective heat transfer coefficients for several potential materials that could fill gaps in the waste-waste package-borehole wall system.....p. 51
Table 5.1: Stable chemical species for common elements in nuclear waste at 122° C in a solution of 20 M calcium, 60 M sodium, and 100 M chloride at a pH of 8.5 and an Eh of -0.3 V.....p. 61
Table 5.2: Potential soluble chemical species formed and their maximum possible concentrations in a deep borehole environment.....p. 64
Table A2.1: Average activities of radionuclides at 23 years post-discharge by waste type.....p. 81
Table A2.2: Decay constant, decay energy, and power per atom present for each radionuclide considered.....p. 83
Table A.2.3: Thermal power output by year for each waste type.....p. 85
Table A2.4: Heat generation rate and distance-dependent temperature gradient by year in previous work.....p. 87

List of Units

Concentration:	M=molarity
	g/L=grams per liter
	g/cm^3=grams per cubic centimeter of water
Density:	g/cm^3=grams per cubic centimeter
Diffusivity:	m^2/day=square meters per day
	cm^2/s=square centimeters per second
Electric potential:	V=volts
	mV=millivolts
Heat flow:	mW/m^2=milliwatts per square meter
Heat transfer coefficient:	W/m^2K= watts per square meter per Kelvin
Hydraulic conductivity:	m/s=meters per second
Leach rates:	g/m^2d=grams dissolved per square meter surface area per day
Length:	km=kilometer
	m=meter
	cm=centimeter
Mass:	g=grams
	mg=milligrams
	MTHM=metric tons heavy metal
Permeability:	$m \cdot cm^2$=meters-square centimeters
Power:	MW=megawatts
	W=watts
Pressure:	kbar=kilobar
	GPa=Gigapascals
Radioactivity:	Ci=curie
Temperature:	°C=Celsius
	K=Kelvin
Thermal conductivity:	W/mK=Watts/meter-Kelvin

CHAPTER 1: INTRODUCTION AND OVERVIEW

Although fuel emplacement in the Yucca Mountain repository is slated to begin in the next decade, the United States will soon exhaust the space for High-Level Waste (HLW) disposal available in that repository as currently licensed and will need additional disposal capacity, and other countries face similar needs. Deep boreholes are a potential solution to this demand for HLW disposal, and offer the additional potential advantage of a lower radionuclide escape probability when compared to that of a near-surface mined repository. Additionally, recent advances in drilling technology have reopened discussions not only because of reduced costs in the excavation of potential deep borehole repositories, but also because such advances have increased the knowledge of conditions that nuclear waste packages are likely to encounter in such a borehole. The objective of this thesis is to develop an improved generic conceptual design for deep borehole repositories for nuclear reactor spent fuel and other high-level waste, based on up-to-date technical knowledge and analysis of key performance attributes.

1.1 Current state of research

In the developing discussion on the potential for deep borehole disposal of nuclear waste, it has become apparent that a significant amount of research and development must be carried out to provide data necessary to evaluate the safety of a potential deep borehole repository. First, although there is some information about the geophysics and geochemistry of formations at depths of up to 12 km from existing very deep boreholes,

such as the borehole on the Kola Peninsula in Russia,[1] the knowledge about the environment at such depths is not comprehensive enough to establish a sufficiently detailed model of the disposal environment to fully evaluate the behavior of radioactive waste packages at such depths. In order to arrive at the worst-case scenario for waste behavior that the safety basis for a repository requires, it is necessary to pursue further geologic exploration, both in general and at specific sites selected for construction of boreholes.

The information necessary from such exploration is extensive. The characteristics of the host rock must be well understood from a variety of perspectives, including porosity, bound and free water content, chemical composition, and thermal behavior. The hydrology of the entire borehole must also be understood, as this influences the ultimate escape path for radionuclides from the waste package. Gases present in the borehole can influence the chemical alteration of radioactive waste and waste packages both directly and indirectly by influencing the surrounding solution chemistry. Additionally, it is imperative that any microbial activity at these depths be well understood, as this affects the oxygen and pH balance of the system, as well as the concentrations of other species such as sulfur.

Thus, once the environment in the borehole at a selected site is understood, it will be necessary to evaluate the behavior of waste forms and packages in such conditions. For example, based on the extensive U.S. program to evaluate Yucca Mountain as a HLW repository, we are well-aware of how spent nuclear fuel behaves under oxidizing conditions. We do not have as much information regarding analogous behavior under reducing conditions which, given the presence of mostly hydrocarbons and noble gases,

as opposed to oxygen gas, at depths of 2-4 km, are the most likely conditions in a very deep borehole. The behavior of the radioactive waste package in the borehole environment is ultimately responsible for any potential radionuclide release to the environment, thus this, as well as the hydrology of the borehole, must be well understood to model radionuclide releases from the repository.

This thesis concentrates on the behavior of spent nuclear fuel, waste packages, and several other waste forms in a very deep borehole. It will also outline information available regarding the hypothesized environment of a very deep borehole. The following sections discuss preliminary ideas about the variables in the design, construction, and operation of such a borehole and the importance of defining these parameters prior to analyzing the behavior of nuclear waste. Specifically, based on proposals from advocates of the very deep borehole disposal method, the parameters for a hypothetical borehole repository will be defined for the purposes of investigation of the behavior of nuclear waste in the specific hypothetical environment. Finally, the chapter concludes with an overview of the research conducted in support of this thesis, including explanations of why these questions are important in the assessment of the feasibility of deep borehole nuclear waste disposal.

1.2 Review of recent borehole repository literature

This section reviews the rather sparse literature on the subject of the deep borehole approach to nuclear waste disposal. Work since the last major study by Kuo at MIT in the early 1990s is briefly summarized.

The engineers' thesis[2] and subsequent paper[3] by Kuo analyzed the thermal considerations of disposal in a deep borehole and performed a basic analysis of radionuclide transport to surface waters. The analyses assumed emplacement of waste at approximately 2.5 km based on the costs of drilling, and found that the ability to retain radionuclides and dissipate heat in a deep borehole were superior to that of a shallow-mined repository.

More recently, Sizek evaluated the centerline waste temperatures for various borehole sizes and cooling times following discharge. Considering the current U.S. regulatory limit of 350° C centerline temperature following disposal,[4] his results indicate that deep borehole disposal could meet regulatory requirements with respect to thermal considerations, as 10 years or more cooling in a borehole of 1 m diameter or less does not result in any temperatures in excess of 350° C.[5]

Another related study examined the potential for the use of the heat from nuclear waste to melt granite in a deep borehole, which would subsequently recrystalize around the waste and retard escape of radionuclides from the waste package. The concept, as proposed by Gibb, would require the waste surface temperature to exceed 700° C and thus would involve significant changes to the regulatory requirements for the waste temperature specifications in a repository.[6]

Finally, the recent study of the future of nuclear power written by an interdisciplinary group at MIT specifically called attention to deep boreholes as deserving of further evaluation for spent fuel disposal.[7] This, combined with recent research efforts, indicate that deep boreholes should be strongly considered as a potential solution for

nuclear waste disposal, but also that significant additional evaluations and research efforts are required before the safety of such a disposal scheme can be assured.

1.3 General concept as basis for current research efforts

The first variable to be considered is the depth of the waste emplacement, as this affects the physical parameters, such as pressure and temperature, and chemical composition to which the waste will be subjected. Chapman and Gibb suggest digging down to 3-5 km, such that crystalline, rather than sedimentary, rocks are reached. Additionally, this range is most favorable due to the fact that below 3 km, lithostatic pressure seals large cracks to make the borehole a more suitable host environment for waste, while below 5 km there is a significant concern regarding borehole collapse. Deeper holes are also not worthwhile because stacks of canisters more than about one kilometer tall can crush the bottom canisters in the stack, which would compromise retrievability and package integrity.

Other aspects of the borehole sizes to be considered include the diameter of each hole and the spacing between them, as these also influence potential changes to hydrology due to the existence of the boreholes. For diameter, Chapman and Gibb suggest a 0.8 m diameter, as this would give enough room for emplacement of traditional waste packages and may reduce costs compared with larger diameter holes.[8] As for the spacing of the boreholes, it is desirable to minimize this such that the footprint of the repository is as small as possible, although the spacing must also be sufficiently large such that the structural integrity of the boreholes is not compromised and that there is

sufficient volume of rock between boreholes provided to absorb decay heat from the waste without significantly compromising rock integrity.

Once the general borehole dimensions are set in the design, there are still several other elements in the design of the disposal scheme to be considered. For example, the boreholes may be lined, which may be either favorable or unfavorable from a radionuclide transport standpoint; lining could act as an extra barrier between the waste and the water supply, although it could also create a hydrologic line to the water table should waste packages fail. A liner also adds extra thermal resistance which will mean higher waste centerline temperatures.

In order to evaluate the potential for deep borehole disposal of nuclear waste given currently available technology, this thesis will start by adopting most of the assumptions similar to those in the concepts proposed by Gibb[9] and Kuo.[10] Waste emplacement will span one km in granitic deposits at the bottom of the borehole, with maximum depths ranging from 4 to 4.5 km depending on the depths necessary to leave approximately one km of crystalline rock above the waste as a barrier to radionuclide transport. Each borehole is assumed to be drilled to a diameter of 60 cm, as this will allow for disposal of wastes in a canister of 50 cm diameter without leading to waste package temperatures above regulatory limits. Figure 1.1 depicts these characteristics in schematic fashion.

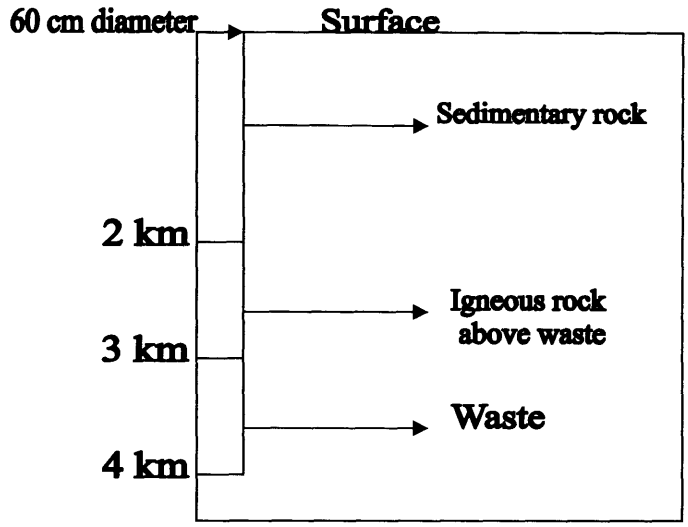

Figure 1.1: Schematic of waste emplacement depth and rock types encountered.

In order to ensure adequate rock volume between boreholes to handle the thermal and mechanical stresses resulting from drilling waste disposal, each borehole will be placed at a distance of 200 m from the next (center to center). Thus, a 20x20 borehole array will take up approximately 16 km^2. Figure 1.2 illustrates an array of boreholes as proposed.

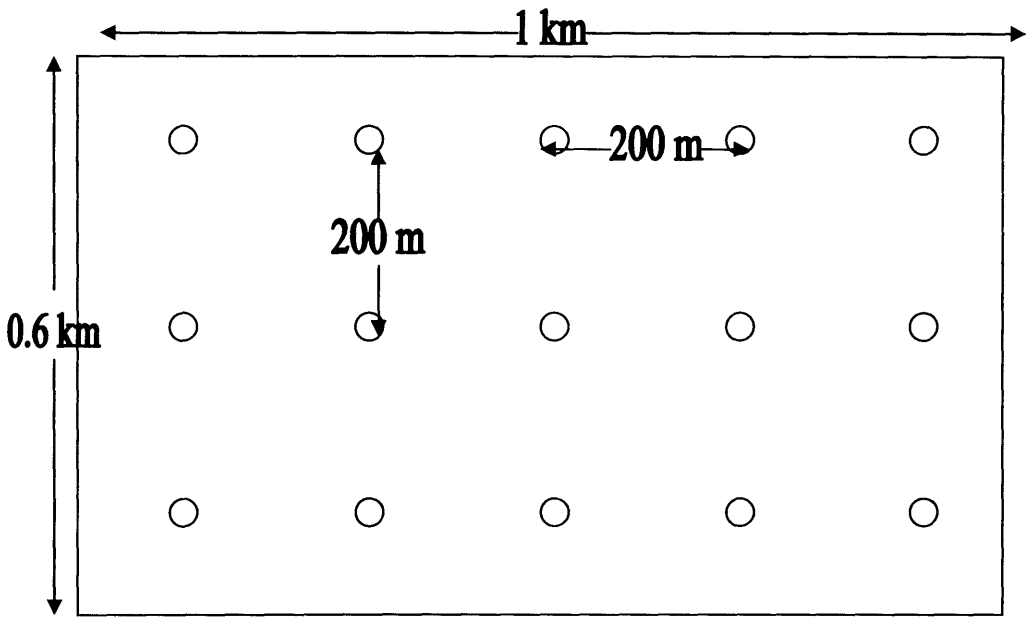

Figure 1.2: Illustration of a portion of the borehole array viewed from above.

Once a borehole is drilled, waste containers are placed vertically on top of one another, and the gap between the rock and the canister wall is filled with a chemically absorbent fill, such as clay or powdered graphite if retrievability is to be made more feasible. Figure 1.3 illustrates a radial profile of the waste, its container, and the fill.

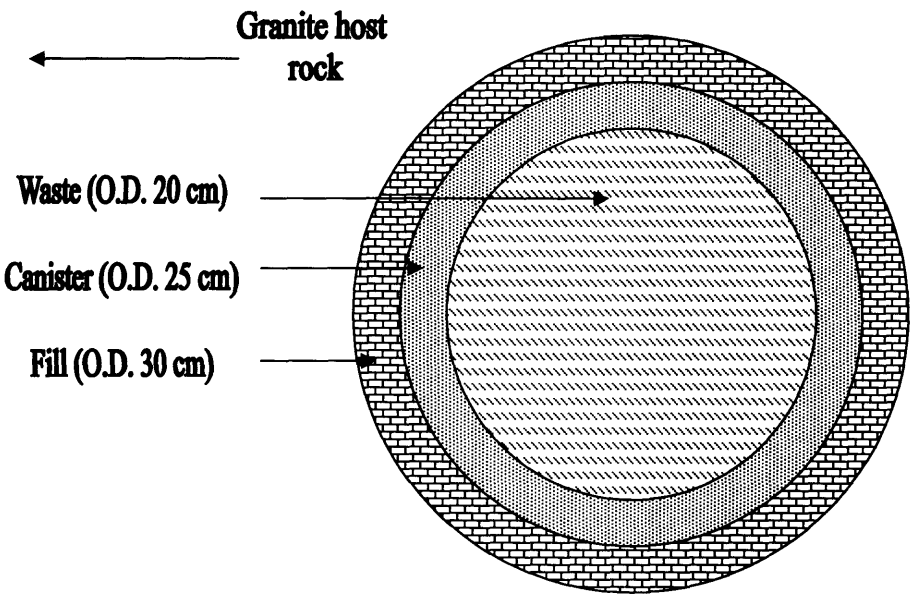

Figure 1.3: Illustration of radial profile of the waste in a borehole.

1.4 Topics of research covered

Description of General Environmental Conditions - As the deepest exploratory borehole in the world at a depth of over 12 km, the very deep Kola borehole in Russia offers some of the most comprehensive data on the environment 2-4 km underground that is currently available. In the excavation of the borehole and subsequent analysis of rocks, water, and gases extracted during the process, a great deal of information was obtained about the geologic properties at various depths of the continental crust. The information available includes rock type, structure, geochemistry, water content, organic and other gases present, and physical rock properties such as porosity. Additionally, recent excavation activities in Europe, particularly Sweden, have broadened the knowledge of the conditions at such depths. Even more recently, geothermal boreholes have been

drilled in granite in the French Alsace, but information is not yet available on the borehole environment.[11] While extensive data is available from the oil and gas industries, this is not as useful, as it is mostly in rock strata which is not of present interest. Chapter 2 of this thesis describes the data available on the environment likely to be encountered in a very deep borehole and draws conclusions about the relevant parameters and their values, which are used as the basis for evaluations presented in the later chapters of this thesis.

Material Suitability – In order to ensure reliability of disposal, both the disposition waste form and the waste package material must be able to withstand the environment of a very deep borehole. In the process of finding suitable forms for waste disposal, scientists have evaluated the potential use of borosilicate glass, ceramics, and unprocessed spent fuel rods as final forms for geologic disposal. While these evaluations primarily concerned the suitability of these waste forms for shallow-level disposal, information about their behavior under higher pressures and temperatures, as well as different chemical conditions, is available.

Chapter 3 presents an evaluation of the suitability of ceramics, borosilicate glass, and spent fuel rods for disposal under conditions expected to be found in a deep borehole. Further, Chapter 3 presents an evaluation of corrosion-resistance characteristics of several potential fabrication materials for waste packages, since the canister creates an additional barrier between the waste and the external environment, and must be compatible with the waste form and the surrounding conditions.

Thermal Properties - Due to the fact that nuclear waste generates energy as radionuclides decay, the problem of thermal loading in any waste repository is one that

requires careful consideration. In a deep borehole, the additional factor of the geothermal gradients in the surrounding rock (about 25° C per km) due to the depth of the waste makes the thermal modeling more complex. Chapter 4 presents an analysis of the heat transfer process(es) coupling the waste, its package, and the surrounding rocks.

Radionuclide Behavior - Since most U.S. nuclear waste management research to this point has centered about the conditions in traditional shallow-mined repositories with a relatively high Eh, or strongly oxidizing conditions, due to the presence of atmospheric oxygen, most of the knowledge we have about the chemical behavior of radionuclides in spent fuel pertains to its behavior under oxidizing conditions. However, data from the Kola Borehole and several other sources indicates that very little oxygen is present in granite at such depths.[12] Although the chemical behavior of radionuclides under these conditions is not thoroughly understood, there is some data on the behavior of spent fuel under reducing conditions, much of which comes from research related to reprocessing. Further preliminary data comes from the Swedish waste management program, as their repository, proposed to be sited in bedrock, would place the waste in reducing conditions. Chapter 5 presents the current state of knowledge regarding spent fuel behavior under these conditions and an analysis of potential concentrations of radionuclides based on an Eh-pH evaluation of stable species. The thesis concludes with a summary, conclusions, and recommendations for future research in Chapter 6. Appendices are included summarizing detailed data in support of the presentation in the main text.

CHAPTER 2: ENVIRONMENTAL MODEL

In order to accurately model the behavior of radioactive waste and potential containers for it in a very deep borehole repository, it is necessary to define the conditions to which the materials will be subjected. While there is a great deal of knowledge available from the oil and gas exploration industries, their experiences involve oil- and gas-bearing strata; thus their experience is not as applicable as may first be assumed. Rather, the disposal of nuclear waste in a deep borehole requires igneous rock with few fractures. The hydrology, geochemistry, and geophysics communities have conducted a significant amount of research on the conditions deep in the earth's crust in such rocks, and a great deal of information is available on the geology, geochemistry, and general physical conditions at depths of 2-5 km beneath the surface. In particular, Russian researchers have gathered extensive data from the Kola Borehole. Other countries, such as the United States and Sweden, have developed data on the interaction between basement granite and the gases and fluids thought to be present at such depths. The following chapter outlines the data currently available from by reviewing the relevant literature, and then sets forth the environmental conditions that will be used in the modeling the behavior of radioactive waste and its containers in very deep boreholes.

2.1 Kola Borehole data

In studying the characteristics of the earth on the Kola Peninsula in Russia, scientists gathered data on the physical properties of the earth down to depths of 14 km.

Specifically, they gathered information about the rocks, including their chemical composition and porosity, fluids, including their abundance, salinity, pH and conductivity, and general physical properties, such as pressures and temperatures. In gathering this information, they divided the regions of the hole studied into complexes of several km, and further divided each complex into series and suites such that general properties at bands of depth throughout the peninsula could be determined.

Geologic Characteristics by Complex, Suite, and Series - The first such complex, the Pechenga complex, extends to a depth of 6840 m and encompasses the depths and rock types of interest for this thesis. Within this complex lie the Nickel series, which extends to a depth of 4884 m, and the Luostari series, which comprises the rest of the complex.[13] In the Nickel series, the first suite, the Materin suite, reaches a depth of 1059 m[14] and consists of mostly igneous rocks with layering indicative of multiple volcanic eruptions.[15] In contrast, the Zhadanov suite underneath it, which extends to 2805 m, consists almost entirely of sedimentary rocks,[16] including siltsones, tuffs, and carbonate-based rocks and few diabases (granites). [17] Thus, this suite would be less suitable for our intended application, and reinforces the importance of drilling deep enough to leave igneous rock above the shallowest waste package.

The Zapolyarny suite, which reaches to 4673 m, is the suite with the most characteristics indicative of the potential for deep borehole nuclear waste disposal under the current concept. Specifically, the suite consists of diabase rocks in sheets with thicknesses between a few meters and several km.[18] These thick sheets lead to a very low hydraulic conductivity, and the basement granite makes this suite ideal for disposal of waste in a deep borehole environment. Below this suite lies the Luchlompol suite,

extending to 4884 m, which contains mostly sedimentary rocks,[19] which indicates that the prospects for nuclear waste disposal under this concept may be impractical at the depths of this series. This suite ends the Nickel series, below which lies the Luostari Series. This series contains mostly igneous rocks, like the Zapolyarny suite and spans approximately 2 km;[20] however, radioactive waste disposal at these depths as opposed to the depths of the Zapolyarny suite would require an additional 2 km of drilling for the same type of host rock, and is thus not as attractive unless it is found that the safety of disposal is improved due to hydrologic or chemical conditions at those depths. Since at first blush, the Zapolyarny suite is the most attractive for the disposal of radioactive waste, the following section concentrates on the chemical, hydrologic, and physical properties in the suite. Figure 2.1 illustrates the suites of rock in the Kola Borehole.

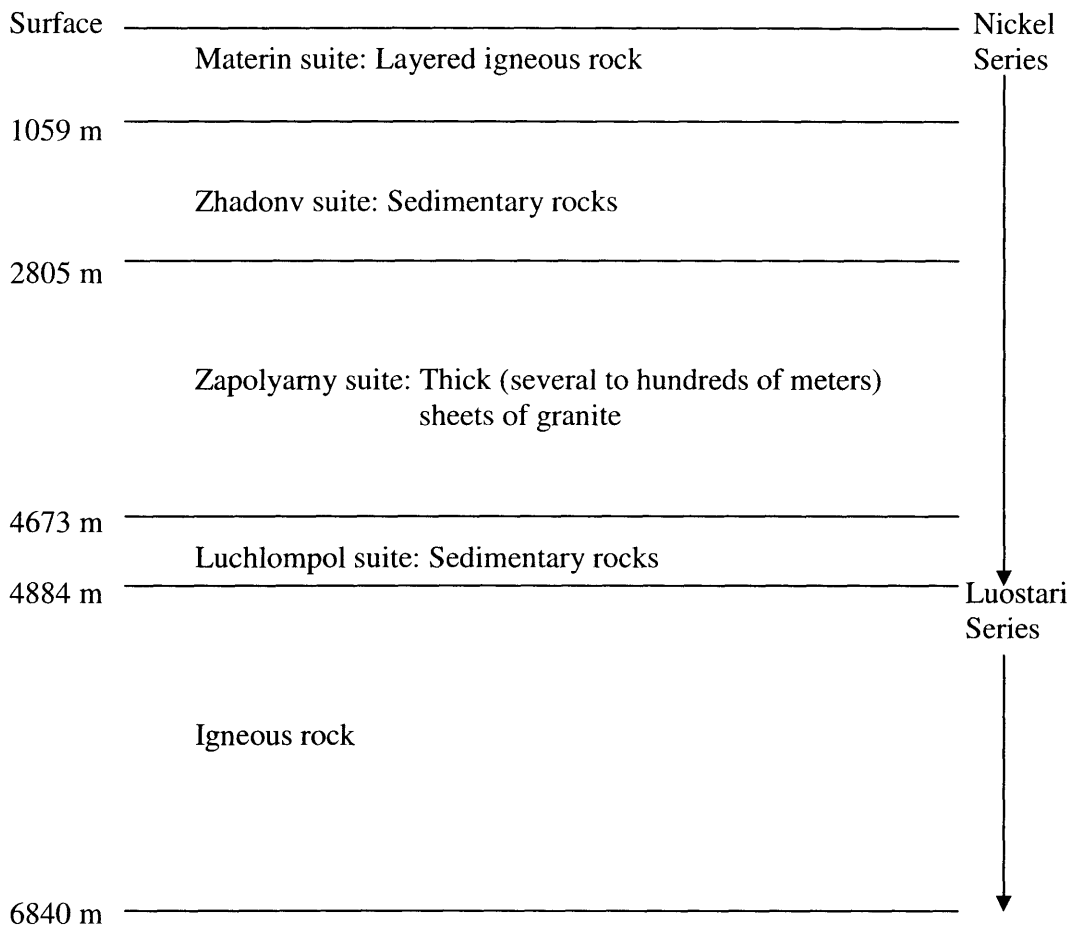

Figure 2.1: Illustration of rock types by suite, up to 6840 m, in the Kola Borehole.

Water Chemistry – Data from the borehole indicate that between 0.8 and 5 km, brine waters are dominant; specifically, sodium/calcium chloride waters are present in waters with pH between 8.5 and 9.[21] Molarities of chloride ion vary between 50 and 150, with the calcium and sodium concentrations varying depending on the local chemical rock composition.[22]

Hydrology and rock characteristics – In general, the porosity of the rocks and the hydraulic conductivity in the Kola Borehole are both relatively low. With the exception of the zone of exogenous fissuring between depths of 500-2000 m, porosity rarely

exceeds 1%, and the coefficients of water conductivity remain lower than 1-2 m^2/day.[23] More specifically, the open porosity in diabase rocks in the Nickel series averages to 0.4%, with a permeability of 3 $m \cdot cm^2$ and a density of approximately 3 g/cm^3.[24]

The diabase rocks found in the Penchenga complex consist of a combination of mostly silicon dioxide, as well as significant contributions from iron, aluminum, and magnesium oxides.[25] Table 2.1 gives the chemical composition of two diabase samples and three actinolitized diabases.

Table 2.1: Chemical composition of diabases in the Kola Borehole.[26]

	Diabase		Actinolitized diabase		
	Prehnite-pumpellyite Facies of metamorphism		Greenschist facies of meta- morphism		
	Sample 226 Rock	Sample 2305 Augite-salite	Sample 9585 Rock	Sample 9508 Actinolite	Sample 9508 Plagioclase
SiO_2	47.70	48.90	47.42	54.98	64.11
TiO_2	1.36	0.92	0.83	0.07	0
Al_2O_3	13.67	4.37	15.72	1.68	21.99
Fe_2O_3	2.01	3.05	3.28	1.41	-
FeO	12.01	10.50	9.70	11.27	
MnO	0.20	0.25	0.17	0.18	&
MgO	7.00	14.66	7.00	15.97	&
CaO	6.30	12.60	9.50	12.84	13.84
Na_2O	1.66	0.40	1.08	&	9.86
K_2O	1.66	0.07	0.47	0.08	0.10
H_2O	0.22	0.82	&	2.13	&
P_2O_3	*	*	0.10	*	&

* not detected
& not discovered

Gas composition – The presence of atmospheric gases in the borehole is generally sparse, with the exception of the zone of exogenous fissuring between 500 and 2000 m, where most of the gases present are atmospheric gases dissolved in water.[27] However, at the depths of interest in the Zapolyarny suite, the dissolved gases consist of nitrogen, methane, and hydrogen.[28] The absence of oxygen indicates that strongly reducing conditions probably exist.

2.2 Other data

Other sources of data regarding behavior of granite-water interactions under various conditions, as well as the pressures and temperatures encountered at various depths, include geothermal investigation results, geochemical studies, and information form previously completed nuclear waste disposal research.

Temperature gradients and other thermal properties – Data from the Fenton Borehole for geothermal exploration in New Mexico indicates a maximum temperature gradient between 55° C/km and 89° C/km, with the temperature at 732 m being 100° C and the temperature at 4.5 km being 320° C.[29] However, that particular borehole is exposed to a great deal of geothermal activity, and the average thermal gradient in the area is 25° C/km.[30] A study that specifically focused upon the thermal properties of crystalline basement rock gave the mean thermal gradient value as 20° C/km, and further gave the mean thermal conductivity of the rock as 3 W/mK. These experimentally derived values result in a heat flow value of 60 mW/m^2.[31]

Water Chemistry – One of the most comprehensive studies of granite-water interaction involved an investigation of Black Forest Granite. The study included in situ studies of water exposed to basement granite as well as lab studies of the composition of granite and leachates from waters exposed to granites extracted from the area.

The water samples taken in situ at a depth of approximately 2000 m took two forms. The first form is mostly sodium chloride brine of about 10 g/L with a neutral pH; the second is a calcium bicarbonate brine of about 2-3 g/L with a pH of 6 and dissolved carbon dioxide at concentrations of 2-3 g/L.[32]

In the laboratory studies of the rock-water interactions, it was found that sodium and potassium concentrations increase with temperature, as well as with decreasing calcium and magnesium concentration, which is indicative of an ion-exchange process.[33] Table 2.2 gives data on the leachates obtained in the laboratory studies after exposure of fine-grained granite to water for approximately one hour at 50 C, as well as the chemical composition of the granites themselves for reference regarding the source of the species found in the leachates. This data gives indication of what kinds of species can be expected in the water, though the actual concentrations will be overestimates. The data indicates that relatively few reactive species, other than the sodium and chloride already present in deep waters, are created by the leaching of granite, which simplifies the analysis of the chemical stability of waste forms and waste package materials.

Table 2.2: Properties of leachates and rocks in a laboratory study of granite-water interactions (50° C with fine grained rock powder for approximately one hour).

Leachate Properties

	Granite Type and % composition of species by weight	
Species	Triberg	Baerhalde
Na	18.71	35.49
K	25.43	47.76
Ca	0.2	0.33
Mg	0.19	0.1
Li	0.15	0.9
Rb	0.11	0.54
Fe	0.48	1.42
Mn	0.02	0.02
Al	8.38	11.3
NO_3	0.23	0.13
SO_4	0.58	0.47
F	6.64	27.19
Cl	18.31	23.46
Br	0.14	0.16
P	0.25	1.76
SiO_2	12.03	8.9

Rock Properties

	Granite Type and % composition of species by weight	
Species	Triberg	Baerhalde
SiO_2	73.89	74.48
TiO_2	0.09	0.06
Al_2O_3	13.57	14.25
Fe_2O_3	1.79	1.3
MnO	0.01	0.02
MgO	0.36	0.09
CaO	0.15	0.34
Na_2O	2.57	3.96
K_2O	5.58	4.74
P_2O_5	0.04	0.28
H_2O	1.14	

Dissolved gases and redox conditions – Another study of granite basement rock groundwater chemistry in Japan found a similar ion-exchange process to that discovered in the analysis of the Black Forest Granite. Researchers found a sodium/calcium-magnesium ion exchange process between the rock and the water, and also found that sodium concentration increases with depth and with decreasing calcium and magnesium concentrations. They further found an Eh of groundwater from basement rocks to be around -300 mV, which they hypothesized to be due to the reduction of Fe(III) ions to Fe(II) ions in the granite controlling the redox potential.[34]

In studying the potential for granite-based radioactive waste repositories, the Swedes constructed the Aspo Hard Rock Laboratory, which involves a series of holes and tunnels in crystalline basement rock that are used as a method of in situ study of conditions likely to be encountered in the current Swedish repository design. In the construction of the repository model, there was a large input of surface water to the anoxic groundwater through a fracture zone, which was used as an opportunity to study the effect of surface water input on the chemistry of deep groundwater. They discovered that while the intruding surface water did contain a great deal of dissolved oxygen, it was quickly consumed by the available dissolved Fe(II) and Mn(II) ions in the granite and associated deep groundwater.[35] Thus, it appears unlikely that oxidizing conditions would ever result from atmospheric intrusion into a deep borehole.

General physical parameters – Previous studies of deep borehole disposal of radioactive waste have made assumptions about physical parameters such as pressure deep in the crust and properties of granite likely to be encountered. Gibb, for example approximates the bulk hydraulic conductivity for water in granite basement rocks to be approximately 10^{-11} m/s based on past studies of diffusion in rock.[36] An older evaluation of the concept from the 1970s estimated a pressure increase of 0.3 kbar/km (or 0.03 GPa/km) and a basement rock density of 2.54 g/cm^3.[37] More recently, Gibb gave the relevant pressure range from 2-5 km as 0.1-0.2 GPa,[38] which is roughly equivalent to the approximation from the earlier study. These values can be validated with a simple use of rock density and elementary physics with the following equation:

$$P = \rho g d \rightarrow \frac{P}{d} = \rho g \qquad (2.1)$$

where P is the pressure at depth, d, g is the acceleration due to gravity (9.8 m/s^2), and ρ is the density of rock as given above. The quantity P/d is therefore the pressure gradient with depth, and is equal to 0.025 GPa/km, roughly equivalent to the values from the studies.

2.3 Description of environment model

Based on the depths required to reach crystalline basement rock in the Kola Borehole, the remainder of this study will be conducted assuming a maximum depth of 4.5 km for waste emplacement, and the values of temperature and pressure at that maximum depth are used because they are the most severe. Accordingly, the following physical parameters will be assumed:

- Pressure: 4.5 km x 0.3 kbar/km + 1.013×10^{-3} kbar (from atmosphere) = 1.35 kbar
- Temperature: 10° C at surface + 4.5 km x 25° C/km = 122° C

Chemically, all previous research indicates the presence of a reducing environment at depths as shallow as 700 m below the surface. Thus, the following chemical parameters will be assumed:

- pH: 8.5
- Eh: -300 mV
- Saline Molarity: 100 M
- Dominant Aqueous Chemical Species: Cl^-, Na^+, K^+, F^-, Al^{+2}, SiO_2^+
- Additional Aqueous Chemical Species Present: Fe^{+2}, Mn^{+2}, Ca^{+2}, Mg^{+2}, Li^+, Rb, NO_3^-, SO_4^{-2}, Br-

- Dissolved Gases: nitrogen (P_{N_2}=.9), methane (P_{CH_4}=0.01), hydrogen (P_{H_2}=0.1)

In terms of properties of the granite, the Black Forest Granite and the granite from the Kola Borehole are similar. The data on the physical parameters are taken from the Kola Borehole study, while the chemical composition of the granite is assumed to be a composite of the two types of granite.

- Permeability: 0.03 mcm^2
- Hydraulic Conductivity: 10^{-11} m/s
- Porosity: 0.4%
- Density: 3 g/cm^3
- Major Chemical Species: SiO_2, AlO_3, Fe_2O_3, Na_2O, K_2O
- Additional Chemical Species Present: TiO_2, MnO, CaO, P_2O_5, H_2O

In general, these conditions are indicative of highly anoxic, reducing chemical conditions due to the prevalence of nitrogen and hydrogen and lack of oxygen at the depths of interest. While this is generally favorable for waste package stability and radionuclide retention, the increased temperature and pressure could have adverse effects, as could the high salinity of the waters. Additionally, the relatively high temperatures could result in melting of fuel if heat cannot be conducted away efficiently via the waste package and granite. The next three chapters evaluate the impact of such parameters on the feasibility of deep borehole disposal of nuclear waste.

CHAPTER 3: MATERIAL SUITABILITY IN BOREHOLE ENVIRONMENT

The following chapter discusses the suitability of various materials, both waste forms and waste package materials, for disposal in a deep borehole environment. The waste forms evaluated include spent nuclear fuel, vitrified HLW, and HLW ceramic forms, while the package materials evaluated include several alloys and pure metals.

3.1 Waste forms

Due to the significant variety in the nuclear wastes that require disposal in the U.S. and across the world, there are several different waste forms that have potential for use in permanent disposal. For example, in the once-through fuel cycle, entire assemblies of spent fuel may be disposed of without further processing, while in the closed fuel cycle, waste incidental to reprocessing is produced and must be solidified and disposed of in a stable form. The following section evaluates three potential waste forms with respect to their suitability for a deep borehole disposal environment.

3.1.1 Spent nuclear fuel

As a major component of the nuclear waste to be disposed of in Yucca Mountain, spent nuclear fuel has been deemed a suitable waste form for disposal in a shallow geologic repository given proper packaging.[39] The results of one study indicate that a deep borehole environment may actually retard the degradation of spent fuel when

compared to the oxidizing environments encountered in a shallow geologic repository in sedimentary rocks. The presence of granite decreased the material loss from UO_2 spent fuel by at least 80% for each waste component, while for MOX fuel the material loss decreased by a factor of 3-5 for each waste component.[40] Given the acceptance of disposal of spent nuclear fuel assemblies in an oxidizing, shallow mined repository, as well as the fact that the presence of granite in a deep borehole will likely stabilize spent fuel assemblies, direct deep borehole disposal of spent fuel appears to be a viable option.

3.1.2 Vitrified HLW

Nuclear waste from countries that reprocess their commercial spent fuel, as well as some wastes from the defense complex in the United States, are no longer in the form of spent fuel assemblies and thus must be otherwise disposed of. One proposed option is vitrification, or containment of the wastes in a solidified glass matrix. The product of the process is generally referred to as HLW Glass, and is relatively stable under traditional repository conditions. While the durability of HLW Glass under environmental conditions of a deep borehole repository is not as well understood, there has been some research regarding the effects of several factors, such as temperature, on the stability of HLW Glass. For example, one study investigated the effects of temperature on glass dissolution, and found a positive relationship between temperature and solubility, as well as diffusion coefficient.[41] Table 3.1 summarizes the results of the study.

Table 3.1: Effect of Temperature on HLW Glass Dissolution and Diffusion (Data from Pigford, et al)

Temperature (° C)	Solubility (g/cm^3)	Diffusion Coefficient (cm^2/s)
20	$5x10^{-5}$	$1x10^{-5}$
50	$8.8x10^{-5}$	$2x10^{-5}$
100	$1.7x10^{-4}$	$4.5x10^{-5}$
150	$2.8x10^{-4}$	$7.9x10^{-5}$
200	$4.2x10^{-4}$	$1.2x10^{-4}$
250	$5.8x10^{-4}$	$1.5x10^{-4}$

Another study on the stability of HLW glass investigated the effects of the presence of granite in the leaching solution. They found that, in general, exposure to granite reduced the leaching of glass matrix components (as opposed to radionuclides vitrified in the matrix). Glass samples of roughly 475 mg were exposed to either 0.2 or 2 g of granite in a 100-day flow-through experiment. The exposure to 0.2 g of granite reduced the leaching of glass matrix components by 25%, while exposure to 2 g of granite reduced the leaching by 50%.[42] While this reduction in leaching is promising, the increased temperature and pressure in a borehole environment will increase the rate of defect propagation, thus adversely affecting the solubility data. The synergistic effect of the increased defect propagation rate and the increase in the chemical dissolution rate of the glass indicates that glass may not be suitable for disposal in a deep borehole.

3.1.3 Ceramic waste forms

Another option being pursued for the disposal of HLW is the use of ceramics. Similar to vitrification, the use of ceramics involves the incorporation of radionuclides from HLW into a ceramic matrix. As with HLW Glass, there is extensive data on the

behavior of ceramic waste forms in traditional repository environments, although some research has been conducted on the effect of pH and temperature on their durability, and such data indicates potential effects of a deep borehole repository environment. For example, one study investigated the effect of temperature and pH on leaching of wastes from Al_2O_3-based nuclear wastes. Using $LaAlO_3$ and $CaAl_{12}O_{19}$ as the ceramic matrix and cerium, neodymium, strontium, and cesium to simulate the most prevalent oxidation states of common radionuclides, they tested the leaching of the ceramics at neutral and acidic pH as well as at temperatures of 90° C and 150° C. They found that aluminum, calcium, and strontium leached at higher rates with increased temperature, while neodymium and cerium leached at lower rates. Additionally, they found very low leach rates, less than 10^{-4} g/m^2d in the neutral pH water. They concluded that in groundwater with near-neutral pH, $LaAlO_3$ can be a suitable host phase for waste.[43]

Another study investigated the ability of a ceramic nuclear waste form to retain radionuclides in neutral pH water. After conducting tests at 90° C for 91 days, they found that the matrix elements leached faster than the radionuclides, indicating that radionuclides are retained well in a ceramic matrix.[44] A recent study more closely investigated the reason for chemical durability of zirconium-based ceramics in neutral pH water, and found that because insoluble $Zr(OH)_4$ is stable in the Eh-pH diagram between pH 1.7 and 10.7, the ceramics do not leach at an appreciable rate. They further found that in 4.1 million years, only 27% of the ceramic volume would have leached.[45] While this is promising for the use of ceramic waste forms in a very deep borehole, it does not necessarily mean that the ceramics are as durable as the long-term volumetric depletion

rate indicates. Specifically, due to radiation damage, actual leach rates of ceramics doped with radioactive wastes are higher than those in experiments without radiation damage.[46]

3.1.4 Summary of waste form susceptibility

In general, waste forms are more durable in the presence of granite and in neutral to alkaline environments, than in a traditional sedimentary rock based shallow repository. However, the increased temperature of a very deep borehole may be problematic for some waste forms, particularly HLW glass, which showed approximately a five-fold increase in dissolution rate between 20° C and 125° C, the hypothesized temperatures in a shallow and deep borehole repository, respectively. Ceramics, on the other hand, show significant durability in tests conducted at temperatures of 90° C and higher, retaining a great deal of the waste at high temperatures under neutral to alkaline conditions. Unprocessed spent nuclear fuel is another waste form suitable for disposal in a deep borehole environment, as the previously cited studies show reduction in the dissolution rate under exposure to granite, and the spent fuel is capable of surviving the thermal environment of a nuclear reactor, which is more severe than that of a very deep borehole. While the conditions of a reactor are more controlled in terms of water chemistry and the operating time is short relative to the time spent in a repository, the lack of water likely in a borehole would halt most corrosion mechanisms.

3.2 Waste package materials

Although robust waste forms have been developed and spent fuel is relatively stable under environmental conditions similar to that of a deep borehole, waste packages are used for greater safety both during handling and after disposal. Traditionally, metals, either pure or alloyed, have been favored due to their strength and durability for significant periods of time. While an evaluation of the strength of a waste package material and design is outside the scope of this chapter, the durability of a metal or alloy in the borehole environment is tantamount to its ability to perform the function of providing an additional barrier to release of radionuclides. The following section gives a brief explanation of corrosion mechanisms and then evaluates several alloys and pure metals in light of the borehole environment and general corrosion mechanisms.

3.2.1 Corrosion mechanisms

Corrosion mechanisms fall into two main categories: general and localized corrosion. General corrosion can take the form of uniform corrosion, or the general ionization and dissolution of a metal in an aggressive environment, and can also take the form of galvanic corrosion, in which the close proximity of two dissimilar metals results in accelerated corrosion of the metal more prone to oxidation.[47] Localized corrosion mechanisms include pitting corrosion, in which a passive oxide film is destabilized and leads to localized pits of corroded metal where the passive film has dissolved,[48] and environmentally-induced cracking, in which stress applied to a metal results in cracking of a lower strength passive oxide film and subsequent exposure of fresh metal to a corrosive environment without a protective oxide film.[49] The next two sections evaluate

the susceptibility of several pure metals and alloys to both general and localized corrosion in a deep borehole environment.

3.2.2 Pure metals

In general, pure metals are more resistant to stress-corrosion cracking, a common form of environmentally-induced cracking, than alloys.[50] Thus, general corrosion is the most significant concern in the evaluation of these metals. In evaluating different metals, Eh-pH diagrams, or Pourbaix diagrams, were constructed using the HSC 5.0 chemistry software package for several potential pure metals to compare the susceptibility of the metals to the borehole environment. The diagrams were constructed for copper, iron, aluminum, zinc, and titanium in an aqueous solution of 20 M calcium, 60 M sodium, and 100 M chloride at 122° C. Figure 3.1 gives an example of the Pourbaix Diagrams constructed for copper. The remaining diagrams are included in Appendix 1.

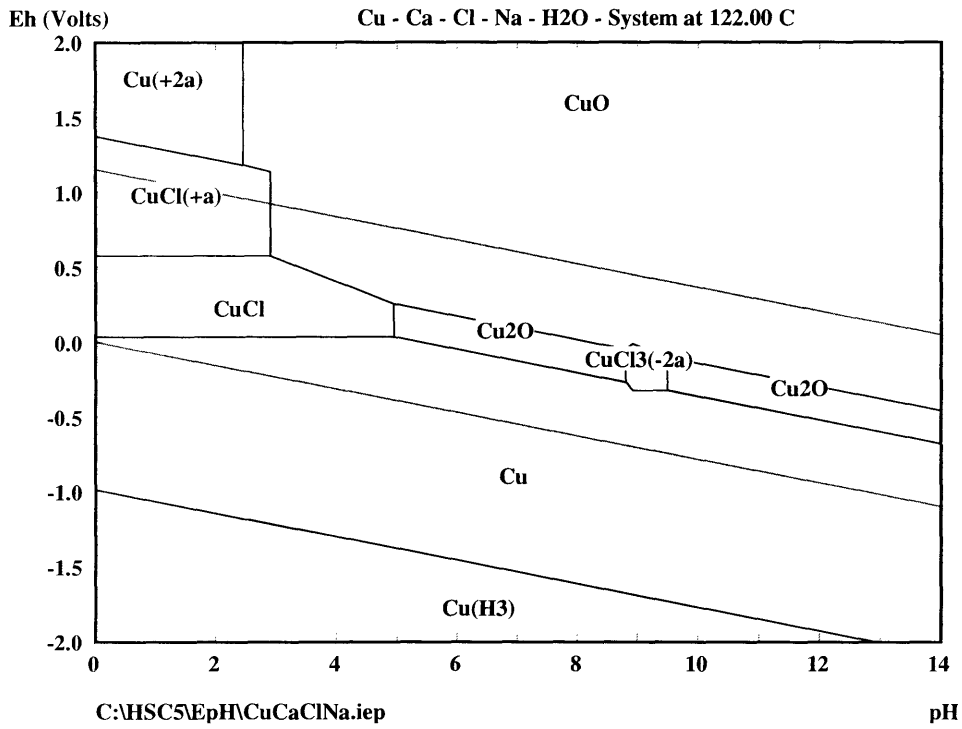

ELEMENTS	Molality	Pressure
Cu	1.000E+00	2.049E+00
Ca	2.000E+01	2.049E+00
Cl	1.000E+02	2.049E+00
Na	6.000E+01	2.049E+00

Figure 3.1: Pourbaix diagram for copper in 20 M calcium, 60 M sodium, and 100 M chloride at 122° C.

The stable state of each metal at an Eh of -0.3 V and a pH of 8.5 in the constructed diagrams was taken as the most likely stable state of each metal in a deep borehole environment. Table 3.2 gives the stable state of each metal in a deep borehole environment.

Table 3.2: Hypothesized stable states of eight different metals for potential use as a waste package material for very deep borehole disposal of nuclear waste.

Metal	Stable state at and Eh of -0.3 V and pH of 8.5 in a solution of 20 M calcium, 60 M sodium, and 100 M chloride at 122° C
Alumnium	$Al_2O_3 \cdot H_2O$
Chromium	$CaO \cdot Cr_2O_3$
Copper	Cu
Iron	HFe_2O^-
Nickel	NiO
Tin	SnO_2
Titanium	$CaO \cdot TiO_2$
Zinc	ZnO

3.2.3 Alloys

Since alloys are more susceptible to localized corrosion than general corrosion, evaluation of an alloy's suitability for a particular application must be evaluated for the specific environment based on previous experience with environmentally-induced cracking and pitting in specific alloy-environment combinations. The following section evaluates the abilities of several groups of alloys to withstand the environmental conditions of a deep borehole based on previous experience with alloy-environment combinations known to cause pitting or environmentally-induced cracking.

Iron/Steels – Due to the fact that iron corrodes readily in the presence of chlorides, it is generally not suitable for the very saline environment of a deep borehole. In alkaline chloride solutions, iron is susceptible to pitting.[51] Carbon steels are also susceptible to pitting in alkaline chloride solutions.[52] Most stainless steels, particularly austenitic stainless steels, are susceptible to stress corrosion cracking in alkaline solutions

of calcium chloride,[53] which is highly concentrated at the depths of disposal being explored here.

Aluminum alloys – Aluminum alloys, like iron and its alloys, tend to be susceptible to pitting in alkaline chloride solutions.[54] They are also susceptible to stress corrosion cracking in near neutral pH solutions with chlorides.[55]

Titanium alloys – Generally, titanium is a noble metal in the galvanic series, and forms a very stable oxide film. However, while it is resistant to pitting in most environments, it is subject to crevice corrosion in chloride solutions at temperatures above 70° C.[56]

Copper alloys – As pure copper metal is stable at the redox potential and pH likely to be encountered in a deep borehole, this indicates that copper alloys may be more suitable for use as a waste package material. In general, copper and its alloys are corrosion resistant in nonoxidizing aqueous environments.[57] This indicates that they might be a good choice for waste package materials, as does the fact that copper is slated for use as a waste package material in the Swedish mined granite repository with reducing chemical conditions.[58] The most common cause of stress corrosion cracking in copper alloys is the presence of sulfides and ammonium,[59] neither of which will be present in significant quantities in a very deep borehole. However, copper alloys are not without their drawbacks in a deep borehole environment. Dezincification, which decreases the strength of a zinc alloy through depletion of the zinc, occurs in brasses in waters under stagnant conditions; and denickelification, a similar process to dezincification for nickels in alloys, occurs in copper-nickel alloys in waters when subjected to high heat flux.[60]

3.2.4 Summary of waste package material susceptibilities

Due to the presence of significant concentrations of chlorides, most alloys are susceptible to localized corrosion, such as stress corrosion cracking, in a deep borehole environment. Additionally, the only metal stable in the pure metal form (i.e. not a passive oxide film) is copper. Since passive oxide films are readily destabilized by chlorides, copper is the most attractive option for waste package materials in very deep boreholes. However, it may be possible to line a stronger, more economic alloy with copper to reduce the costs of disposal. Such an alloy would have to be evaluated for the potential for galvanic corrosion with copper prior to use, but the possibility remains if lower cost and higher strength than can be achieved with pure copper become necessary.

3.3 Conclusions

The discussions in this chapter highlight the capabilities available with deep borehole disposal of nuclear waste, as well as the constraints. While safety may be enhanced by reduced dissolution of ceramic waste forms and spent nuclear fuel, waste package materials are susceptible to corrosion by the concentrated chloride environment. However, pure copper metal waste packages, or plating of pure copper on a higher-strength, lower-cost alloy, are both possibilities for a corrosion resistant waste package material. In general, although saline environments are aggressive corrosion accelerators, the absence of oxygen removes this problem in the corrosion of potential waste forms and waste package materials. Regardless of the exact materials selected, it is clear that both

waste forms and waste package materials exist that can survive the conditions in a very deep borehole. It should also be noted that the assumption that the borehole is flooded with saline water is a conservative one. In some mid-continental sites, the borehole could well remain dry. However, since many countries (e.g. Japan, Korea, and Taiwan) may need to use near or off-shore sites, the presence of saline water is a recommended presumption.

CHAPTER 4: THERMAL ANALYSIS

Since the radioactive decay of nuclear waste produces energetic particles that thermally heat the waste itself, as well as its surrounding container and environment, it is imperative that any disposal scheme used be capable of handling the heat produced by the waste. First, the environment must be able to absorb the thermal decay heat without being significantly altered; second, it must be able to conduct heat at a sufficient rate such that the centerline waste temperature does not exceed a specified safety level. While the calculations of the centerline temperatures that would be reached inside the waste package are left to future work, it is possible to make preliminary assumptions that the centerline temperature will remain below unsafe levels if it can be verified that heat is conducted away from the waste package effectively. The following chapter discusses the method used to calculate the time dependent heat production, the method used to estimate the temperature of the waste surface and surrounding environment, and the results of the analysis.

4.1 Calculation of thermal output of waste

In order to calculate the thermal output of a particular kind of waste, each isotope and its respective decay rate and decay energy was considered separately. Thermal outputs were calculated for high-level waste glass, pressurized water reactor (PWR) spent nuclear fuel, and boiling water reactor (BWR) fuel. Data on average radionuclide contents of each type of waste were taken from the U.S. Department of Energy Office of

Civilian Radioactive Waste Management,[61] and a time-dependent model of the radionuclide content for each type of waste was constructed based on that data and that from the 15th Edition of the Chart of the Nuclides.[62] The results were then verified by comparison to ORIGEN-based calculations.[63]

While a simple decay model can be used for some of the radionuclides, several are the daughter products of other radionuclides in the waste, and thus they are both produced and destroyed. An additional complication is that the data is reported for 23 years after discharge. For most radionuclides, which do not have a production source in the waste, the time-dependent number of atoms, N(t), at time, t, is given by

$$N(t) = \frac{A(23)}{\lambda} e^{-\lambda(t-23)} \tag{4.1}$$

where λ is the decay constant in s^{-1} and A(23) is the activity in Bq at 23 years following discharge (as reported by DOE).

For those radionuclides that had parent source material following discharge, a more complex solution was used. The contribution from a parent material was accounted for as:

$$N_d(t) = N_p(t) e^{\lambda_p t} \tag{4.2}$$

where $N_p(t)$ is the number of parent nuclides at time, t, and $N_d(t)$ is the contribution to the number of daughter product atoms by the decay of the parent nuclide at time, t. Factored into the first relation for the decay of radionuclides, the number of daughter product nuclides at time t is give as:

$$N_d(t) = \left[\frac{A(23)}{\lambda_d} + N_p(23) \cdot (1 - e^{-\lambda_p (t-23)}) \right] \cdot e^{-\lambda_d (t-23)} \tag{4.3}$$

Table 4.1 lists the daughter nuclides for which this technique needed to be used, and the parent nuclides that contributed to the post-discharge source of the daughter product in the waste.

Table 4.1: Daughter isotopes with parent source material in waste.

Daugter Isotope	Parent Nuclide(s) in Waste
Niobium-93m	Zirconium-93
Actinium-227	Protactinium-231, Uranium-235
Thorium-230	Uranium-234
Uranium-233	Neptunium-237
Uranium-235	Uranium-238, Plutonium-238
Uranium-236	Plutonium-240
Uranium-238	Plutonium-242
Neptunium-237	Americium-241
Plutonium-238	Americium-242/242m, Curium-242
Plutonium-239	Americium-243, Curium-243
Plutonium-240	Curium-244
Plutonium-241	Curium-245
Plutonium-242	Curium-246
Americium-241	Plutonium-241

Once the time-dependent number of atoms for each radionuclide for a particular type of waste was calculated, the time-dependent power output was calculated by multiplying the number of atoms at a given time by the average decay power per number of atomic disintegrations. The average power per atom is calculated by taking the total energy emitted per decay, accounting for the decay energy of all short-lived daughter products and daughter products not otherwise accounted for in the radionuclide evaluation, and multiplying it by the decay constant. The relation is given by:

$$P(t) = N_p(t) \cdot \lambda_p \cdot E_{decay} \tag{4.3}$$

where E_{decay} is the total energy per decay accounting for the energy of decay of short-lived daughter products.

Based on average radionuclide contents at 23 years,[64] the decay heat power generated for each type of waste studied (BWR Spent Fuel, PWR Spent Fuel, and HLW Glass) was calculated. Figure 4.2 graphically depicts this method with a flowchart.

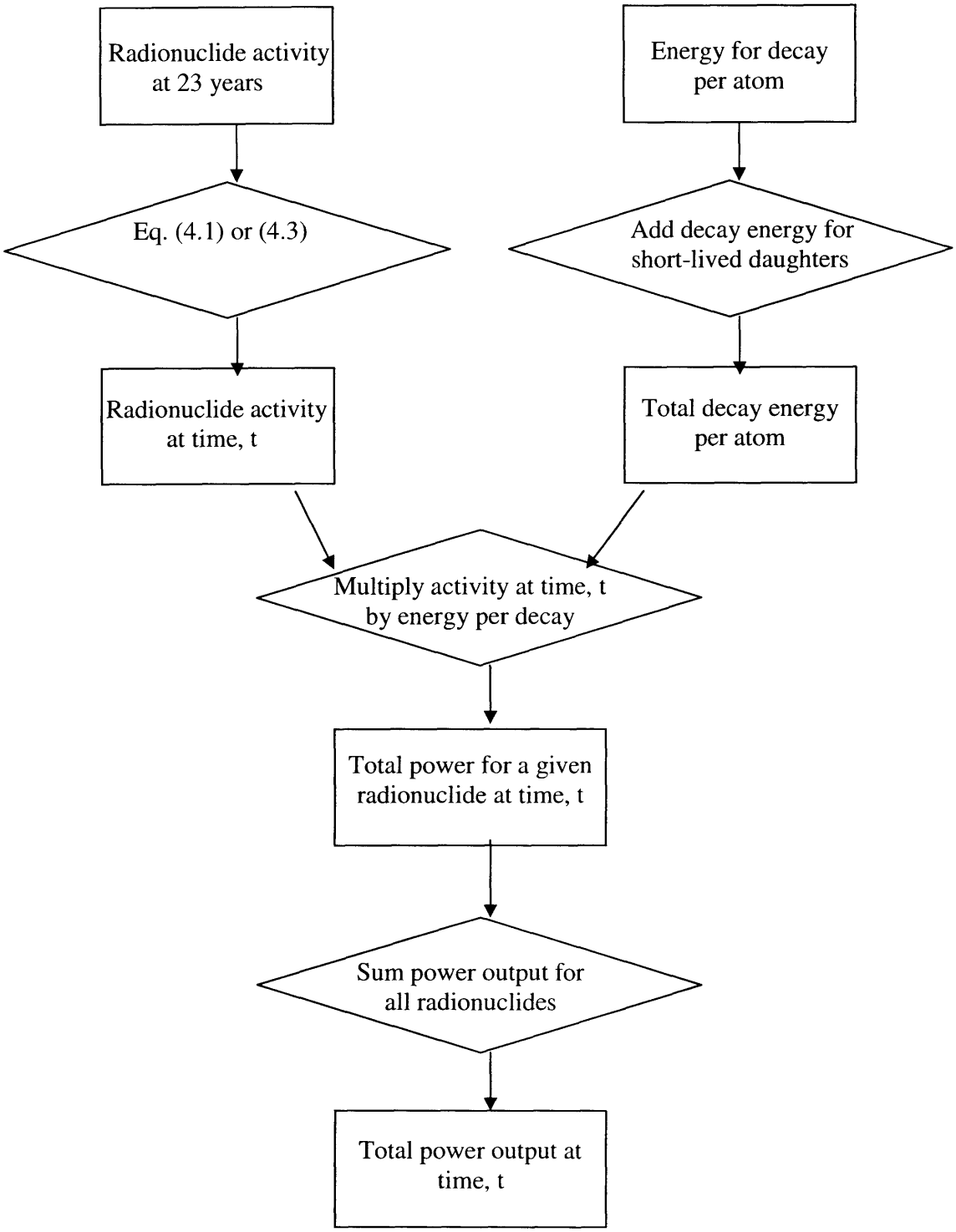

Figure 4.1: Flowchart for calculation of P(t) from radionuclide activities at 23 years as reported by DOE and radionuclide decay energies.

The method was confirmed by comparison of the thermal output values calculated by ORIGEN for a burnup of 37.5 MW(thermal)/MTHM, and it was found that at both 100 years and 1000 years following discharge, the results were within 20% (assuming an average of approximately 0.5 MTHM per assembly).[65,6667] Figure 4.3 illustrates the decay power per assembly (or canister, in the case of HLW Glass) over time.

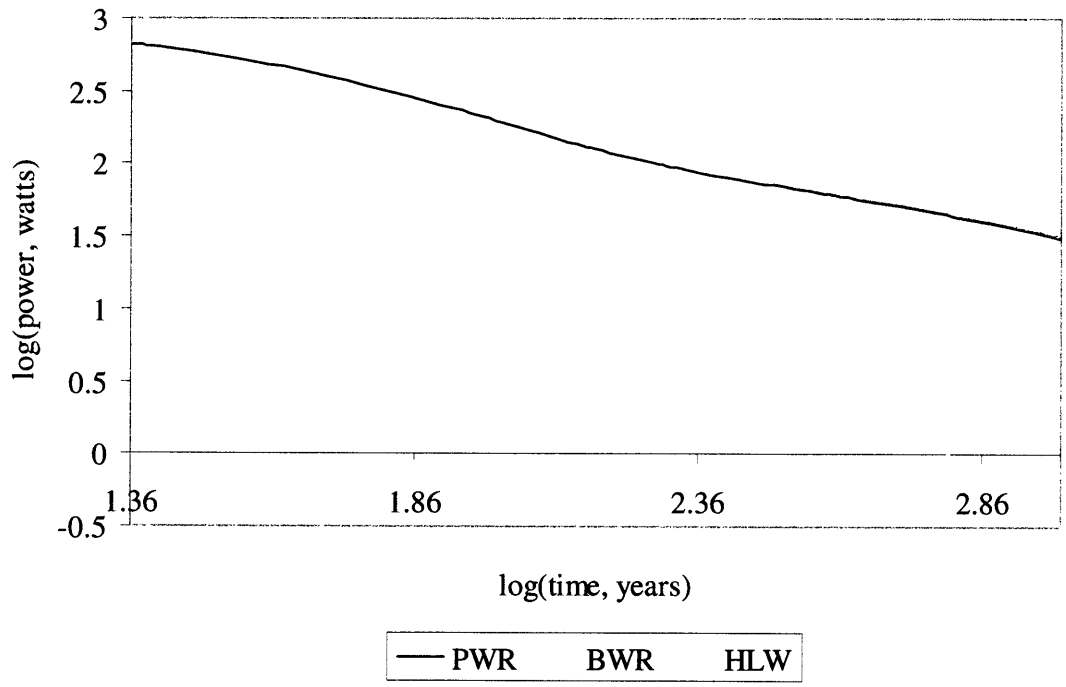

Figure 4.2: Log-log plot of thermal output of waste over time.

In general, the time-dependent total thermal output of waste can be approximated in the form of $P(t)=a \cdot t^{-b}$, where a and b are constants determined in fitting the data to a curve. Table 4.2 gives the values of the constants and the one-sigma error, as well as the R-squared value for the fitting of each type of waste's thermal output to the power law curve.

Table 4.2: Parameters from fitting of time-power output data to power law decay curve.

Waste	a	Error (σ)	b	Error (σ)	R-squared
BWR	325	170	0.835	0.013	0.99
PWR	873	51	0.551	0.029	0.85
HLW	771	58	0.697	0.046	0.8

4.2 Temperature gradient in waste package canister wall

The temperature gradient through the wall of the waste package can be modeled as the result of a current of heat flux, Q (W), moving through a resistance, R (K/W), resulting in a change in temperature, ΔT, between the inner and outer walls of the package. Figure 4.4 graphically depicts this model

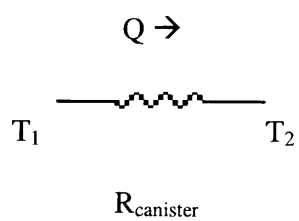

Figure 4.3: Model of thermal resistance circuit for flow of heat through copper waste package canister wall.

The thermal resistance, $R_{canister}$, was calculated using the relation for a hollow cylinder, which is given as:

$$R_{cylinder} = \frac{\ln\left(\frac{r_o}{r_i}\right)}{2\pi Lk} \tag{4.4}$$

where r_o and r_i are the outer and inner radii, respectively, L is the length of the cylinder in meters, and k is the thermal conductivity of the material in W/m·K.[68] Assuming a value of 398 W/mK for the thermal conductivity of copper, [69] the thermal resistance of the copper was calculated as follows:

$$R_{canister} = \frac{\ln\left(\frac{r_{canister}}{r_{waste}}\right)}{2\pi L_{canister} k_{copper}} = \frac{\ln\left(\frac{0.25m}{0.2m}\right)}{2\pi \cdot 5m \cdot 378W/m \cdot K} = 1.88 \cdot 10^{-5} \frac{K}{W} \tag{4.5}$$

The temperature change can thus be calculated, in °C, for any given time at which the heat generation is known by the following relation:

$$\Delta T = (T_{in} - T_{out}) = Q \cdot R_{canister} \tag{4.6}$$

where T_{in} is the inner wall temperature and T_{out} is the outer wall temperature. Figure 4.5 gives the results of the temperature change calculation over time.

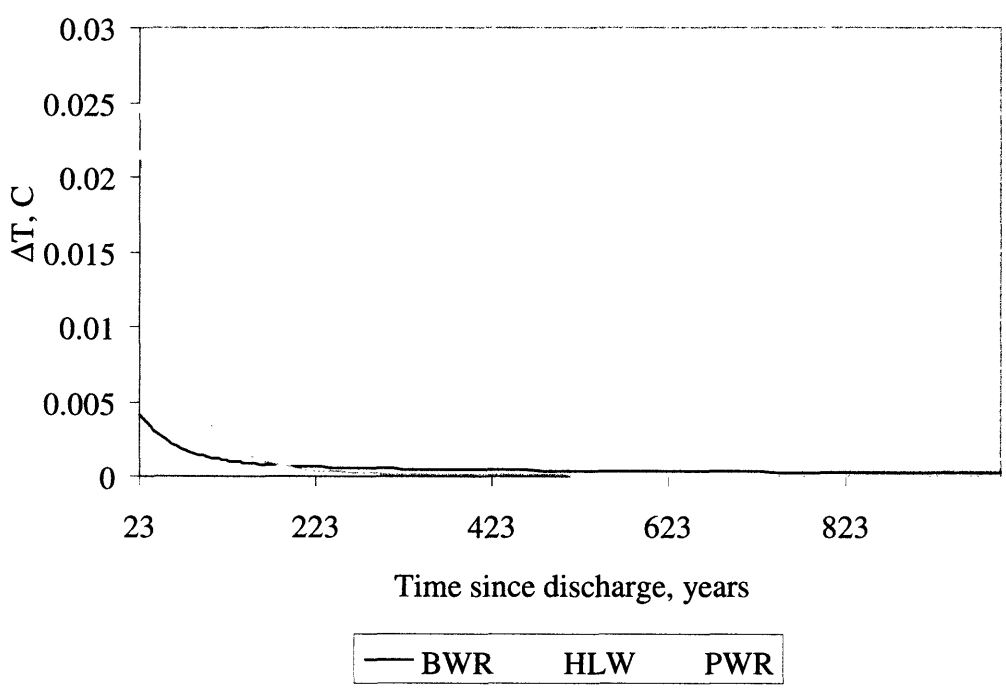

Figure 4.4: Temperature gradient across copper canister wall with exposure to three different waste types over time.

4.3 Temperature gradient in gaps

Since gaps between the waste and the waste package, and between the waste package and the fill or granite, will inevitably exist, it is important to evaluate what kind of temperature gradients would occur for different materials with the potential to fill the gap. In general, the temperature gradient across a gap can be approximated as:

$$\Delta T = q'' \frac{\delta}{k} \tag{4.7}$$

where k is the thermal conductivity of the substance filling the gap in W/mK, q" is the thermal flux in W/m^2, and δ is the width of the gap in m. The quantity δ/k is also called the effective heat transfer coefficient, h, and has units of W/m^2K.

In analyzing the temperature gradient across potential gaps, it was assumed that the gaps would not exceed 1 cm, and that the heat flux imparted to the material would not significantly affect its thermal conductivity. Thus, the effective heat transfer coefficient could be calculated as a constant for each of the materials analyzed. Table 4.3 gives the thermal conductivities and effective heat transfer coefficients for various materials.

Table 4.3: Thermal conductivities and effective heat transfer coefficients for several potential materials that could fill gaps in the waste-waste package-borehole wall system.

Material	k (W/m·K)	h (W/m^2K)
Graphite granules	141[70]	14100
Water	0.6836[71]	68.36
Argon	0.217[72]	21.7
Oil	0.134[73]	13.4
Gas	0.054[74]	5.4

The effective heat transfer coefficient can then be used to arrive at a value for the temperature gradient for a given heat flux. Figure 4.6 gives the results of this calculation for the five different materials that could fill a gap.

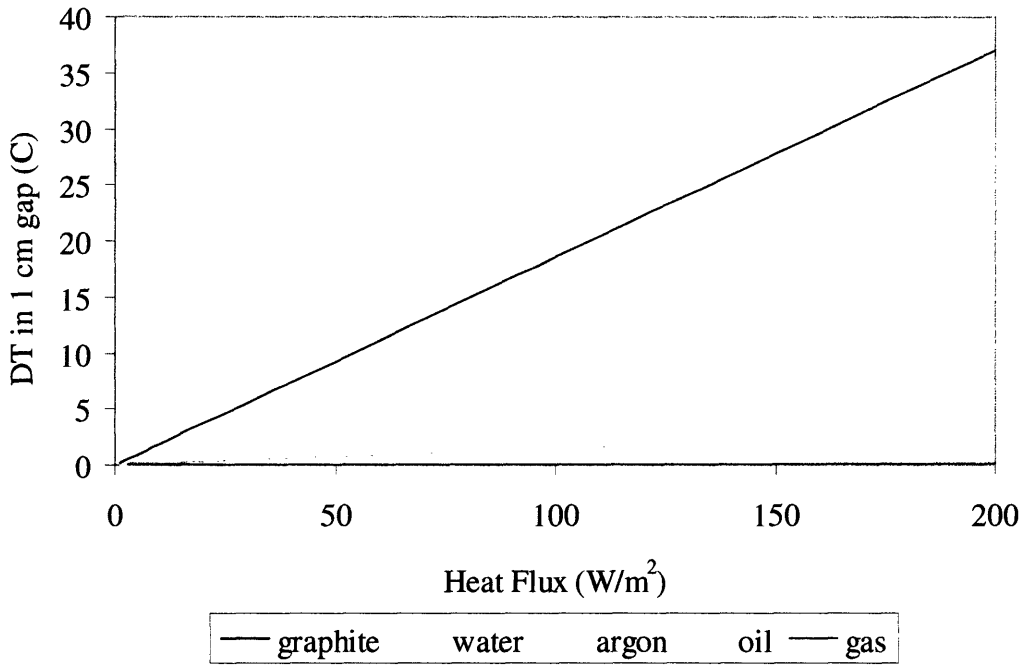

Figure 4.5: Temperature drop across a gap filled with various materials as a function of heat flux.

4.4 Temperature gradient in granite

Although analytical solutions for the transient conduction of heat from the edge of the borehole through the granite are difficult to arrive at, several previous works have presented numerical solutions to the calculation of temperature gradient from the borehole to the ambient granite temperatures. Since temperature gradient and heat flux at the borehole wall are directly proportional at a given time from emplacement and

distance from the borehole, it is possible to use these results to find the temperature gradient that would exist for the heat generation for waste packaged two assemblies to a canister, as is envisioned with the current concept. The thermal profile for the current concept was thus calculated as follows:

$$\Delta T_{current} = \frac{\Delta T_{numerical}}{Q_{numerical}} \cdot Q_{current} \tag{4.8}$$

where $Q_{current}$ is the power produced with the current concept of waste packaging for deep borehole disposal, $Q_{numerical}$ and $\Delta T_{numerical}$ are the associated power production and temperature gradient from numerical simulations in past results,[75] and $\Delta T_{current}$ is the temperature gradient calculated for the current concept. The data for the temperature gradient calculations was taken at the borehole wall and at radial distances of 4 m, 10m, 20 m, and 42 m from the wall and at times of 1, 4, 10, 20, 50, 100, 250, 500, 1000, 5000, and 10,000 years from emplacement. In the analysis, it was assumed that all waste was placed in the borehole 25 years after discharge. The results were then computed for each elapsed time-radial distance data point from the numerical simulation, as well as for the heat flux from the conceptualized HLW, BWR, and PWR heat-loaded waste packages. Figure 4.7 gives an example of the results for the temperature gradient for the three different waste types 10 years after emplacement, while the remainder of the results are given in Appendix 2.

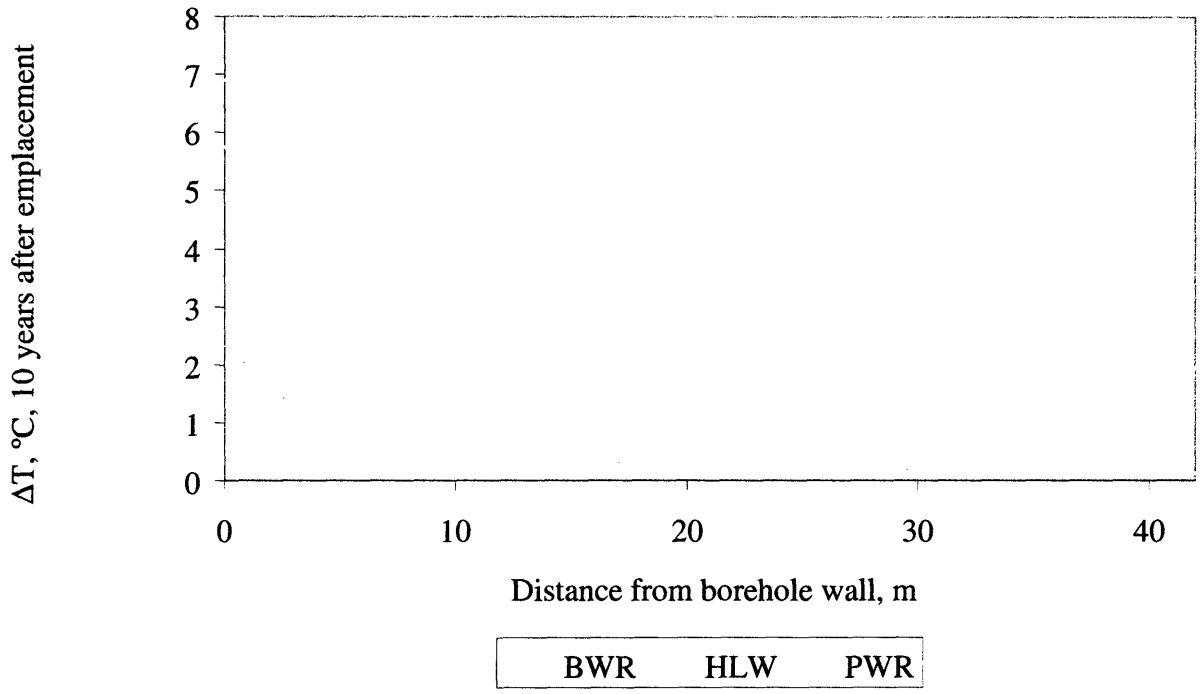

Figure 4.6: Radially-dependent temperature gradient for three different waste types 10 years after emplacement.

4.4 Summary

While the thermal output of the wastes are high soon after generation and non-trivial levels of power output continue long after disposition, it appears that the environment is not adversely affected, and that heat can be dissipated from the waste package efficiently provided gaps are not filled with extremely low thermal conductivity materials. The temperature gradient in the waste package canister wall is small, as are potential temperature gradients in gaps filled by several different types of materials. Further, the temperature gradient in the granite is not significant, thus indicating that adverse environmental effects due to thermal output are minimal. At 10 years after emplacement, the total ΔT from the inside wall of the of the canister to the far field

amounts to, at most, 0.02° C (canister wall) + 10° C (gap filled with oil at a heat flux of 50 W/m^2) + 7° C (PWR spent fuel) < 20° C, which is inconsequential. Thus, future work can be focused on the temperature inside the canister, in the waste form itself.

CHAPTER 5: CHEMICAL BEHAVIOR OF RADIONUCLIDES

The following chapter describes a basic model of the hypothesized chemical behavior of radionuclides based on the conditions likely to be encountered in deep borehole disposal of radioactive waste. The first section outlines currently available experimental data on chemical behavior and solubility of radionuclides in environments similar to those encountered in deep granite deposits. The second section calculates hypothesized concentrations of 14 radionuclides commonly found in spent nuclear fuel and other nuclear wastes by, first finding the stable species based on Eh-pH analysis of the radionuclide in a particular environment, and second calculating the concentration of soluble species created by dissolution of the stable species using solubility products.

5.1 Previous data on chemical behavior under reducing conditions

Since the model of the environment of a deep borehole being used in this study assumes a pH of 8 and an Eh of -300 mV, relevant results from previous research generally deal with anoxic or reducing conditions and their effect on the speciation and dissolution of spent fuel and its components. Generally, reducing conditions result in lower solubilities for the radionuclides that will comprise the majority of nuclear wastes.

A study comparing the dissolution of spent fuel in two different flow-through experiments, one with reducing conditions and one with oxidizing conditions, found that the reducing conditions resulted in lower dissolution of spent fuel components. The reducing conditions, which were achieved by saturation of the flow-through solution with

hydrogen gas, resulted in lower concentrations of radionuclides in the solutions. Most radionuclides were of such low concentrations in the reducing condition solutions that they were below detection limits. Even though the uranium and cesium concentrations were above detection limits, they were found to be four orders of magnitude lower than the concentrations found under oxidizing conditions.[76]

Another study of corrosion of spent fuel found that anoxic conditions and enhanced reducing capacity greatly decreased the solubility of the actinide components of spent fuel. The test involved dissolution of spent fuel with and without exposure to oxygen (oxic and anoxic, respectively). In the anoxic dissolution test, unoxidized iron powder was verified to be present throughout the test, thus indicating that the reducing capacity of the solution was not exhausted at any point. They found that when compared to oxic conditions, anoxic conditions resulted in lower concentrations for all radionuclides other than cesium, and that the strongest effect was observed for the actinides, with the concentration of plutonium being reduced by a factor of 100.[77]

In addition to studies of spent fuel dissolution and solubility, several researchers have investigated the dissolution of specific radionuclides in spent fuel under reducing conditions. One such study investigated the speciation of uranium oxides in Allard groundwater, which simulates groundwater conditions likely to be encountered at great depths in granite bedrock with its salinity, pH, and reducing capacity. They found that in a solution with a pH of 9 and an Eh of -0.3 V, the concentration of soluble uranium asymptotically approached 5×10^{-7} M after two years.[78] The asymptotic concentration of uranium is well below the concentrations naturally found in drinking water in some areas; the molarities in drinking water wells in British Columbia, Canada, for example, average

1.7×10^{-5} M.[79] In the United States, the Environmental Protection Agency limits on alpha disintegration rate at 15 pCi/L[80] would limit the uranium concentration to 10^{-5} M, assuming no other alpha emitters present.

Another study of the dissolution of uranium oxide found that the presence of dissolved hydrogen gas suppresses the oxidation-dissolution process. With hydrogen-gas saturated solutions, hexavalent (soluble) uranium did not reach values higher than 2×10^{-7} M, while in the presence of iron, which enhances the reducing capacity of the solution, the concentrations do not exceed 10^{-11} M.[81]

Due to the high mobility and solubility of technetium (a radionuclide common in spent fuel and other nuclear wastes) under oxidizing conditions, it is imperative to understand how it would behave in a reducing environment to compare the performance of a deep borehole repository to that of a shallow mined repository. A study of the behavior of technetium under reducing conditions in salt brines found that the final concentrations were much lower than under oxidizing conditions. Under oxidizing conditions, Tc(VII) is formed and is highly soluble, while under reducing conditions, insoluble Tc(IV) hydrous oxides, including $TcO(OH)_2$, $TcO_2 \cdot 2H_2O$, and $TcO_2 \cdot H_2O$, are formed. In brines, the addition of iron powder to arrive at reducing conditions dropped the technetium concentrations from their initial values of 10^{-5} M to 10^{-7} M in 50 days and further to 10^{-8} M in 500 days. However, the addition of iron powder had no effect on the concentration of technetium in fresh waters.[82] This indicates that for some waste components, particularly technetium, the combination of reducing conditions and the presence of salt brines may inhibit their dissolution, making deep borehole disposal more favorable from a safety perspective.

Generally, these results indicate that reducing conditions are more favorable for the containment of radionuclides in the geologic disposal of nuclear waste. Further, those studies that involved exposure to brines and other groundwater conditions characteristic of deep granitic bedrock also indicated a potential for enhanced containment of radionuclides. However, the previously completed studies do not analyze the maximum concentrations that would likely be encountered under conditions that would be intrinsic in deep borehole disposal of nuclear waste. The following two sections will discuss, based on the conditions outlined in chapter 2 of this thesis, the chemical forms of various radionuclides that are likely to be stable as well as their estimated solubilities.

5.2 Probable chemical state of waste components

With an estimate of an aqueous system's pH and Eh, as well as the concentration of any aqueous species likely to be present in such a system, it is possible to predict which species or radionuclides will be stable by using Pourbaix diagrams, which graph the stable species of a specific element along a pH-Eh plot. If the concentrations of other aqueous species are considered in the construction of such a diagram, it is possible to pinpoint the stable species of a particular element by simply locating the pH-Eh point of the solution. However, since a very deep borehole environment is likely to present a chemical system with very concentrated brines, standard Pourbaix diagrams are not useful in determining the species that would likely be formed with very deep borehole disposal of nuclear waste.

Since standard Pourbaix diagrams are not applicable to a deep borehole environment, HSC 5.0 Chemical Reaction and Equilibrium Software was used to produce the appropriate diagrams. With an extensive database of thermodynamic and equilibrium constants for most elements, the program is able to produce suitable Pourbaix diagrams for a wide variety of aqueous systems and major input elements. For the purposes of finding the stable species of radionuclides in a deep borehole environment, each radionuclide was diagrammed in HSC 5.0 separately at 122° C with ionic concentrations of 20 M for calcium, 60 M for sodium, and 100 M for chloride. Figure 5.1 is an example of the final result of the construction of a suitable Pourbaix diagram, and graphically represents the stable chemical species of americium at various pH and Eh values.

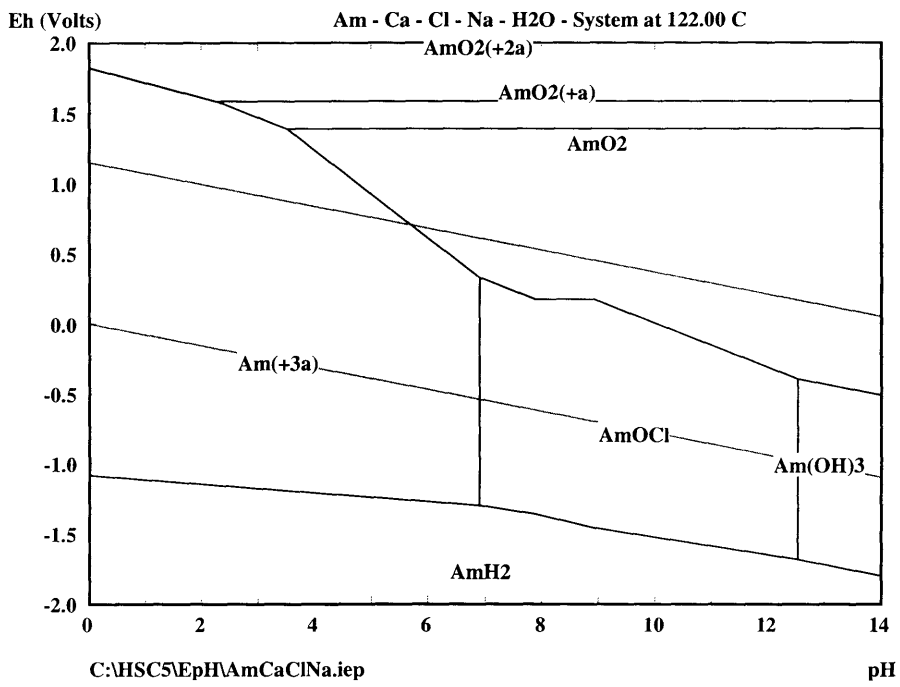

Figure 5.1: Pourbaix diagram for americium in a 20 M calcium, 60 M sodium, and 100 M chloride solution at 122° C.

In this example, the graph of the stable chemical species shows that americium oxychloride (AmOCl) is the stable species at a pH of 8.5 and an Eh of -0.3 V. The Pourbaix diagrams for 14 other radionuclides commonly found in nuclear waste were also produced and are located in Appendix 3, while Table 5.1 gives the stable chemical states for these radionuclides. These nuclides were selected to be representative of the components found in nuclear waste. For example, americium, curium, neptunium, plutonium, thorium, and uranium are long-lived actinides; cesium, iodine, strontium, and technetium are important fission products; the remaining nuclides are activation products produced in the fuel cladding during operation.

Table 5.1: Stable chemical species for common elements in nuclear waste at 122° C in a solution of 20 M calcium, 60 M sodium, and 100 M chloride at a pH of 8.5 and an Eh of -0.3 V.

Element	Stable Chemical State at pH 8.5 and Eh -0.3 V at 122° C in a solution of 20 M calcium, 60 M sodium, and 100 M chloride
Americium	AmOCl
Carbon	$CaCO_3$
Cesium	Cs^+
Cobalt	$Co(OH)_2$
Curium	CmOCl
Iodine	I_3^-
Nickel	NiO
Neptunium	NpO_2
Plutonium	PuO_2OH
Strontium	$SrCl^+$
Technetium	Tc
Thorium	$Th(H_3)_{3.75}$
Uranium	U_3O_8
Zirconium	$CaZrO_3$

5.3 Solubilities of chemical species formed

In order to determine the maximum concentration of the radionuclides in a deep borehole environment, the solubility product (equilibrium constant with respect to dissolution) is used to find the equilibrium concentration of the radionuclide given the other ions present in the solution. For example, with reactants A and B in molar quantities a and b resulting in products C and D in quantities c and d, the reaction is written as follows:

$$aA + bB \rightarrow cC + dD \tag{5.1}$$

and the equilibrium constant, K, is given as

$$K = \frac{[C]^c [D]^d}{[A]^a [B]^b} \tag{5.2}$$

where [X] is the concentration, or activity, of component X. Water and all solid species are assigned an activity of one in these calculations, while all aqueous species are expressed in units of molarity and dissolved gases are expressed in terms of their partial pressures.

The equilibrium constants for most species were obtained from the Common Thermodynamic Database Project (CTDP). The temperature of the system was approximated as 125° C, and since the log of an equilibrium constant generally increases linearly with temperature, it is possible to extrapolate values of K in most cases. If the CTDP did not provide a value of K for a particular chemical species, HSC 5.0 was used to extract the Gibb's Free Energy values, ΔG, for the chemical species in question, as well as any substances involved in the reaction, at 125° C. The free energy for the reaction, $\Delta G_{reaction}$, can thus be calculated as

$$\Delta G_{reaction} = c\Delta G_C + d\Delta G_D - a\Delta G_A - b\Delta G_B \tag{5.3}$$

and the equilibrium constant for the reaction can be calculated as:

$$K = \exp\left(\frac{-\Delta G_{reaction}}{RT}\right) \tag{5.4}$$

where R is the universal gas constant (8.314 J/mol·K) and T is the temperature in Kelvin.

Once the value of the equilibrium constant was obtained through data from either the CTDP or HSC 5.0, the value of the concentration of the soluble species formed in the dissolution of the stable species for each radionuclide was calculated. Appendix 4 thoroughly discusses the process of calculating these concentrations, while Table 5.2 summarizes the soluble species formed and the maximum concentration possible in a deep borehole environment.

Table 5.2: Potential soluble chemical species formed and their maximum possible concentrations in a deep borehole environment.

Element	Stable Chemical State at pH 8.0 and Eh -0.3 V at 122° C in a solution of 20 M calcium, 60 M sodium, and 100 M chloride	Potential Resulting Soluble Species	Maximum Concentration of Soluble Species (M)
Americium	AmOCl	Am^{+3}	$10^{-13.13}$
Carbon	$CaCO_3$	HCO_3^-	$10^{-9.363}$
Cesium	Cs^+	Cs^+	41.45
Cobalt	$Co(OH)_2$	Co^{+2}	$10^{-16.94}$
Curium	CmOCl	Cm^{+3}	$10^{-18.995}$
Iodine	I_3^-	I_3^-	$10^{-8.006}$
Nickel	NiO	Ni^{+2}	$10^{-8.899}$
Neptunium	NpO_2	Np^{+4}	$10^{-46.18}$
Plutonium	PuO_2OH	PuO_2^+	$10^{-5.13}$
Strontium	$SrCl^+$	$SrCl^+$	$10^{-12.129}$
Technetium	Tc	TcO^{+2}	$10^{-15.053}$
Thorium	$Th(H_3)_{3.75}$	Th^{+4}	$10^{-9.435}$
Uranium	U_3O_8	UO_2^+/UO_2^{+2}	$10^{-13.16}$
Zirconium	$CaZrO_3$	Zr^{+4}	$10^{-38.89}$

5.4 Summary of Chemical Model

The combination of the previous results available from the literature and the analysis undertaken in this thesis provide an excellent basis for the assertion that radionuclides can be better contained in the anoxic aqueous environment of a very deep borehole than that of an oxic shallow geologic repository. For example, plutonium can easily reach aqueous concentration values on the order of 10^{-2} M in aerated systems with species common in natural surface waters.[83] Few of the nuclides would reach solvated quantities in the parts per billion range, and most of those that do are medium half-life

isotopes that are unlikely to migrate to the surface for potential human exposure prior to their decay.

CHAPTER 6: CONCLUSIONS

The previous chapters of this thesis discussed evaluations of many aspects of deep borehole disposal of nuclear waste, including materials selection concerns, long-term thermal behavior modeling, and spent fuel durability in the disposal environment. In general, the results presented indicate that deep boreholes are a viable option for permanent disposition of nuclear waste. However, the results also raise many questions that must be answered before deep borehole disposal can be implemented with an adequate assurance of safety. This chapter summarizes the results of the research completed in support of this thesis, and outlines future work that must be done in support of the safety basis for deep borehole nuclear waste disposal.

6.1 Summary of results

Probable environmental conditions – The data summarized in Chapter 2 of this thesis indicate the general environmental conditions likely to be encountered in a deep borehole. First, the temperature of the host rock at a depth of approximately 4-4.5 km will probably range from 120-130° C, if a geothermally inactive region is selected. Second, granite and other igneous rocks, will be the dominant host rock between 2.5 and 4.5 km deep over 95% of the earth.[84] Finally, although water will be extremely sparse, that which does exist will be near-neutral pH with a reducing Eh and high salinity. Because saline water represents the most hostile environment hypothesized, our analyses are based on its presence.

Materials selection – Based on the environmental conditions assumed, Chapter 3 presents an evaluation of several potential waste forms and waste package materials on the basis of their hypothesized durability in a deep borehole. While it appears that, with respect to chemistry, ceramics, borosilicate glass, and spent nuclear fuel are considerably more stable in a reducing environment than an oxidizing environment, borosilicate glass may not be a favorable option due to the high increase of dissolution rate with temperature increase. Thus, ceramics and unprocessed spent fuel may be the best options for disposal waste forms. For waste package materials, the saline conditions render many alloys susceptible to environmentally-induced cracking. However, pure copper appears to be a viable option that is nonreactive in the assumed borehole environment. As noted earlier, this is the current material of choice in Sweden.

Thermal analysis – The thermal analysis presented in Chapter 4 indicates that the heat output and temperature gradients taking place in and outwards from the waste package canister wall are likely acceptable. For most materials that could potentially fill any gaps between the waste and the waste package or the package and the fill, the temperature gradient is small for loadings of up to two PWR assemblies per canister.

Radionuclide chemical behavior – The theoretical solubility analysis presented in Chapter 5 shows that the concentrations of most radionuclides are relatively low – and in general several orders of magnitude less than in oxidizing environments, as indicated by the reduction in plutonium solubility. Those radionuclides that do reach substantial concentrations, such as cesium, are the mid-lived isotopes (e.g. 30.07 years for Cs-137) that are unlikely to be released from a repository before they have substantially decayed.

6.2 Future work

Site-specific environmental data – While the data from the Kola Borehole and other information cited in Chapter 2 give a preliminary idea about the environment that waste will encounter in a very deep borehole, the specific data for a borehole site will vary. Further exploration should be completed before designating a site as suitable for deep borehole disposal. One promising new technology for this purpose is ground penetrating radar, which can detect major voids or faults that would disqualify an area for borehole disposition. Future work should investigate the potential of this new technology, including the potential depths of penetration by radar and the costs associated with exploration using the technology. Further analysis of the applicability of the latest oil and gas borehole assessment methods – such as seismic and well logging – is also in order.[85]

Materials selection – The current state of research on corrosion and durability of waste forms indicates that waste forms may be more durable in a very deep borehole than in a traditional shallow mined repository. However, no tests cited in Chapter 3 specifically simulated the temperature, salinity, pH, and Eh values that are anticipated in a borehole. Future work must verify that waste forms can survive all the physical and chemical conditions of borehole disposal simultaneously. Additionally, while Chapter 3 discussed the general considerations for prevention of corrosion through materials selection, specific tests simulating deep borehole environmental conditions should be conducted with copper, the material that appears most promising based on current data, and other materials, such as copper alloys or copper plated metals, that may be suitable.

Radionuclide transport – In order to determine the potential radiological releases from a deep borehole repository to human uptake pathways, the potential rate of diffusion of radionuclides from the emplacement site in the borehole to surface or subsurface waters consumed by humans must be determined. Preliminary data, such as that from the Kola Borehole, indicate that the rate of diffusion through solid granite is extraordinarily slow. For example, previous works have found the diffusivity of Tc-99 in granite to be 1.4×10^{-12} m^2/s.[86] However, it must be verified that the drilling process does not adversely affect this property of granite, and that the borehole is plugged in such a way that a hydraulic pathway of reduced impedance to the surface is not formed.

Confirmation of radionuclide chemical behavior - Although the results presented in Chapter 5 indicate that most radionuclides are insoluble in a deep borehole environment due to the reducing conditions present, little experimental data exists to support the theoretical calculations based on Eh-pH stability predictions. In order to confirm the low solubility of most radionuclides, long-term solubility tests must be carried out under environmental conditions that closely approximate those of a deep borehole.

Thermal analysis enhancement – While the thermal analysis of Chapter 4 indicates that the thermal output of the waste will not be a major problem for safety of disposal in deep boreholes, more detailed analysis must be completed before the thermal integrity of the system can be assured. With respect to the temperature of the waste inside the package, several potential package fill materials, from metals to silicon carbide to powdered graphite, could help conduct heat away from the waste. These materials should be evaluated in specific thermal analyses to determine which fill material is best suited to

reduce the centerline temperature, and further, it must be verified that the centerline waste temperature does not exceed a tolerable level. Another potential enhancement to the thermal analysis is a transient analysis of the heat dissipation through the granite, and determination of the temperature and thermal stress history due to the disposal of waste. Before deep borehole disposal can be verified as a safe option, it must be concluded that the thermal dissipation through the granite will not impair its ability to isolate the waste from human uptake pathways.

Stress analysis – Since in the current concept for the deep borehole disposal of nuclear waste, packages will be stacked on top of each other for approximately one km, a great deal of force will be exerted on the canisters at the bottom of the stack. The problem may be of greater concern if the packages are not well-packed, exhibit manufacturing defects, or are not filled with a material that gives the inside of the package enough strength to avoid collapse of the package walls. In order to ensure that packages are not crushed, as crushing or wall collapse would remove the secondary radionuclide transport barrier and compromise ease of retrievability if this requirement is desired, the stresses imparted to the waste packages must be evaluated for designs optimized to withstand this burden.

Drilling and sealing methods – While it is certainly possible to drill to depths of 5 km, the cost and time required to reach that depth must not be prohibitive if deep borehole disposal is to be used widely. Additionally, the drilling method cannot result in the creation of fissures in the granite host rock, as this would increase the hydraulic conductivity of the rock and reduce the time to potential human exposure. While some increase in the hydraulic gradient with drilling is unavoidable, a potential method for

combating this is the use of an effective material for a plug between the waste and the sedimentary rocks above. For example, Ceramicrete, a new material composed mostly of magnesium oxide and developed by Argonne National Laboratory, readily absorbs water, thus any intruding waters would be quickly absorbed by the plug. Another option includes clays with high sorption capabilities for trapping radionuclides and retarding their release to the environment, should they eventually leach from the waste form. Since the plug zone will span about 1 km in granite and up to 2 km in the ubiquitous sedimentary overlay, the opportunity exists for using a diverse sequence of several plugging methods each several hundred meters in extent.

Economic analysis – In order for very deep borehole disposal of nuclear waste to be considered a viable option, several aspects of the cost of disposal in such a manner must be evaluated. Most importantly, the costs of drilling must be assessed as a function of depth, as this would affect the optimal depth of waste emplacement. Several advanced drilling techniques have been developed recently, which could significantly reduce costs. For example, work in the Ukraine has recently increased the speed by a factor of 2-3 and reduced the costs of drilling deep boreholes by using a standard oil well drill unit with high-frequency hydrostatic vibrators.[87] While this would make it possible to drill even deeper, it is not likely, however, that depths significantly different than those specified in this thesis would qualify because of the constraints governing security, retrievability, and maintenance of canister integrity. Of even greater interest with respect to economic analysis is optimization of borehole diameter. For example, it may be possible to meet thermal constraints with as many as four PWR assemblies per canister, which would significantly reduce the unit cost, in $/MTHM, of HLW disposal.

In summary, detailed design of the loaded waste canister and of the borehole plug are high priority topics for future engineering analyses; in the chemistry area dissolution rates and solubility measurements of real or simulated waste in anoxic brines are in order. Assuming successful completion of these recommended additional studies, it is reasonable to presume that deep boreholes could become a viable, if not preferable, candidate for next-generation repository service both in the U.S. and worldwide.

APPENDIX 1: POURBAIX DIAGRAMS FOR POTENTIAL WASTE PACKAGE MATERIALS

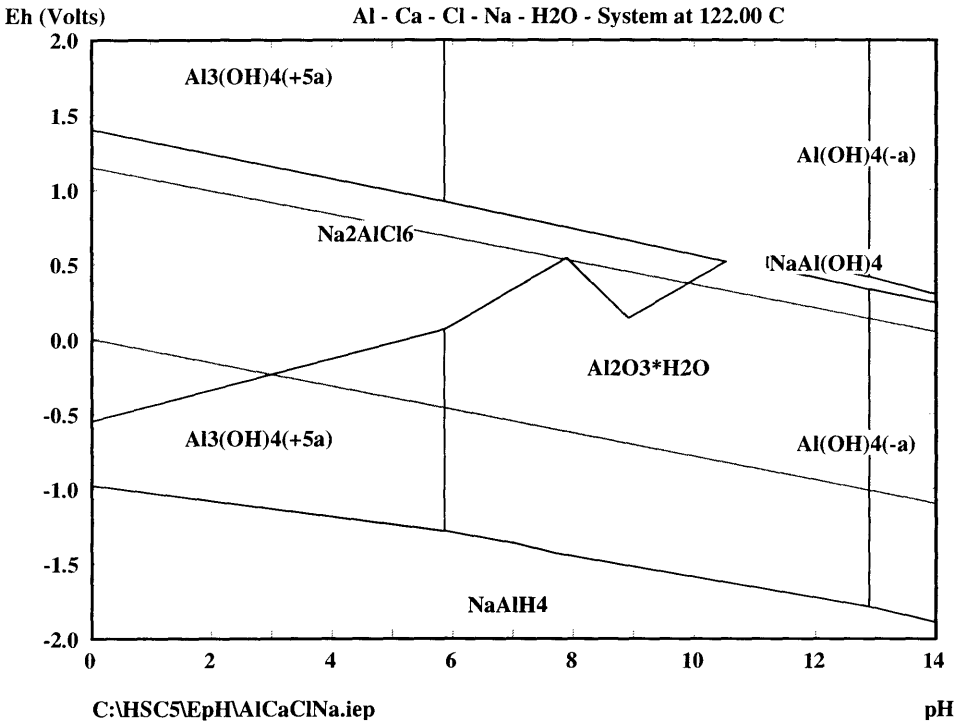

ELEMENTS	Molality	Pressure
Al	1.000E+00	2.049E+00
Ca	2.000E+01	2.049E+00
Cl	1.000E+02	2.049E+00
Na	6.000E+01	2.049E+00

Figure A1.1: Pourbaix diagram for aluminum in 20 M calcium, 60 M sodium, and 100 M chloride at 122° C.

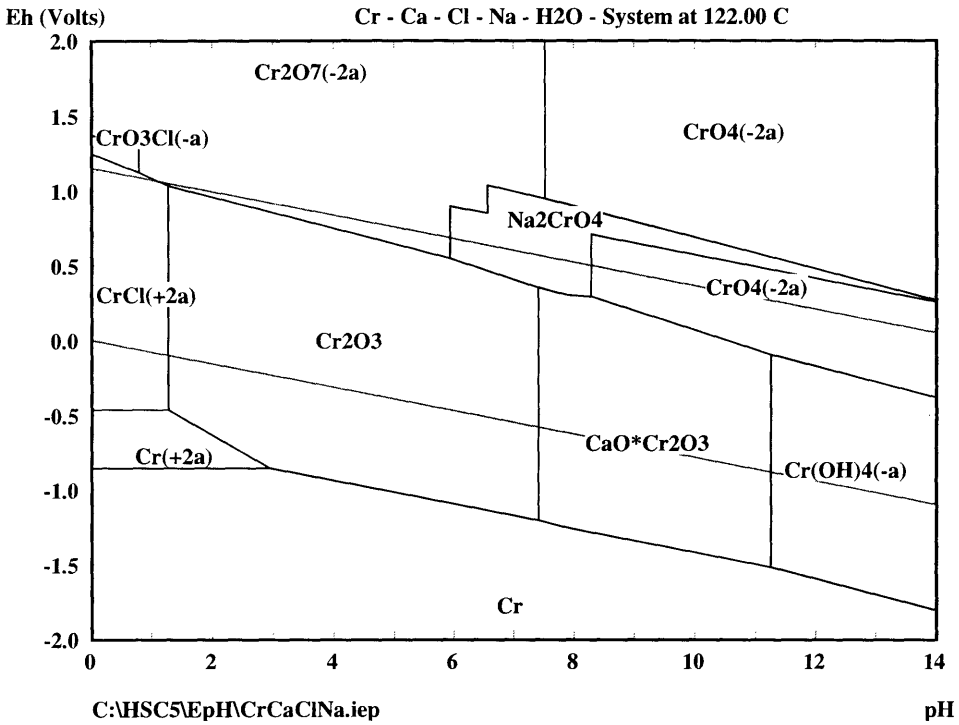

ELEMENTS	Molality	Pressure
Cr	1.000E+00	2.049E+00
Ca	2.000E+01	2.049E+00
Cl	1.000E+02	2.049E+00
Na	6.000E+01	2.049E+00

Figure A1.2: Pourbaix diagram for chromium in 20 M calcium, 60 M sodium, and 100 M chloride at 122° C.

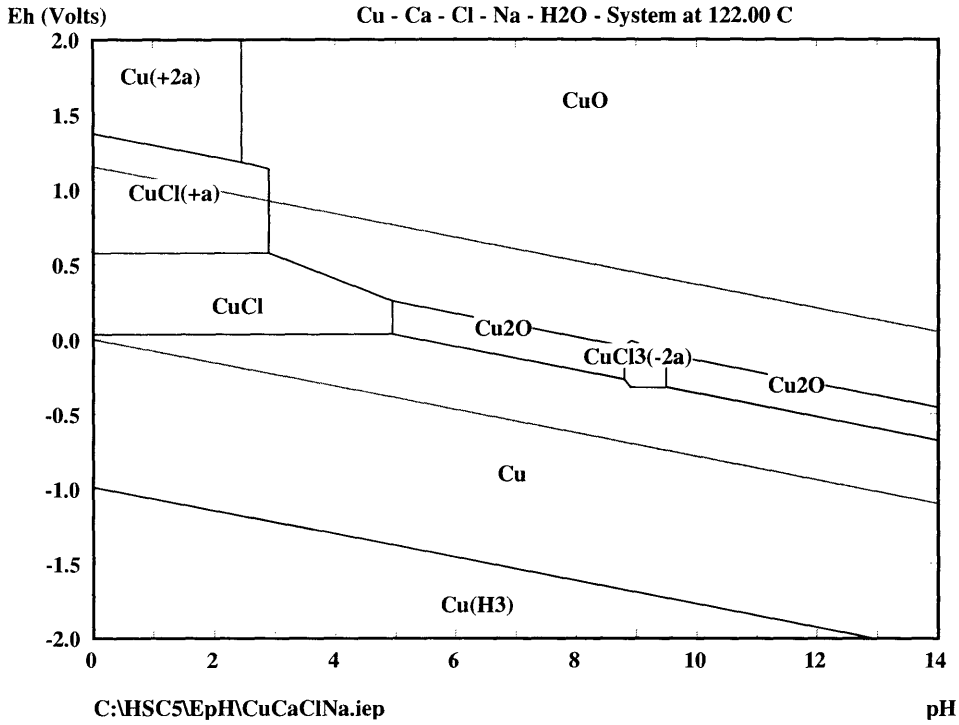

ELEMENTS	Molality	Pressure
Cu	1.000E+00	2.049E+00
Ca	2.000E+01	2.049E+00
Cl	1.000E+02	2.049E+00
Na	6.000E+01	2.049E+00

Figure A1.3: Pourbaix diagram for copper in 20 M calcium, 60 M sodium, and 100 M chloride at 122° C.

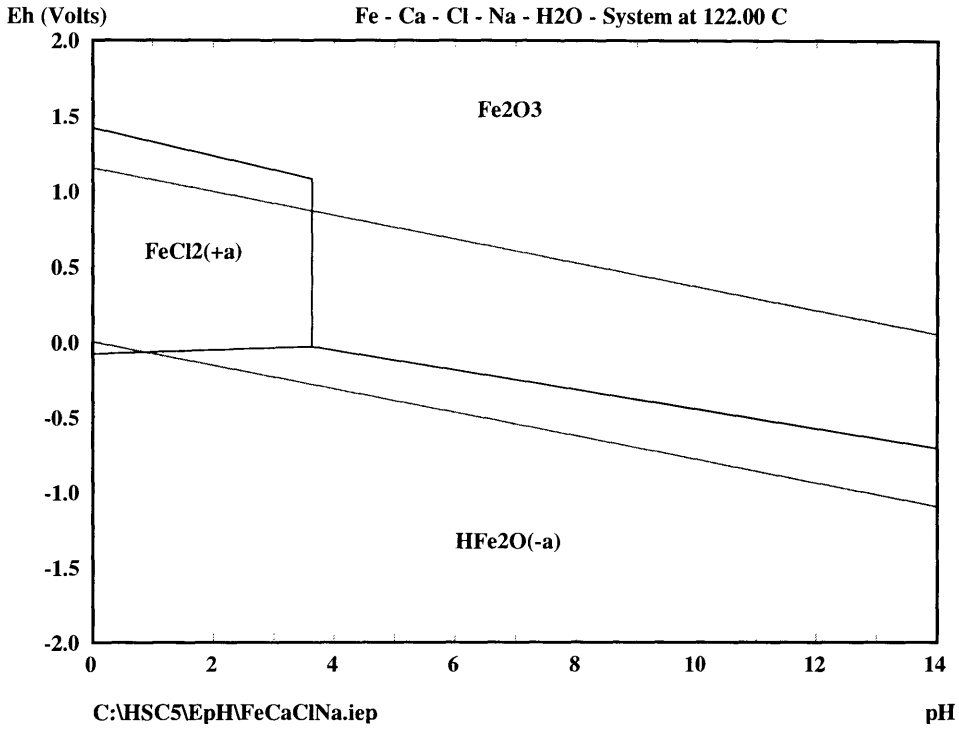

ELEMENTS	Molality	Pressure
Fe	1.000E+00	2.049E+00
Ca	2.000E+01	2.049E+00
Cl	1.000E+02	2.049E+00
Na	6.000E+01	2.049E+00

Figure A1.4: Pourbaix diagram for iron in 20 M calcium, 60 M sodium, and 100 M chloride at 122° C.

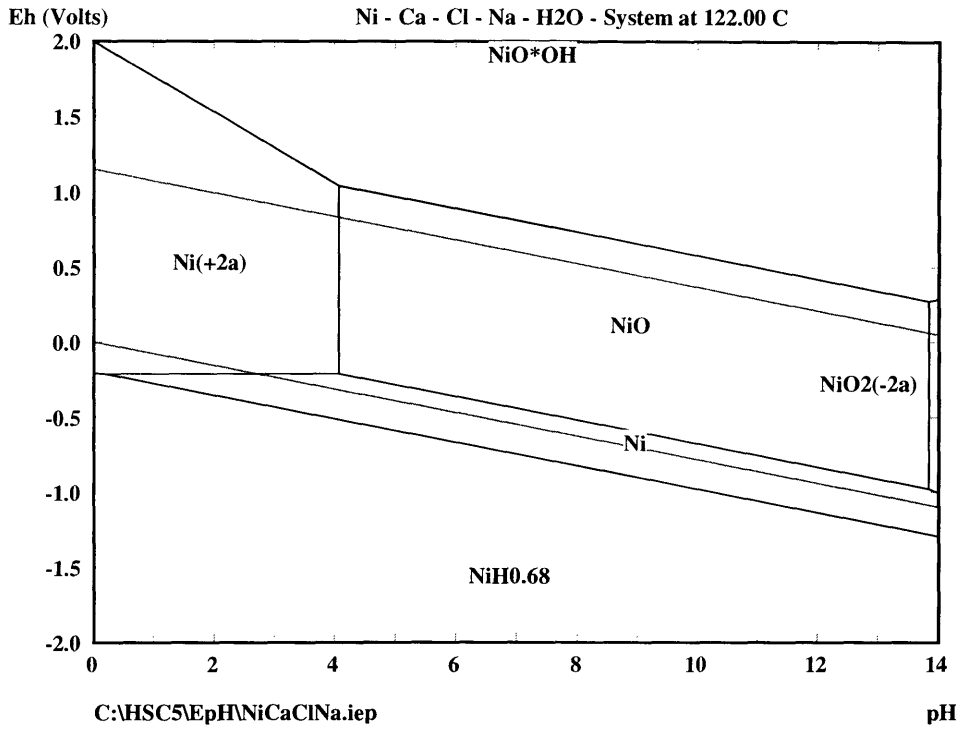

ELEMENTS	Molality	Pressure
Ni	1.000E+00	2.049E+00
Ca	2.000E+01	2.049E+00
Cl	1.000E+02	2.049E+00
Na	6.000E+01	2.049E+00

Figure A1.5: Pourbaix diagram for nickel in 20 M calcium, 60 M sodium, and 100 M chloride at 122° C.

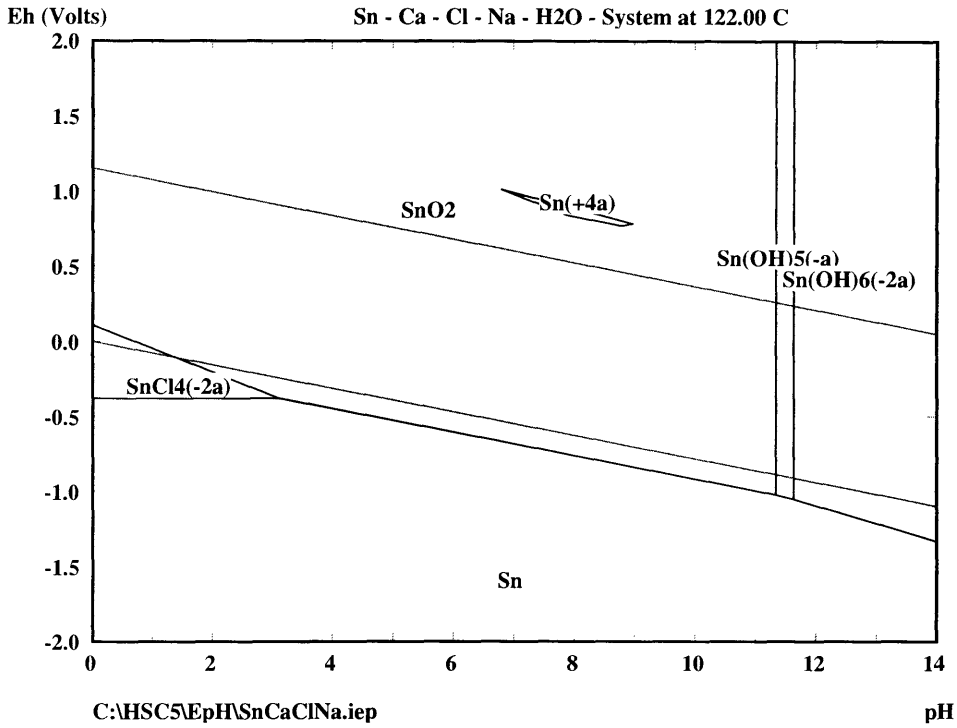

ELEMENTS	Molality	Pressure
Sn	1.000E+00	2.049E+00
Ca	2.000E+01	2.049E+00
Cl	1.000E+02	2.049E+00
Na	6.000E+01	2.049E+00

Figure A1.6: Pourbaix diagram for tin in 20 M calcium, 60 M sodium, and 100 M chloride at 122° C.

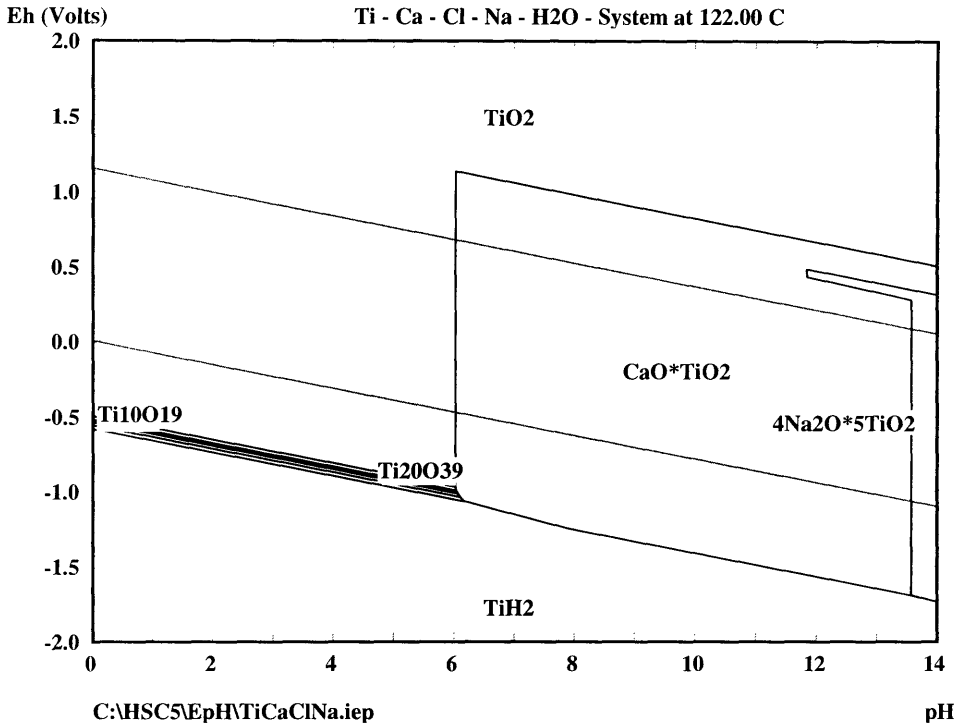

ELEMENTS	Molality	Pressure
Ti	1.000E+00	2.049E+00
Ca	2.000E+01	2.049E+00
Cl	1.000E+02	2.049E+00
Na	6.000E+01	2.049E+00

Figure A1.7: Pourbaix diagram for titanium in 20 M calcium, 60 M sodium, and 100 M chloride at 122° C.

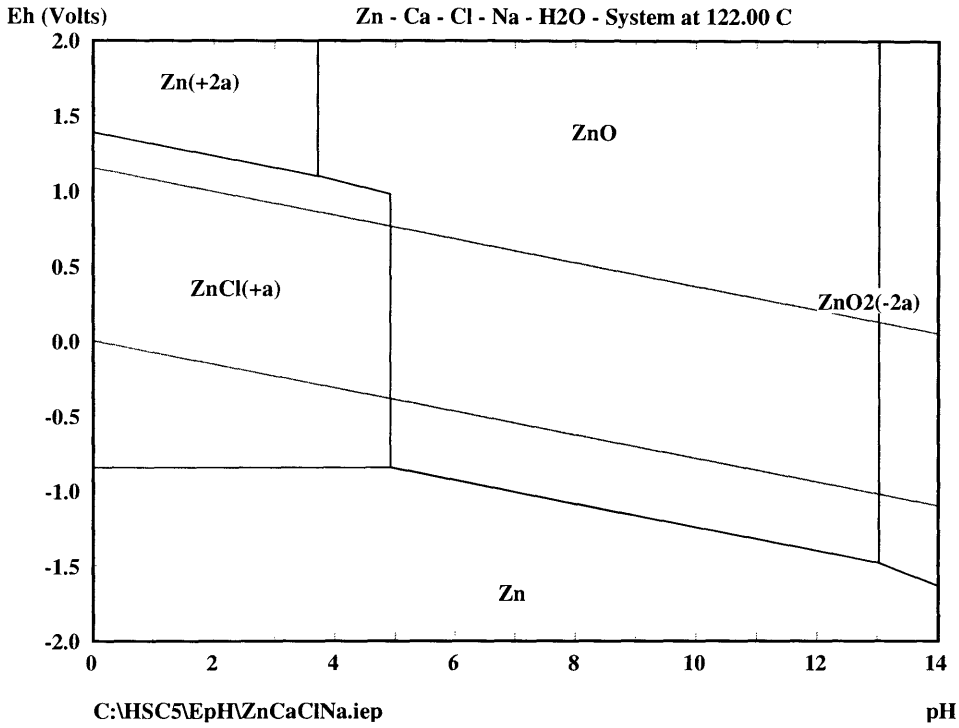

ELEMENTS	Molality	Pressure
Zn	1.000E+00	2.049E+00
Ca	2.000E+01	2.049E+00
Cl	1.000E+02	2.049E+00
Na	6.000E+01	2.049E+00

Figure A1.8: Pourbaix diagram for zinc in 20 M calcium, 60 M sodium, and 100 M chloride at 122° C.

APPENDIX 2: DATA USED IN THERMAL ANALYSIS

Table A2.1: Average activities of radionuclides at 23 years post-discharge by waste type.[88]

	Activity at 23 years following discharge		
Nuclide	PWR (Ci/assembly)	BWR (Ci/assembly)	SRS HLW (Ci/can)
Hydrogen-3	1.20E+02	4.20E+01	-
Carbon-14	6.00E-01	2.90E-01	-
Chlorine-36	5.50E-03	2.10E-03	-
Iron-55	3.40E+00	9.50E-01	-
Cobalt-60	2.20E+02	6.50E+01	4.50E+01
Nickel-59	1.30E+00	3.40E-01	1.80E-02
Nickel-63	1.90E+02	4.50E+01	2.10E+00
Selenium-79	2.30E-01	7.70E-02	1.80E-01
Krypton-85	1.10E+03	3.70E+02	-
Strontium-90	2.30E+04	7.50E+03	2.90E+04
Zirconium-93	1.20E+00	4.60E-01	5.00E+00
Niobium-93m	8.10E-01	3.10E-01	2.20E+00
Niobium-94	6.00E-01	1.90E-02	-
Technetium-99	7.30E+00	2.40E+00	2.50E+00
Ruthenium- 106	3.30E-02	1.40E-02	2.40E+00
Palladium- 107	6.60E-02	2.40E-02	1.20E-02
Cadmium- 11 3m	1.10E+01	4.00E+00	-
Antimony- 125	2.60E+01	1.10E+01	-
Tin-126	4.50E-01	1.50E-01	4.30E-01
Iodine- 129	1.80E-02	6.10E-03	-
Cesium- 134	4.40E+01	1.60E+01	1.20E+01
Cesium- 135	2.70E-01	9.90E-02	6.70E-02
Cesium- 137	3.40E+04	1.10E+04	2.40E+04
Promethium- 147	1.30E+02	4.90E+01	-
Samarium- 151	1.90E+02	6.60E+01	5.50E+02
Europium- 154	9.60E+02	3.20E+02	-
Europium- 155	1.60E+02	5.70E+01	-
Actinium-227	7.60E-06	2.60E-06	-
Thorium-230	1.40E-04	4.50E-05	4.00E-06
Radon-226	0.00E+00		-
Protactinium-231	1.60E-05	5.40E-06	-
Uranium-232	2.10E-02	6.20E-03	-
Uranium-233	3.10E-05	9.10E-06	-
Uranium-234	6.50E-01	2.10E-01	2.70E-02
Uranium-235	8.00E-03	2.60E-03	-

Uranium-236	1.40E-01	4.50E-02	-
Uranium-238	1.40E-01	5.70E-02	8.30E-03
Neptunium-237	2.40E-01	7.10E-02	6.80E-02
Plutonium-238	1.90E+03	6.00E+02	5.00E+02
Plutonium-239	1.80E+02	6.00E+01	6.20E+00
Plutonium-240	2.80E+02	9.30E+01	4.10E+00
Plutonium-241	2.40E+04	8.90E+03	5.40E+02
Plutonium-242	1.00E+00	4.00E-01	5.80E-03
Americium-24 1	1.60E+03	6.10E+02	2.60E+01
Americium-242/242m	1.10E+01	4.70E+00	-
Americium-243	1.40E+01	5.20E+00	1.80E-01
Curium-242	9.10E+00	3.90E+00	-
Curium-243	9.70E+00	3.80E+00	-
Curium-244	9.00E+02	3.50E+02	8.30E+00
Curium-245	2.10E-01	7.90E-02	-
Curium- 246	4.70E-02	1.70E-02	-

Table A2.2: Decay constant, decay energy, and power per atom present for each radionuclide considered.[89]

Nuclide	Decay constant (y^{-1})	Energy (J)	Power/atom (W)
Hydrogen-3	5.63E-02	2.98E-15	5.31E-24
Carbon-14	4.58E-04	2.52E-14	3.65E-25
Chlorine-36	2.30E-06	1.14E-13	8.29E-27
Iron-55	2.54E-01	1.03E-15	8.25E-24
Cobalt-60	1.32E-01	5.09E-14	2.12E-22
Nickel-59	9.12E-06	1.19E-15	3.43E-28
Nickel-63	6.93E-03	1.07E-14	2.36E-24
Selenium-79	1.07E-06	5.88E-14	1.99E-27
Krypton-85	6.44E-02	1.10E-13	2.25E-22
Strontium-90	2.41E-02	4.53E-13	3.46E-22
Zirconium-93	4.62E-07	9.61E-15	1.41E-28
Niobium-93m	4.31E-02	6.09E-15	8.31E-24
Niobium-94	3.47E-05	7.58E-14	8.33E-26
Technetium-99	3.25E-06	4.71E-14	4.86E-27
Ruthenium- 106	6.80E-01	5.73E-13	1.24E-20
Palladium- 107	1.07E-07	6.41E-15	2.17E-29
Cadmium- 113m	4.92E-02	9.45E-14	1.47E-22
Antimony- 125	2.51E-01	4.84E-14	3.86E-22
Tin-126	2.77E-06	3.44E-13	3.03E-26
Iodine- 129	4.41E-08	2.40E-14	3.36E-29
Cesium- 134	3.36E-01	1.05E-13	1.12E-21
Cesium- 135	3.01E-07	3.36E-14	3.21E-28
Cesium- 137	2.31E-02	8.23E-14	6.02E-23
Promethium- 147	2.65E-01	3.59E-14	3.01E-22
Samarium- 151	7.70E-03	1.22E-14	2.97E-24
Europium- 154	8.07E-02	9.29E-14	2.38E-22
Europium- 155	1.46E-01	2.40E-14	1.11E-22
Actinium-227	3.19E-02	2.98E-12	3.02E-21
Thorium-230	9.19E-06	1.52E-12	4.42E-25
Radon-226	4.33E-04	1.72E-12	2.37E-23
Protactinium-231	2.11E-05	8.03E-13	5.38E-25
Uranium-232	9.93E-03	2.63E-12	8.29E-22
Uranium-233	4.35E-06	7.73E-13	1.07E-25
Uranium-234	2.82E-06	7.63E-13	6.81E-26
Uranium-235	9.85E-10	7.53E-13	2.35E-29
Uranium-236	2.96E-08	7.20E-13	6.75E-28
Uranium-238	1.55E-10	1.06E-12	5.19E-30

Neptunium-237	3.24E-07	8.08E-13	8.30E-27
Plutonium-238	7.90E-03	8.79E-13	2.20E-22
Plutonium-239	2.88E-05	8.26E-13	7.53E-25
Plutonium-240	1.06E-04	8.27E-13	2.77E-24
Plutonium-241	4.81E-02	3.33E-15	5.09E-24
Plutonium-242	1.85E-06	7.85E-13	4.60E-26
Americium-241	1.60E-03	8.78E-13	4.46E-23
Americium-242/242m	6.07E-04	1.51E-13	2.91E-24
Americium-243	9.40E-05	9.15E-13	2.73E-24
Curium-242	4.26E-03	9.79E-13	1.32E-22
Curium-243	2.38E-02	9.27E-13	7.00E-22
Curium-244	3.69E-02	9.30E-13	1.09E-21
Curium-245	8.15E-05	8.59E-13	2.22E-24
Curium- 246	1.46E-04	8.63E-13	3.98E-24

Table A2.3: Thermal power output by year for each waste type

Time (years)	BWR Power/Assembly (W)	PWR Power/Assembly (W)	HLW Glass Power/Can (W)
23	220	661	577
25	212	636	551
30	193	578	490
35	176	526	436
40	161	480	388
45	147	440	346
50	135	403	308
55	125	371	274
60	115	342	245
65	107	316	218
70	99.2	293	195
75	92.5	273	174
80	86.4	254	155
85	80.9	237	138
90	76.0	222	124
95	71.6	209	111
100	67.7	197	99.1
105	64.1	186	88.7
110	60.9	176	79.5
115	58.0	168	71.4
120	55.4	160	64.1
125	53.0	152	57.6
130	50.9	146	51.8
135	48.9	140	46.6
140	47.2	135	42.0
145	45.5	130	38.0
150	44.1	125	34.3
160	41.5	117	28.1
170	39.3	111	23.2
180	37.4	105	19.3
190	35.8	100	16.1
200	34.4	96.1	13.6
220	32.1	89.3	9.87
240	30.2	83.8	7.42
260	28.7	79.4	5.78
280	27.4	75.6	4.64
300	26.2	72.3	3.84

320	25.2	69.4	3.26
340	24.3	66.8	2.83
360	23.5	64.5	2.50
380	22.7	62.3	2.23
400	22.0	60.3	2.02
440	20.7	56.4	1.71
480	19.5	53.5	1.48
520	18.5	50.6	1.31
560	17.5	48.1	1.18
600	16.7	45.8	1.07
650	15.7	43.1	0.970
700	14.8	40.7	0.891
750	13.9	38.5	0.827
800	13.2	36.5	0.775
850	12.5	34.7	0.731
900	11.9	33.0	0.693
950	11.3	31.5	0.660
1000	10.8	30.1	0.630

Table A2.4: Heat generation rate and distance-dependent temperature gradient by year in previous work.[90]

Time from emplacement (years)	Volumetric Power Generation (W/m^3)		radius from wall (m)				
			0	4	10	20	42
1	484		11.5	3	0.5	0.25	0
4	427		13	5	2	0.5	0.25
10	369		13	6	3	1.5	0.25
50	199		9.5	5.5	4.5	3	2.5
100	126	ΔT, °C	8.25	7	5	4.5	4
250	66.3		8.75	7.5	7	6.75	6.5
500	40.1		10.25	9.5	9.25	9	8.75
1000	24.0		12.5	12	12	12	12
5000	7.22		20.5	20.5	20.5	20.5	20.5

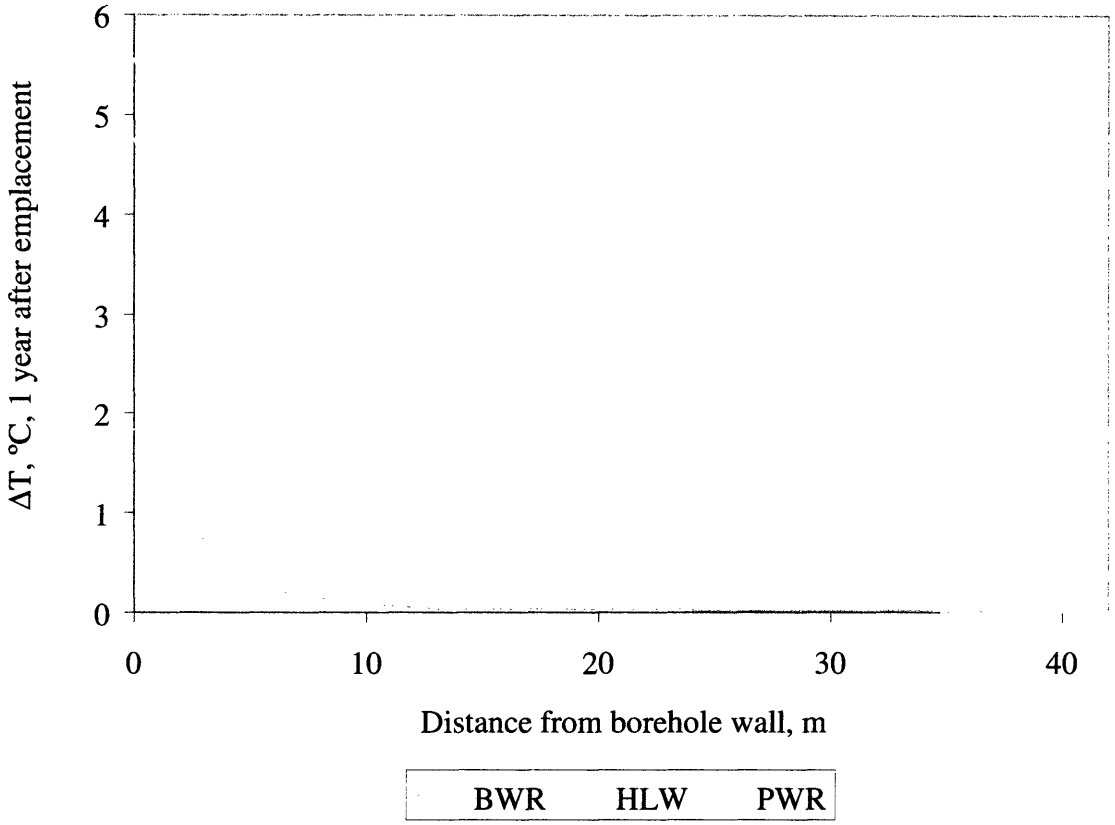

Figure A2.1: Radially-dependent temperature gradient for three different waste types 1 year after emplacement.

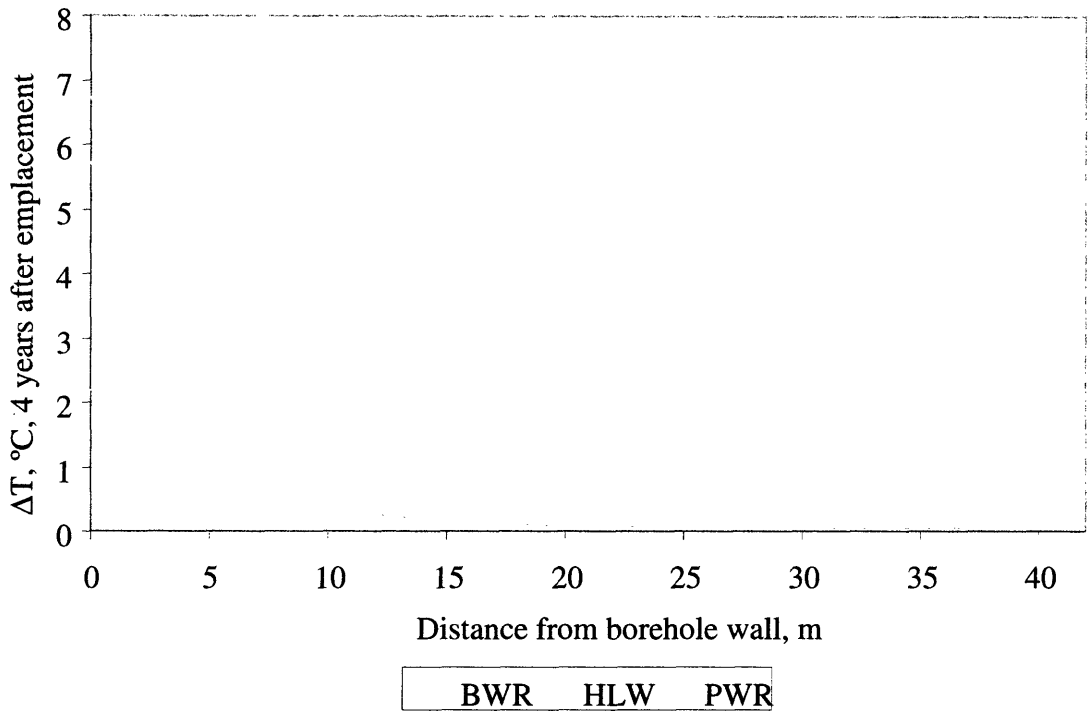

Figure A2.2: Radially-dependent temperature gradient for three different waste types 4 years after emplacement.

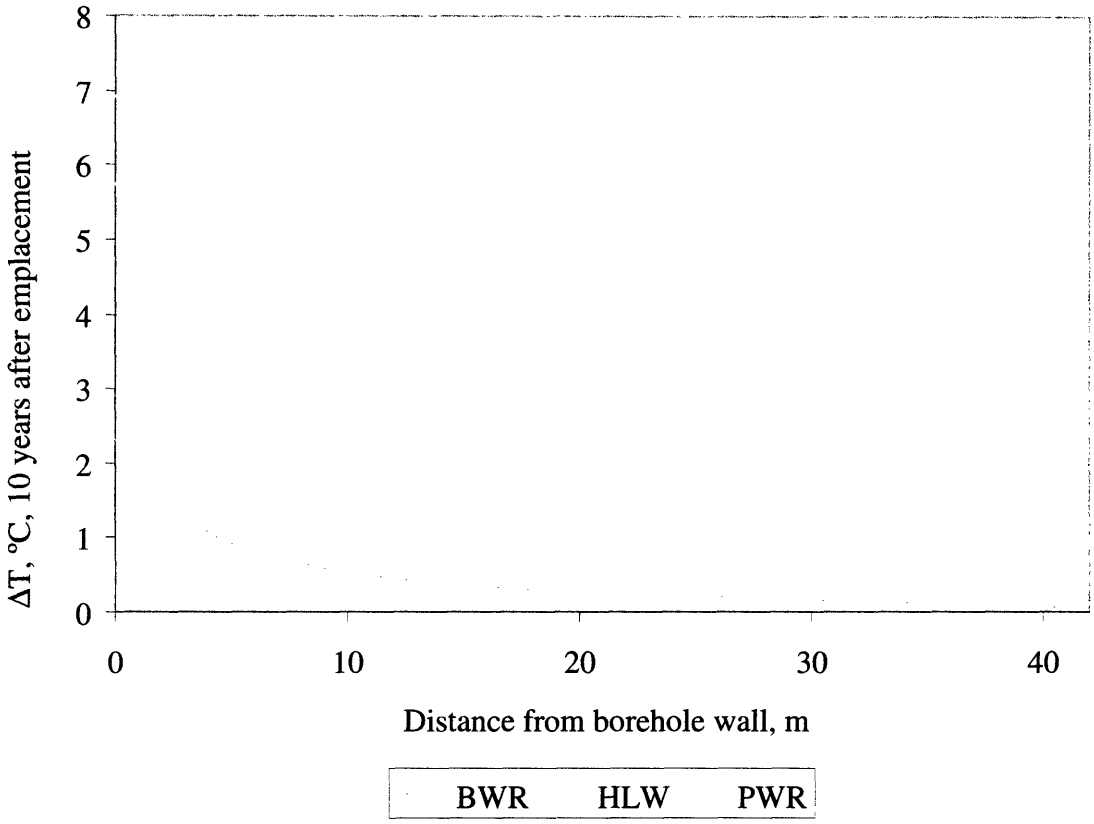

Figure A2.3: Radially-dependent temperature gradient for three different waste types 10 years after emplacement.

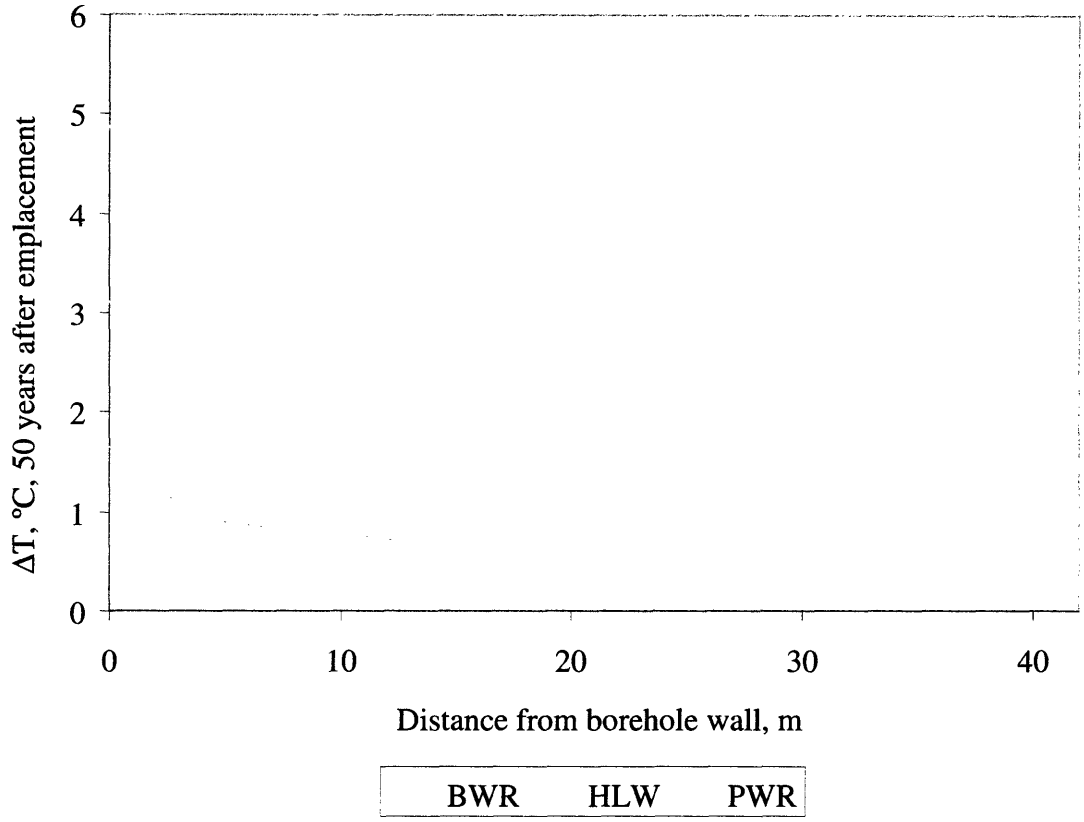

Figure A2.4: Radially-dependent temperature gradient for three different waste types 50 years after emplacement.

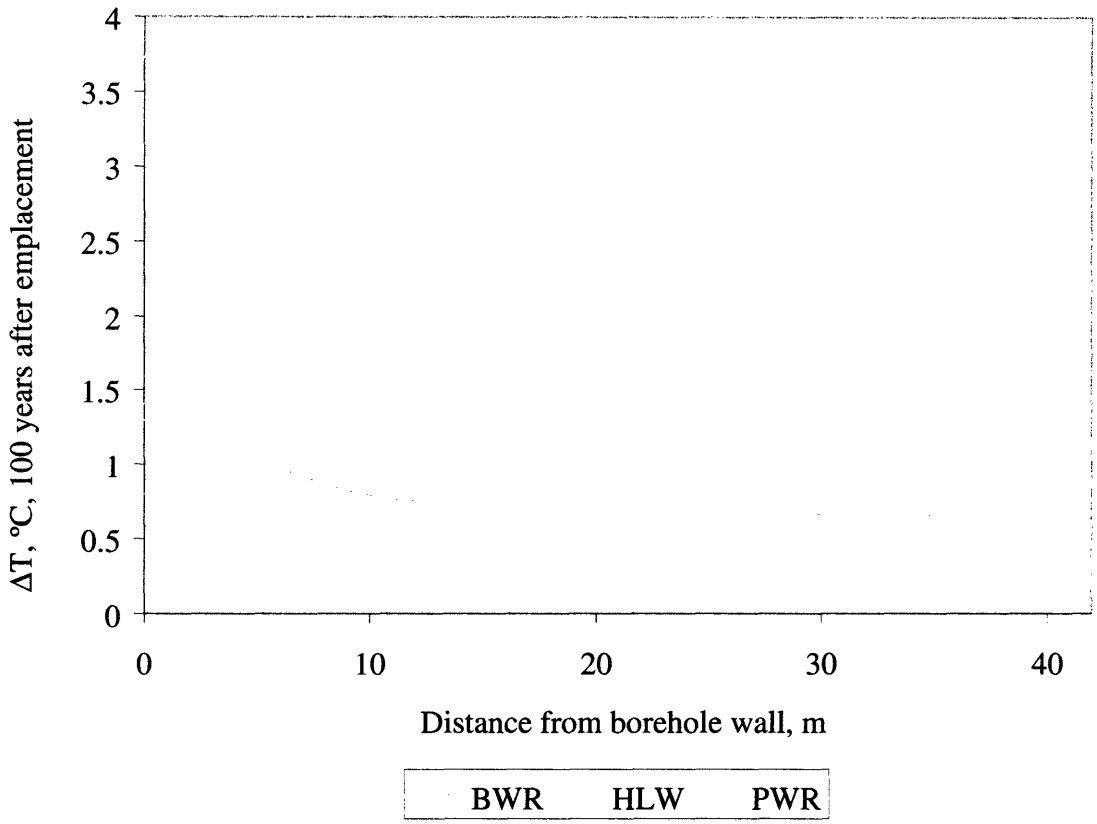

Figure A2.5: Radially-dependent temperature gradient for three different waste types 100 years after emplacement.

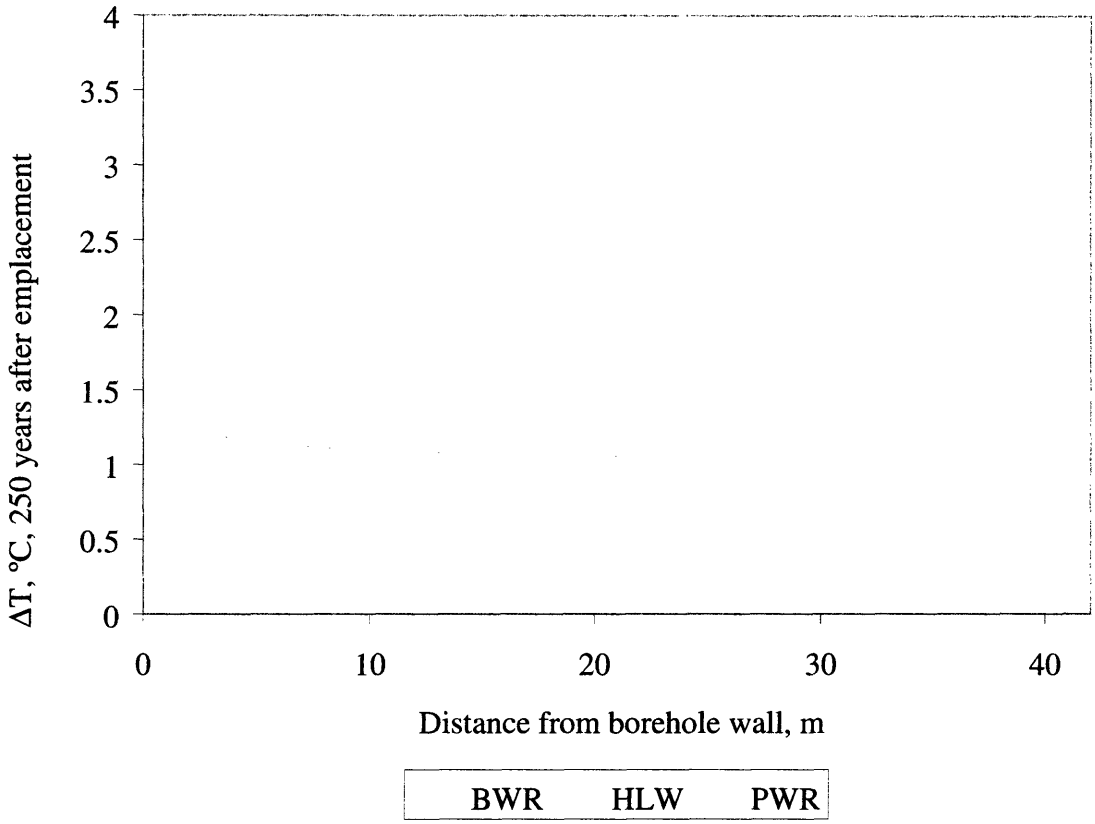

Figure A2.6: Radially-dependent temperature gradient for three different waste types 250 years after emplacement.

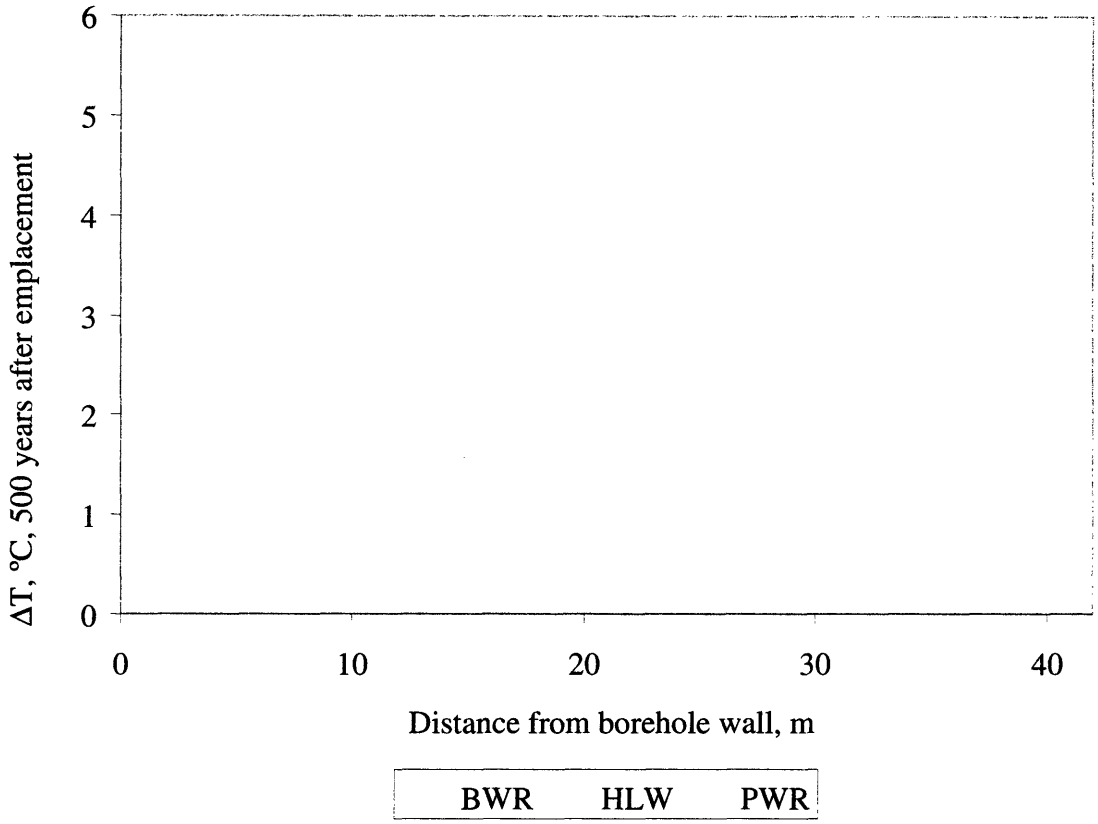

Figure A2.7: Radially-dependent temperature gradient for three different waste types 500 years after emplacement.

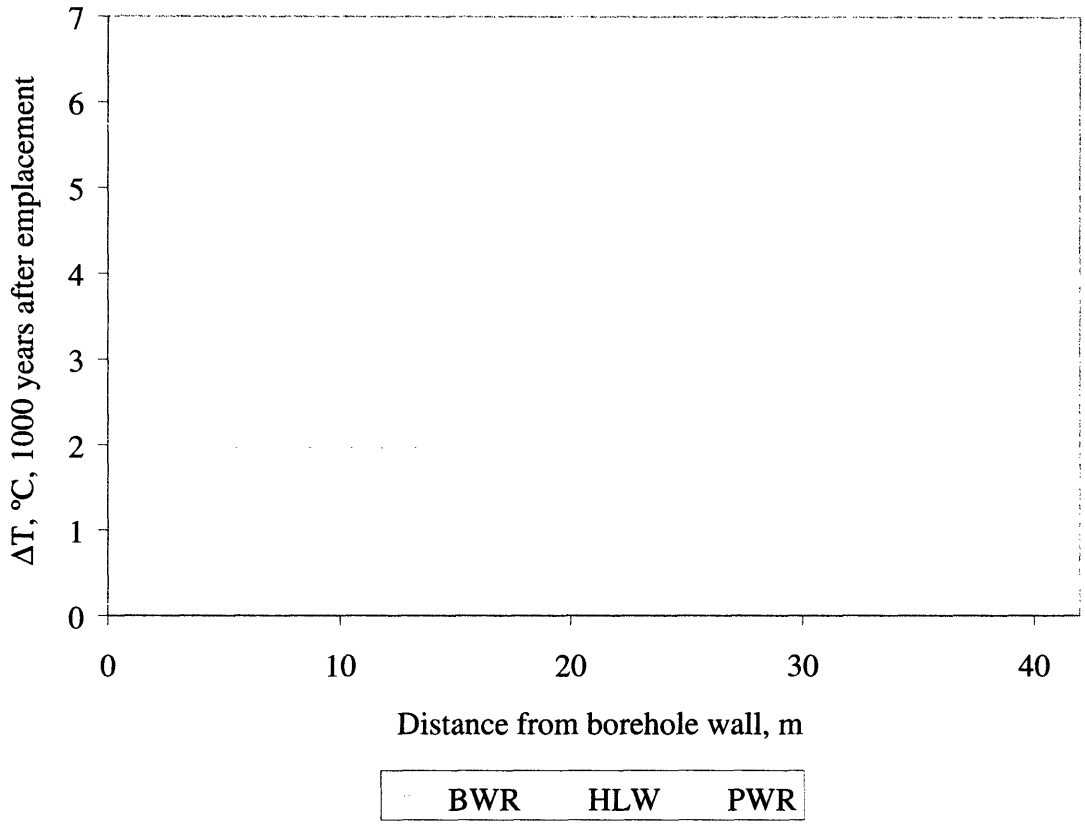

Figure A2.8: Radially-dependent temperature gradient for three different waste types 1000 years after emplacement.

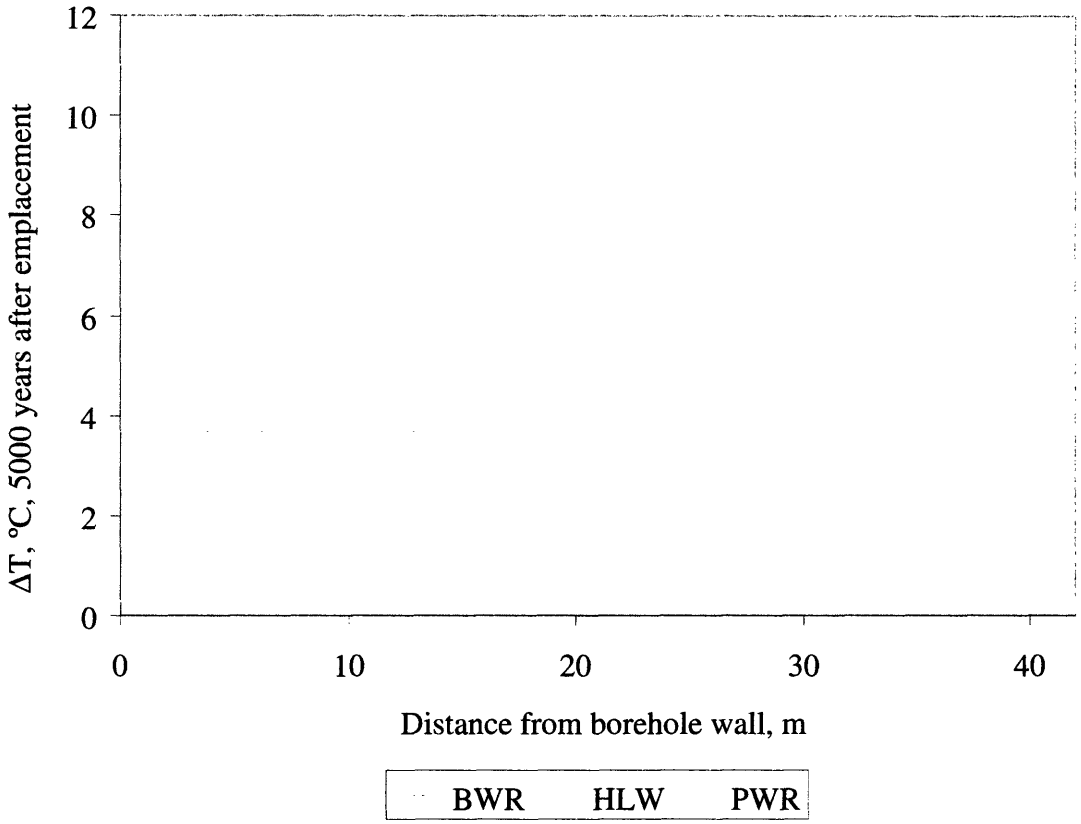

Figure A2.9: Radially-dependent temperature gradient for three different waste types 5000 years after emplacement.

APPENDIX 3: POURBAIX DIAGRAMS OF RADIONUCLIDES COMMON IN NUCLEAR WASTE

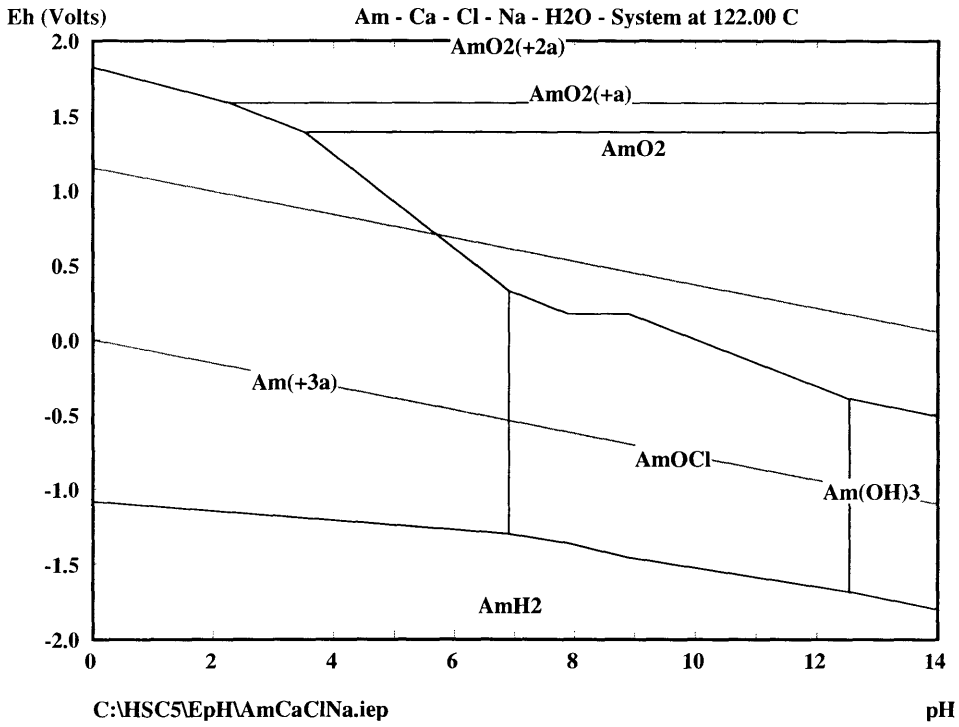

ELEMENTS	Molality	Pressure
Am	1.000E+00	2.049E+00
Ca	2.000E+01	2.049E+00
Cl	1.000E+02	2.049E+00
Na	6.000E+01	2.049E+00

Figure A3.1: Pourbaix diagram for americium at 122° C with 20 M calcium, 60 M sodium and 100 M chloride. The stable state at pH 8.5 and Eh -0.3 V is AmOCl.

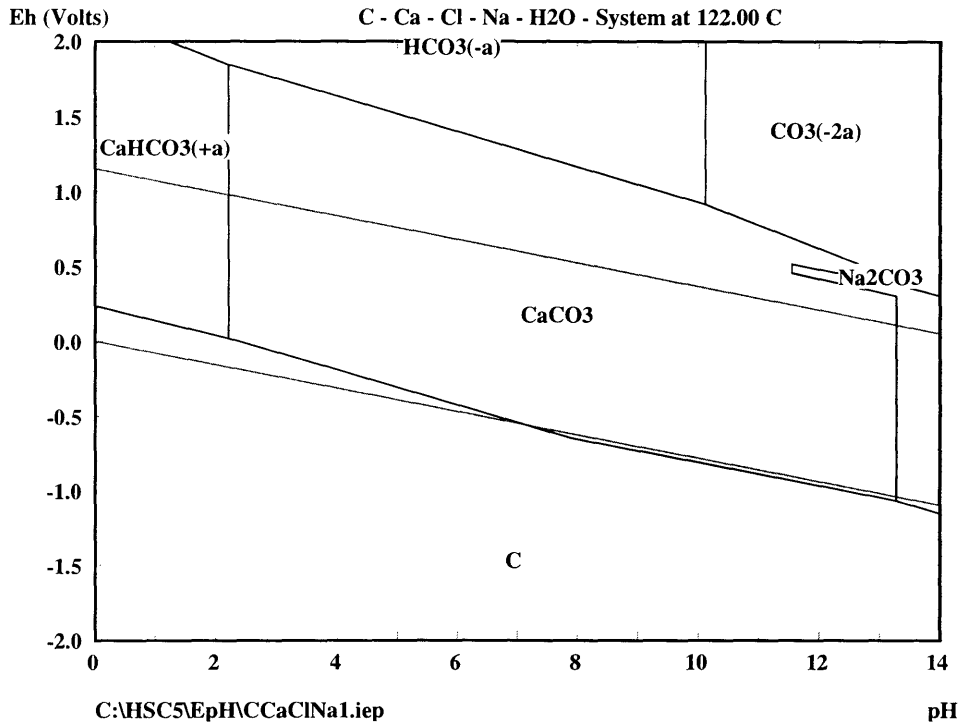

ELEMENTS	Molality	Pressure
C	1.000E+00	2.049E+00
Ca	2.000E+01	2.049E+00
Cl	1.000E+02	2.049E+00
Na	6.000E+01	2.049E+00

Figure A3.2: Pourbaix diagram for carbon at 122° C with 20 M calcium, 60 M sodium and 100 M chloride. The stable state at pH 8.5 and Eh -0.3 V is $CaCO_3$.

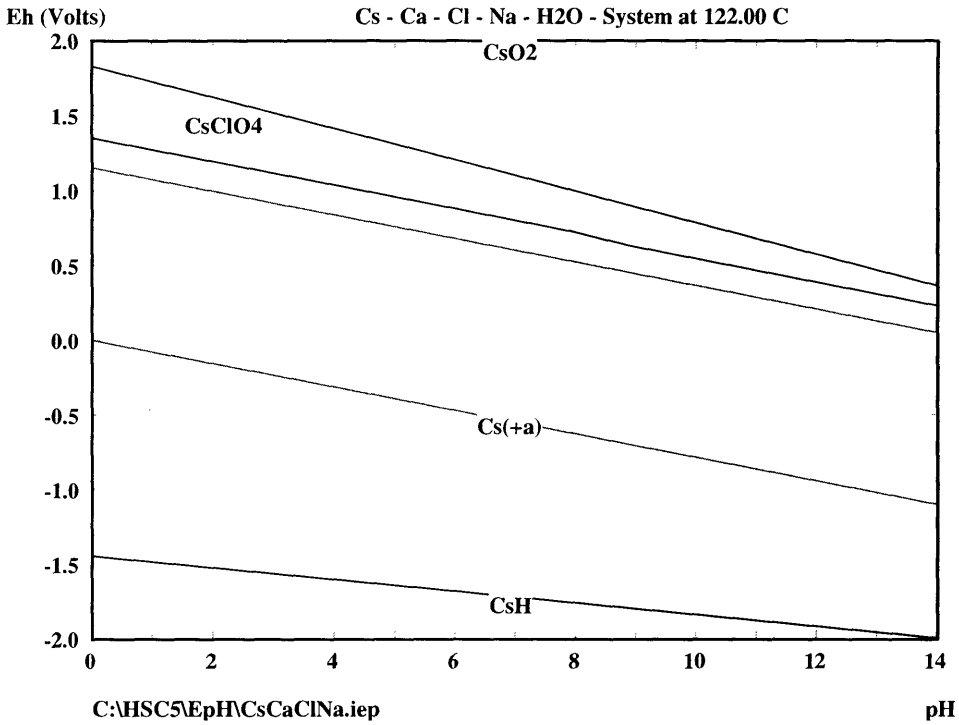

ELEMENTS	Molality	Pressure
Cs	1.000E+00	2.049E+00
Ca	2.000E+01	2.049E+00
Cl	1.000E+02	2.049E+00
Na	6.000E+01	2.049E+00

Figure A3.3: Pourbaix diagram for cesium at 122° C with 20 M calcium, 60 M sodium and 100 M chloride. The stable state at pH 8.5 and Eh -0.3 V is Cs^+.

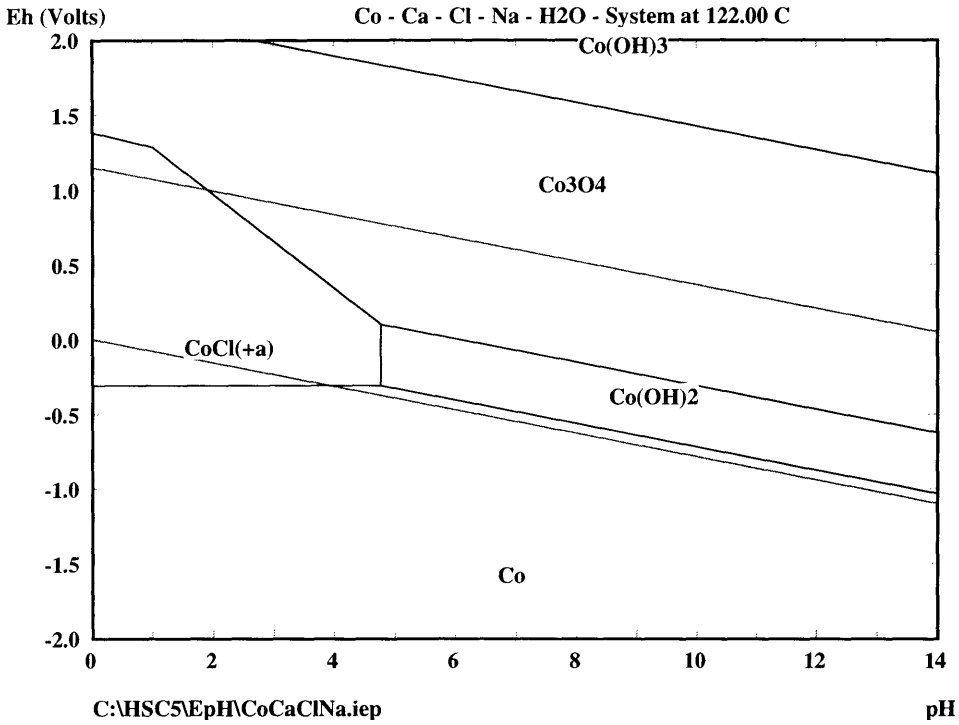

ELEMENTS	Molality	Pressure
Co	1.000E+00	2.049E+00
Ca	2.000E+01	2.049E+00
Cl	1.000E+02	2.049E+00
Na	6.000E+01	2.049E+00

Figure A3.4: Pourbaix diagram for cobalt at 122° C with 20 M calcium, 60 M sodium and 100 M chloride. The stable state at pH 8.5 and Eh -0.3 V is $Co(OH)_2$.

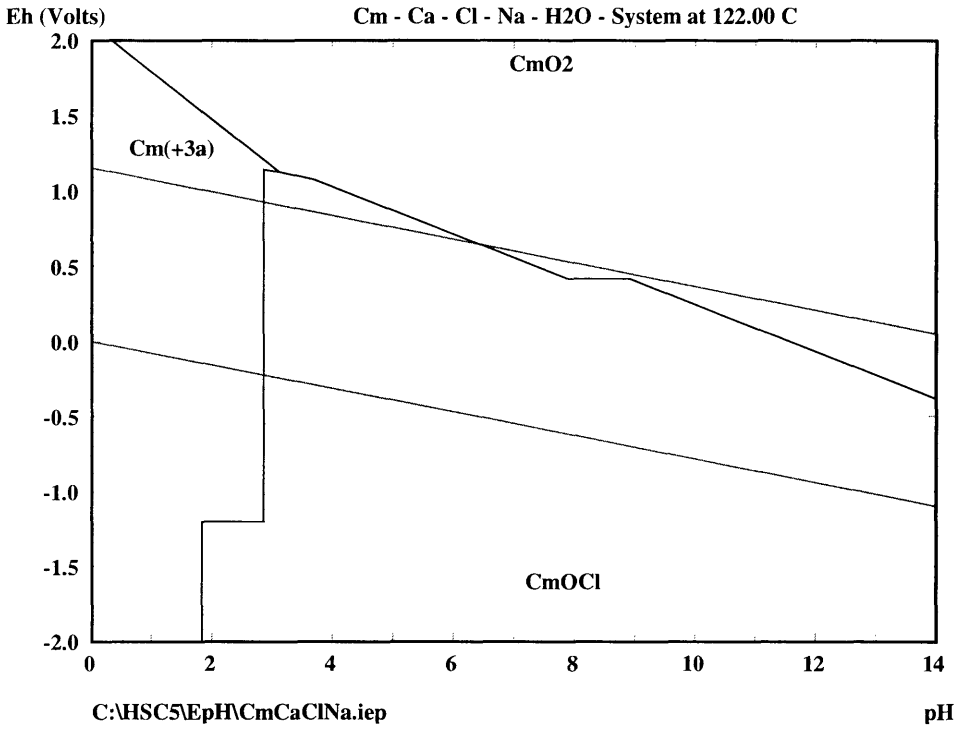

ELEMENTS	Molality	Pressure
Cm	1.000E+00	2.049E+00
Ca	2.000E+01	2.049E+00
Cl	1.000E+02	2.049E+00
Na	6.000E+01	2.049E+00

Figure A3.5: Pourbaix diagram for curium at 122° C with 20 M calcium, 60 M sodium and 100 M chloride. The stable state at pH 8.5 and Eh -0.3 V is CmOCl.

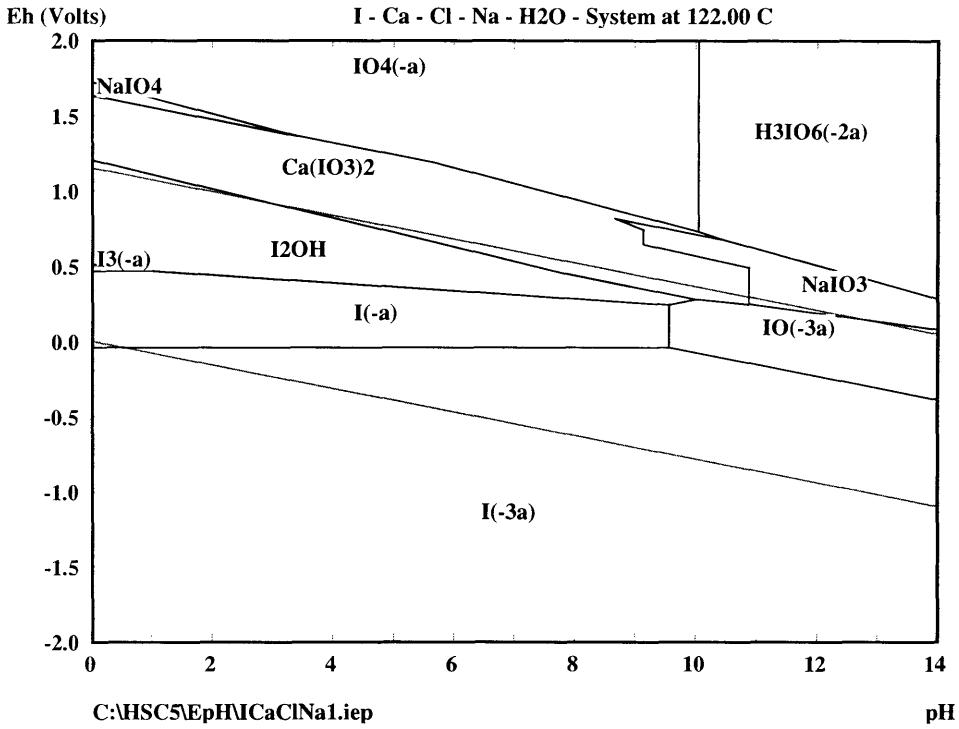

ELEMENTS	Molality	Pressure
I	1.000E+00	2.049E+00
Ca	2.000E+01	2.049E+00
Cl	1.000E+02	2.049E+00
Na	6.000E+01	2.049E+00

Figure A3.6: Pourbaix diagram for iodine at 122° C with 20 M calcium, 60 M sodium and 100 M chloride. The stable state at pH 8.5 and Eh -0.3 V is I_3^- (error in HSC 5.0 gives the stable state as I^{-3}).

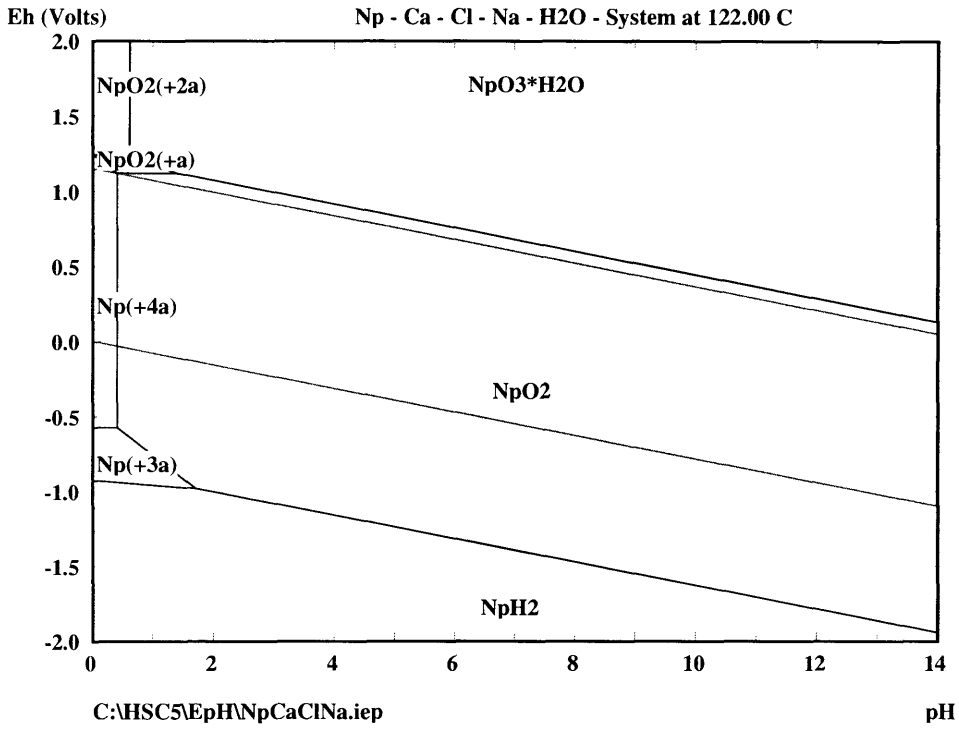

ELEMENTS	Molality	Pressure
Np	1.000E+00	2.049E+00
Ca	2.000E+01	2.049E+00
Cl	1.000E+02	2.049E+00
Na	6.000E+01	2.049E+00

Figure A3.7: Pourbaix diagram for neptunium at 122° C with 20 M calcium, 60 M sodium and 100 M chloride. The stable state at pH 8.5 and Eh -0.3 V is NpO_2.

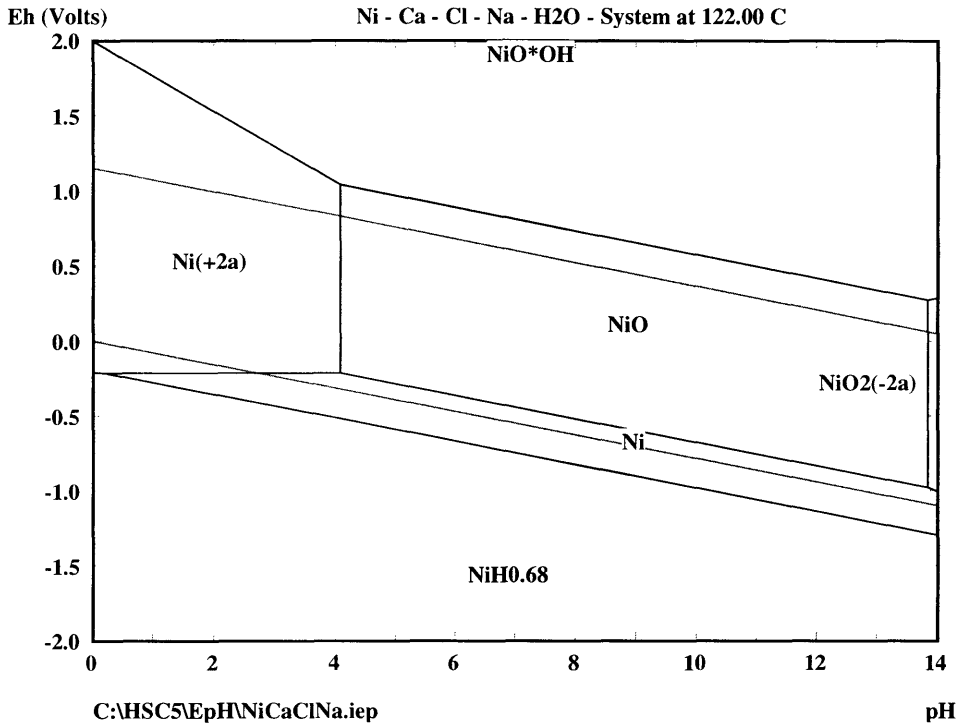

ELEMENTS	Molality	Pressure
Ni	1.000E+00	2.049E+00
Ca	2.000E+01	2.049E+00
Cl	1.000E+02	2.049E+00
Na	6.000E+01	2.049E+00

Figure A3.8: Pourbaix diagram for nickel at 122° C with 20 M calcium, 60 M sodium and 100 M chloride. The stable state at pH 8.5 and Eh -0.3 V is NiO.

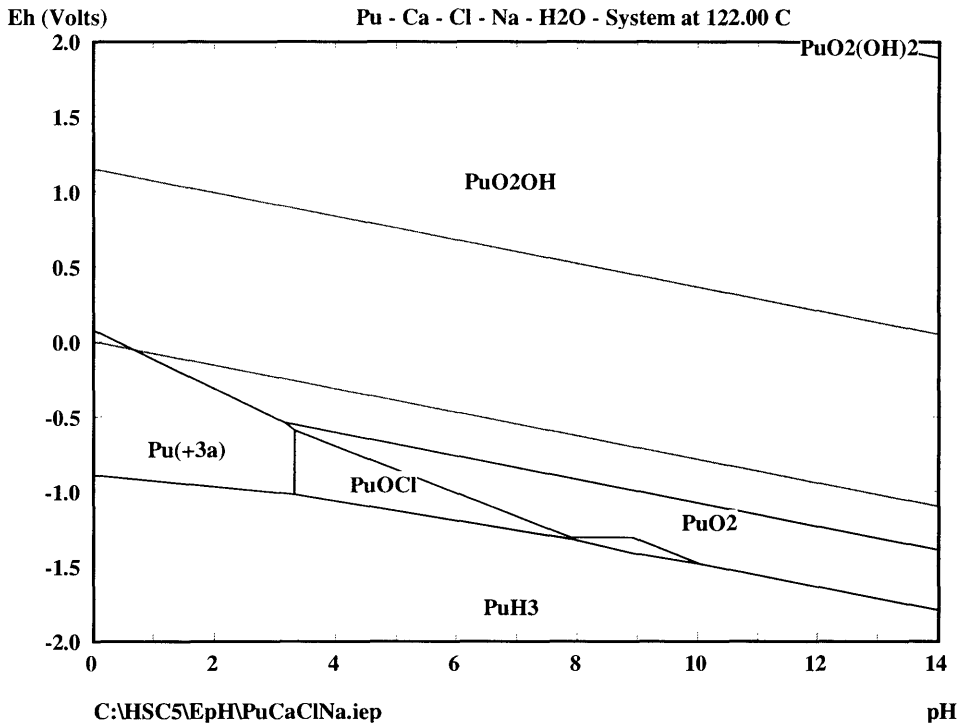

ELEMENTS	Molality	Pressure
Pu	1.000E+00	2.049E+00
Ca	2.000E+01	2.049E+00
Cl	1.000E+02	2.049E+00
Na	6.000E+01	2.049E+00

Figure A3.9: Pourbaix diagram for plutonium at 122° C with 20 M calcium, 60 M sodium and 100 M chloride. The stable state at pH 8.5 and Eh -0.3 V is PuO_2OH.

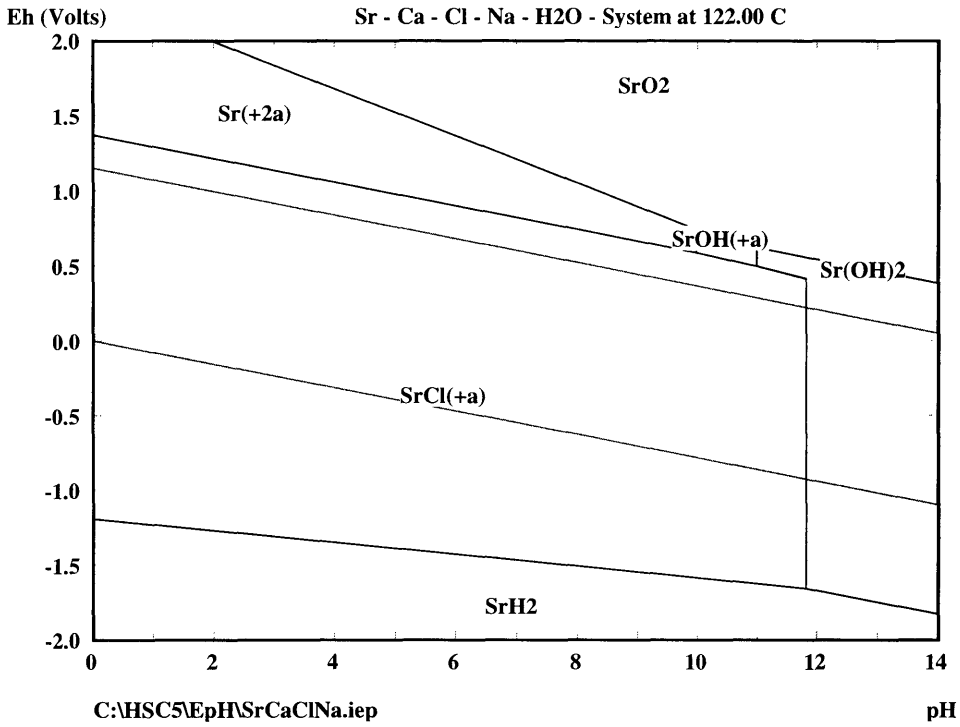

ELEMENTS	Molality	Pressure
Sr	1.000E+00	2.049E+00
Ca	2.000E+01	2.049E+00
Cl	1.000E+02	2.049E+00
Na	6.000E+01	2.049E+00

Figure A3.10: Pourbaix diagram for strontium at 122° C with 20 M calcium, 60 M sodium and 100 M chloride. The stable state at pH 8.5 and Eh -0.3 V is $SrCl^+$.

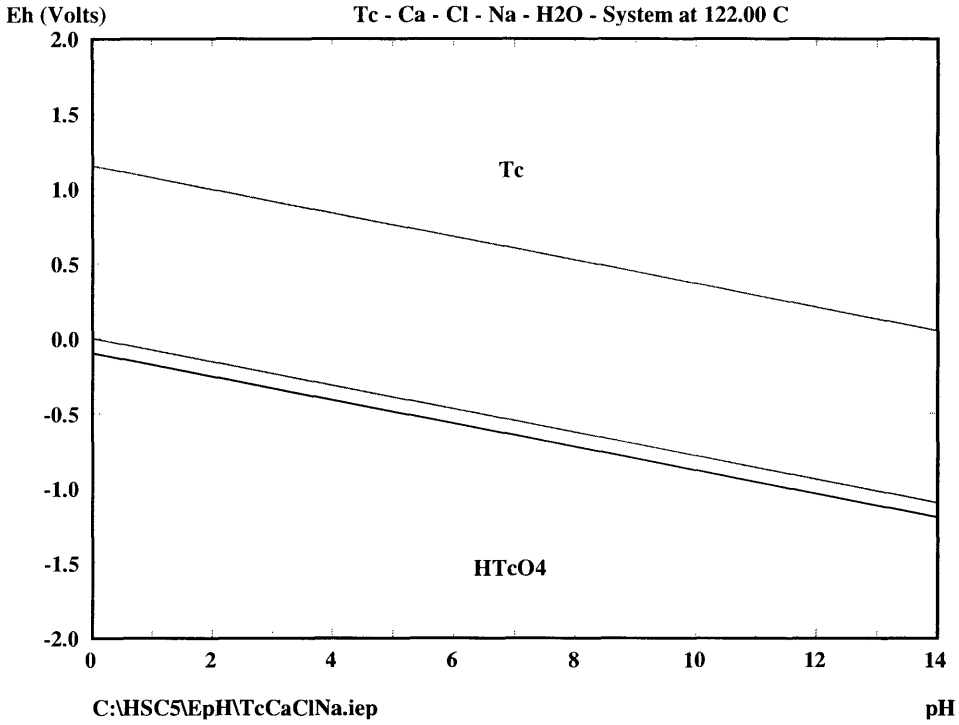

ELEMENTS	Molality	Pressure
Tc	1.000E+00	2.049E+00
Ca	2.000E+01	2.049E+00
Cl	1.000E+02	2.049E+00
Na	6.000E+01	2.049E+00

Figure A3.11: Pourbaix diagram for technetium at 122° C with 20 M calcium, 60 M sodium and 100 M chloride. The stable state at pH 8.5 and Eh -0.3 V is Tc.

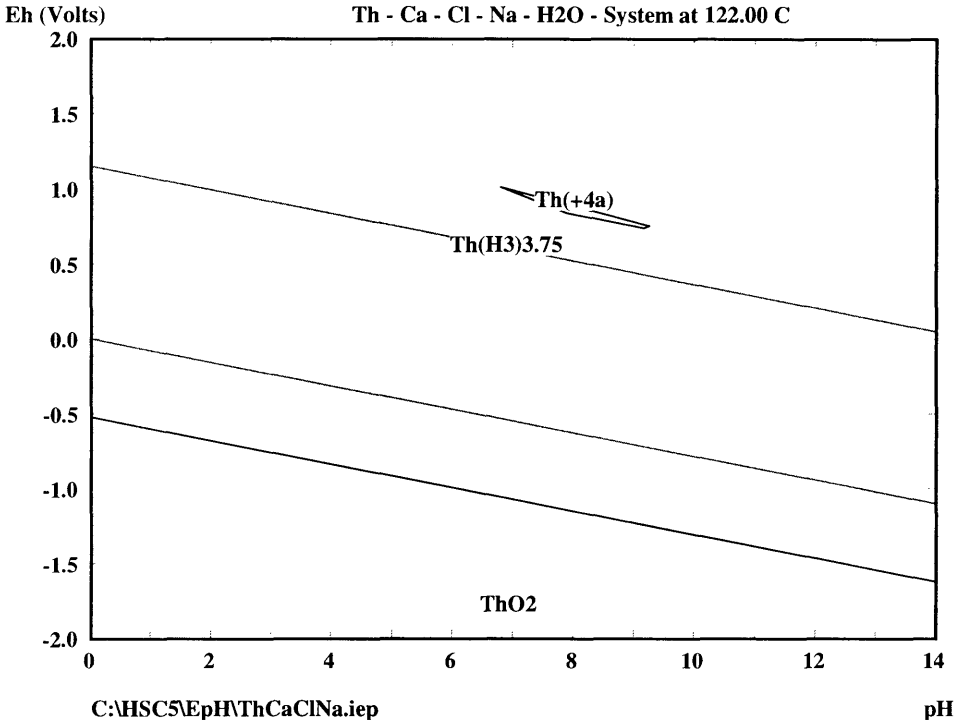

ELEMENTS	Molality	Pressure
Th	1.000E+00	2.049E+00
Ca	2.000E+01	2.049E+00
Cl	1.000E+02	2.049E+00
Na	6.000E+01	2.049E+00

Figure A3.12: Pourbaix diagram for thorium at 122° C with 20 M calcium, 60 M sodium and 100 M chloride. The stable state at pH 8.5 and Eh -0.3 V is $Th(H_3)_{3.75}$.

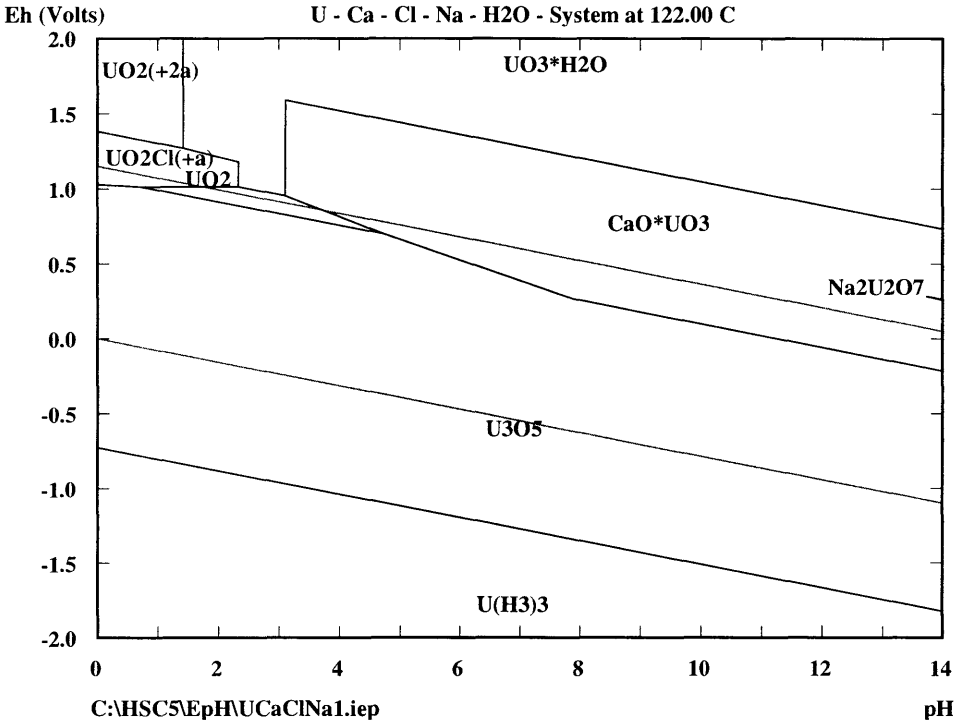

ELEMENTS	Molality	Pressure
U	1.000E+00	2.049E+00
Ca	2.000E+01	2.049E+00
Cl	1.000E+02	2.049E+00
Na	6.000E+01	2.049E+00

Figure A3.13: Pourbaix diagram for uranium at 122° C with 20 M calcium, 60 M sodium and 100 M chloride. The stable state at pH 8.5 and Eh -0.3 V is U_3O_8 (error in HSC 5.0 gives the stable state as U_3O_5).

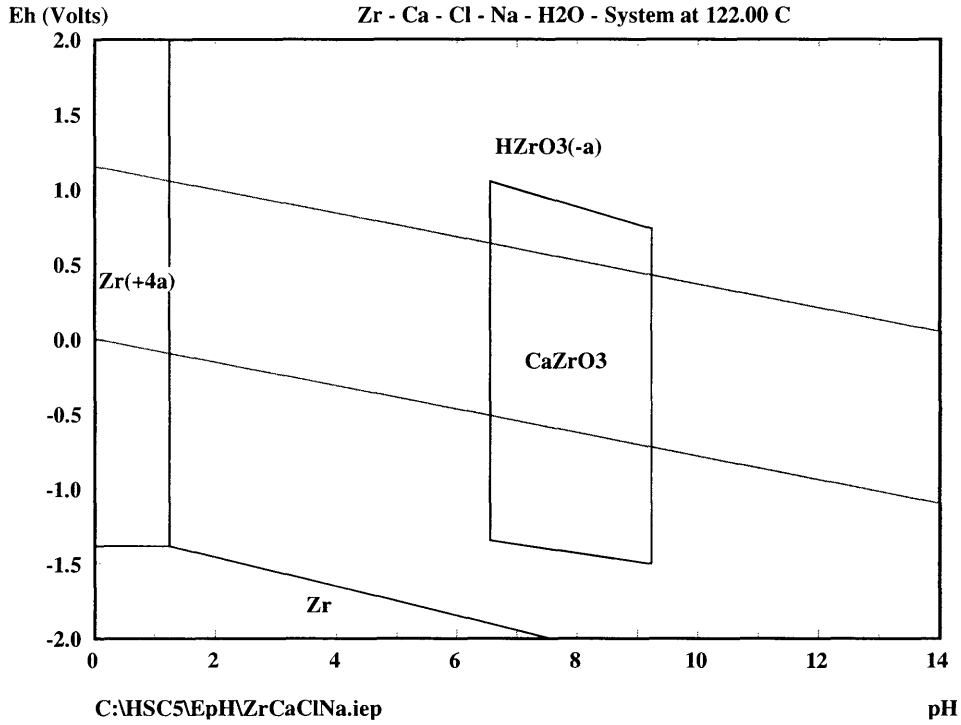

ELEMENTS	Molality	Pressure
Zr	1.000E+00	2.049E+00
Ca	2.000E+01	2.049E+00
Cl	1.000E+02	2.049E+00
Na	6.000E+01	2.049E+00

Figure A3.14: Pourbaix diagram for zirconium at 122° C with 20 M calcium, 60 M sodium and 100 M chloride. The stable state at pH 8.5 and Eh -0.3 V is $CaZrO_3$.

APPENDIX 4: SOLUBILITY OF COMMON RADIONUCLIDES IN NUCLEAR WASTE IN A DEEP BOREHOLE ENVIRONMENT

This appendix details the calculations that support the values of the maximum estimated concentrations listed for 14 radionuclides in Table 5.2. The sources for solubility products and free energy values include the Common Thermodynamic Database Project[91] and HSC 5.0 Chemistry Software, and these values are used to calculate the maximum anticipated concentrations for each radionuclide.

A4.1 Americium

Reaction:
$Am^{+3} + Cl^{-} + H_2O \rightarrow AmOCl + 2H^{+}$

Solubility product:
From the CTDP information on AmOCl, log(K(75° C))=-8.29 and log(K(100° C))=-7.08.

$$\log(K(125^{\circ}C) = \frac{\log(K(100^{\circ}C) - \log(K(75^{\circ}C)}{25^{\circ}C} \times 25^{\circ}C + \log(K(100^{\circ}C) = -5.87$$

Solubility of Am^{+3}:

$$K(125^{\circ}C) = \frac{[H^{+}]^2}{[Am^{+3}][Cl^{-}]} \rightarrow [Am^{+3}] = \frac{(10^{-8.5})^2}{100 \cdot 10^{-5.87}} = 10^{-13.13}$$

A4.2 Carbon

Reaction:
$Ca^{+2} + HCO_3^{-} \rightarrow CaCO_3 + H^{+}$

Solubility product:
From the CTDP information on $CaCO_3$, log(K(100° C))=-0.7743 and log(K(150° C))=-0.0999.

$$\log(K(125^{\circ}C) = \frac{\log(K(100^{\circ}C) + \log(K(150^{\circ}C)}{2} = -0.4371$$

Solubility of HCO_3^{-} (radioactive carbon):

$$K(125^{\circ}C) = \frac{[H^{+}]}{[Ca^{+2}][HCO_3^{-}]} \rightarrow [HCO_3^{-}] = \frac{10^{-8.5}}{20 \cdot 10^{-0.4371}} = 10^{-9.363}$$

A4.3 Cesium

Reaction:
$Cs^{+} + Cl^{-} \rightarrow CsCl$

Solubility product:
From the CTDP information on CsCl, log(K(100° C))=0.2611 and log(K(150° C))=0.5039.

$$\log(K(125^\circ C) = \frac{\log(K(100^\circ C) + \log(K(150^\circ C)}{2} = 0.3825$$

Solubility of Cs^+:

$$K(125^\circ C) = \frac{1}{[Cs^+][Cl^-]} \rightarrow [Cs^+] = \frac{100}{10^{0.3825}} = 41.45$$

A4.4 Cobalt

Reaction:
$Co^{+2} + 2H_2O \rightarrow Co(OH)_2 + 2H^+$

Solubility product:
From HSC 5.0 data at 125° C, $\Delta G(Co(OH)_2)$=-576.94 J/mol, $\Delta G(Co^{+2})$=103.55 J/mol, $\Delta G(H_2O)$=-314.73 J/mol, and $\Delta G(H^+)$=0 J/mol.
ΔG(reaction)= $\Delta G(Co(OH)_2)$ - $\Delta G(Co^{+2})$ - 2x $\Delta G(H_2O)$ = -576.94 J/mol – 2x-314.73 J/mol + 103.55 J/mol = 156.07 J/mol

$$K(125^\circ C) = e^{\frac{-\Delta G(reaction)}{RT}} = e^{-0.1247} = 0.8827$$

Solubility of Co^{+2}:

$$K(125^\circ C) = \frac{[H^+]^2}{[Co^{+2}]} \rightarrow [Co^{+2}] = \frac{[10^{-8.5}]^2}{0.8827} = 10^{-16.94}$$

A4.5 Curium

Reaction:
$Cm^{+3} + Cl^- + H_2O \rightarrow CmOCl + 2H^+$

Solubility product:
From HSC 5.0 data at 125° C, $\Delta G(CmOCl)$=-1004.9 J/mol, $\Delta G(Cm^{+3})$=-540.34 J/mol, $\Delta G(Cl^-)$=-187.93 J/mol, $\Delta G(H_2O)$=-314.73 J/mol, and $\Delta G(H^+)$=0 J/mol.
ΔG(reaction)= $\Delta G(CmOCl)$ - $\Delta G(Cl^-)$ - $\Delta G(Cm^{+3})$ - $\Delta G(H_2O)$ = -1004.9 J/mol + 187.93 J/mol + 540.34 J/mol + 314.73 J/mol = 38.1 J/mol

$$K(125^\circ C) = e^{\frac{-\Delta G(reaction)}{RT}} = e^{-0.01151} = 0.9885$$

Solubility of Cm^{+3}:

$$K(125^\circ C) = \frac{[H^+]^2}{[Cm^{+3}][Cl^-]} \rightarrow [Cm^{+3}] = \frac{[10^{-8.5}]^2}{0.9885 \cdot 100} = 10^{-18.995}$$

A4.6 Iodine

$H_2 + 3I_2 \rightarrow 2I_3^- + 2H^+$

Solubility product:
From HSC 5.0 data at 125° C, $\Delta G(H_2)$=-52.33 J/mol, $\Delta G(I_3^-)$=-145.16 J/mol, $\Delta G(I_2)$=-47.56 J/mol, and $\Delta G(H^+)$=0 J/mol.
ΔG(reaction)= 2x$\Delta G(I_3^-)$ - 3x$\Delta G(I_2)$ - $\Delta G(H_2)$ = 2x-145.16 J/mol – 3x-47.56 J/mol + 52.33 J/mol = -95.31 J/mol

$$K(125^\circ C) = e^{\frac{-\Delta G(reaction)}{RT}} = e^{0.0288} = 1.0292$$

Solubility of Cm^{+3}:

$$K(125^\circ C) = \frac{[H^+]^2[I_3^-]}{P_{H_2}} \rightarrow [I_3^-] = \sqrt{\frac{[10^{-8.5}]^2}{0.1 \cdot 1.0292}} = 10^{-8.006}$$

A4.7 Nickel

Reaction:
$H_2O + Ni^{+2} \rightarrow NiO + 2H^+$

Solubility product:
From the CTDP information on NiO, log(K(100° C))=-8.9384 and log(K(150° C))= -7.2623.

$$\log(K(125^\circ C) = \frac{\log(K(100^\circ C) + \log(K(150^\circ C)}{2} = -8.10035$$

Solubility of Ni^{+2}:

$$K(125^\circ C) = \frac{[H^+]^2}{[Ni^{+2}]} \rightarrow [Ni^{+2}] = \frac{(10^{-8.5})^2}{10^{-8.10035}} = 10^{-8.899}$$

A4.8 Neptunium

Reaction:
$Np^{+4} + 2H_2O \rightarrow NpO_2 + 4H^+$

Solubility product:
From the CTDP information on NpO_2, log(K(75° C))=11.1 and log(K(100° C))=11.64.

$$\log(K(125^\circ C) = \frac{\log(K(100^\circ C) - \log(K(75^\circ C)}{25^\circ C} \times 25^\circ C + \log(K(100^\circ C) = 12.18$$

Solubility of Np^{+4}:

$$K(125^\circ C) = \frac{[H^+]^4}{[Np^{+4}]} \rightarrow [Np^{+4}] = \frac{(10^{-8.5})^4}{100 \cdot 10^{12.18}} = 10^{-46.18}$$

A4.9 Plutonium

Reaction:
$PuO_2^+ + H_2O \rightarrow PuO_2OH + H^+$

Solubility product:
From the CTDP information on PuO_2OH, log(K(75° C))=-4.09 and log(K(100° C))=-3.73.

$$\log(K(125^\circ C) = \frac{\log(K(100^\circ C) + \log(K(150^\circ C)}{2} = -3.37$$

Solubility of PuO_2^+:

$$K(125^\circ C) = \frac{[H^+]}{[PuO_2{}^+]} \rightarrow [PuO_2{}^+] = \frac{(10^{-8.5})}{10^{-3.37}} = 10^{-5.13}$$

A4.10 Strontium

Reaction:
$2SrCl^+ + H_2 \rightarrow 2Sr + 2Cl^- + 2H^+$

Solubility product:
From HSC 5.0 data at 125° C, $\Delta G(H_2)$=-52.33 J/mol, $\Delta G(Cl^-)$=-187.95 J/mol, $\Delta G(Sr)$=-22.31 J/mol, $\Delta G(SrCl^+)$=-729.48 J/mol, and $\Delta G(H^+)$=0 J/mol.
ΔG(reaction)= 2x$\Delta G(Sr)$ + 2x$\Delta G(Cl^-)$ - 2x$\Delta G(SrCl^+)$ - $\Delta G(H_2)$ = 2x-22.31 J/mol + 2x-187.95 J/mol– 2x-729.48 J/mol + 52.33 J/mol = -986.11 J/mol

$$K(125^\circ C) = e^{\frac{-\Delta G(reaction)}{RT}} = e^{0.2979} = 1.347$$

Solubility of $SrCl^+$:

$$K(125^\circ C) = \frac{[H^+]^2[Cl^-]^2}{[SrCl^+]P_{H_2}} \rightarrow [SrCl^+] = \frac{(10^{-8.5})^2(100)^2}{1.347 \cdot 0.1} = 10^{-12.129}$$

A4.11 Technetium

Reaction:
$TcO^{+2} + 2H_2 \rightarrow 2H^+ + Tc + H_2O$

Solubility product:
From HSC 5.0 data at 125° C, $\Delta G(H_2)$=-52.33 J/mol, $\Delta G(Tc)$=-13.51 J/mol, $\Delta G(TcO^{+2})$=-89.09 J/mol, $\Delta G(H_2O)$=-314.73 J/mol, and $\Delta G(H^+)$=0 J/mol.
ΔG(reaction)= $\Delta G(TcO^{+2})$ + 2x$\Delta G(H_2)$- 2x$\Delta G(Tc)$ - $\Delta G(H_2O)$ = -13.51 J/mol + 2x-314.73 J/mol – 2x-89.09 J/mol + 52.33 J/mol = -412.46 J/mol

$$K(125^\circ C) = e^{\frac{-\Delta G(reaction)}{RT}} = e^{0.1242} = 1.1322$$

Solubility of TcO^{+2}:

$$K(125^\circ C) = \frac{[H^+]^2}{[TcO^{+2}]P_{H_2}{}^2} \rightarrow [TcO^{+2}] = \frac{(10^{-8.5})^2}{1.1322 \cdot 0.1^2} = 10^{-15.053}$$

A4.12 Thorium

Reaction:
$Th^{+4} + 7.625H_2 \rightarrow Th(H_3)_{3.75} + 4H^+$

Solubility product:
From HSC 5.0 data at 125° C, $\Delta G(H_2)$=-52.33 J/mol, $\Delta G(Th(H_3)_{3.75})$=-251.53 J/mol, $\Delta G(Th^{+4})$= 600.82 J/mol, and $\Delta G(H^+)$=0 J/mol.
ΔG(reaction)= $\Delta G(Th(H_3)_{3.75})$ – 7.625x$\Delta G(H_2)$- $\Delta G(Th^{+4})$= -251.53 J/mol – 600.82 J/mol – 7.625x-52.33 J/mol = -453.33 J/mol

$$K(125^\circ C) = e^{\frac{-\Delta G(reaction)}{RT}} = e^{0.1369} = 1.147$$

Solubility of Th^{+4}:

$$K(125^\circ C) = \frac{[H^+]^4}{[Th^{+4}]P_{H_2}{}^{7.625}} \rightarrow [Th^{+4}] = \frac{(10^{-8.5})^4}{1.147 \cdot 0.1^{7.625}} = 10^{-9.435}$$

A4.13 Uranium

Reaction:
$2UO_2^+ + UO_2^{+2} + 2H_2O \rightarrow U_3O_8 + 4H^+$

Solubility product:
From the CTDP information on U_3O_8, log(K(75° C))=5.27 and log(K(100° C))=5.94.

$$\log(K(125^\circ C) = \frac{\log(K(100^\circ C) - \log(K(75^\circ C)}{25^\circ C} \times 25^\circ C + \log(K(100^\circ C) = 6.61$$

Solubility of UO_2^+ and UO_2^{+2}:

$$K(125^\circ C) = \frac{[H^+]^4}{[UO_2{}^+]^2[UO_2{}^{+2}]} \rightarrow [UO_2{}^+]^2[UO_2{}^{+2}] = \frac{(10^{-8.5})^4}{10^{6.61}} = 10^{-40.61}$$

$$2[UO_2{}^+] = [UO_2{}^{+2}] \rightarrow 2[UO_2{}^+]^3 = 10^{-40.61} \rightarrow [UO_2{}^+] = 10^{-13.637} \; and \; [UO_2{}^{+2}] = 10^{-13.336}$$

$$[U_{aq}] = [UO_2{}^+] + [UO_2{}^{+2}] = 10^{-13.16}$$

A4.14 Zirconium

Reaction:
$Ca^{+2} + Zr^{+4} + 3H_2O \rightarrow CaZrO_3 + 6H^+$

Solubility product:
From the CTDP information on $CaZrO_3$, log(K(100° C))=-15.5372 and log(K(150° C))= -11.2811.

$$\log(K(125^\circ C) = \frac{\log(K(100^\circ C) + \log(K(150^\circ C)}{2} = -13.409$$

Solubility of Zr^{+4}:

$$K(125^{\circ}C) = \frac{[H^{+}]^{6}}{[Ca^{+2}][Zr^{+4}]} \rightarrow [Zr^{+4}] = \frac{(10^{-8.5})^{6}}{20 \cdot 10^{-13.409}} = 10^{-38.89}$$

References

[1] Kozlovsky, Y.A., *The Superdeep Well of the Kola Peninsula*, Springer-Verlag, New York, 1984. p. 12.
[2] Kuo, Weng-Sheng, *Evaluation of Deep Drillholes for High-Level Nuclear Waste Disposal*, Nuclear Engineer's Thesis, Massachusetts Institute of Technology, 1991.
[3] Kuo, et al, "Reevaluation of the Deep-Drillhole Concept for Disposing of High-Level Nuclear Waste," *Nuclear Science Journal*, Volume 32, Number 3, June 1995. pp. 229-248.
[4] *Final Environmental Impact Statement of for a Geologic Repository for the Disposal of Spent Nuclear Fuel and High-Level Radioactive Waste at Yucca Mountain, Nye County, Nevada*, U.S. Department of Energy Office of Civilian Radioactive Waste Management, Washington, DC, Feburary 2002.
[5] Sizgek, "Thermal considerations in a very deep borehole nuclear waste repository for synroc," *Materials Research Society Symposium Proceedings,* Volume 663, 2001. p. 819-826.
[6] Gibb, Fergus and Attrill, Phillip, "Granite recrystallization: the key to the nuclear waste problem?" *Geology*, Volume 31, Number 8, August 2003. p. 657-660.
[7] *MIT Study on Nuclear Energy*, Massachusetts Institute of Technology, Cambridge, MA, August, 2003.
[8] Gibb, F. G., "A New Scheme for the Very Deep Geological Disposal of High Level Radioactive Waste," *Journal of the Geological Society*, London, Volume 157, 2000. p. 27-36.
[9] Gibb, 2003.
[10] Kuo, 1991.
[11] *New Scientist*, May 15, 2004. p. 29.
[12] Kozlovsky, p. 284.
[13] Kozlovsky, et al, p. 40.
[14] Ibid, p. 41.
[15] Ibid, p. 43.
[16] Ibid, p. 44.
[17] Ibid, p. 50.
[18] Ibid, p. 51.
[19] Ibid, p. 42.
[20] Ibid, p. 53.
[21] Ibid, p. 276.
[22] Ibid, p. 286.
[23] Ibid, p. 272.
[24] Ibid, p. 332.
[25] Ibid, p. 77.
[26] Ibid, p. 77.
[27] Ibid, p. 277.
[28] Ibid, p. 286.
[29] Raleigh, et al, *Observation of the Continental Crust Through Drilling I*, Springer-Verlag, Berlin, 1984. p. 275-276.
[30] Ibid, p. 274.
[31] Khristoforova, et al, "Temperature Distribution and Anomalies in the Crystalline Basement of the Tataria Arch," *Physics and Chemistry of the Earth (A)*, Volume 25, Number 6-7, 2000, p. 597-604.
[32] Stober and Bucher, *Water-Rock Interaction*, Kluwer Academic Publishers, Dordrecht, 2002. p. 63.
[33] Ibid, p. 86.
[34] Iwatsuki and Yoshida, "Groundwater chemistry and fracture mineralogy in the basement granitic rock in the Tono uranium mine area, Gifu Prefecture, Japan – Groundwater composition, Eh evolution analysis by fracture filling materials," *Geochemical Journal*, Volume 33, 1999. p. 19-32.
[35] Banwart, et al, "Large-scale intrusion of shallow water into a vertical fracture zone in crystalline bedrock: Initial hydrochemical perturbation during tunnel construction at the Aspo Hard Rock Laboratory, southeastern Sweden," *Water Resources Research*, Volume 30, Number 6, June 1994, p. 1747-1763.
[36] Ibid.
[37] Logan, Stanley, "Deep self-burial of radioactive wastes by rock-melting capsules," *Nuclear Technology*, Volume 21, February 1974. p. 111-124.
[38] Gibb, 2000.

[39] DOE, 2002.
[40] Glatz, et al. "Influence of granite on the leaching behavior of different nuclear waste forms," *Journal of Nuclear Materials*, Volume 223, 1995. p. 84-89.
[41] Pigford, et al, "Effect of repository heating on dissolution of glass waste," *Transactions of the American Nuclear Society*, Volume 44, 1982. p. 115-116.
[42] Glatz, et al.
[43] Hayakawa and Kamizono, "Leaching of Al_2O_3-Based Nuclear Waste Forms," *Journal of Nuclear Science and Technology*, Volume 39, Number 7, 1993. p. 673-679.
[44] Morss, et al, "Cerium, uranium, and plutonium behavior in glass-bonded sodalite, as ceramic nuclear waste form," *Journal of Alloys and Compounds*, Volume 303-304, 2000. p. 42-48.
[45] Kamizono, et al, " Durability of zirconium-containing waste forms in water," *Journal of the American Ceramics Society*, Volume 74, Number 4, 1991. p. 863-864.
[46] Weber, et al "Radiation effects in crystalline ceramics for the immobilization of high-level nuclear waste and plutonium," *Journal of Materials Research*, Materials Research Society, Warrendale, PA, June 1998. p. 1434-1484.
[47] Jones, Denny, *Principles and Prevention of Corrosion*, Prentice Hall, Upper Saddle River, NJ, 1996. p. 11.
[48] Ibid, p. 15.
[49] Ibid, p. 17-19.
[50] Ibid, p. 237.
[51] Ibid, p. 199.
[52] Ibid, p. 515.
[53] Ibid, p. 255.
[54] Ibid, p. 199.
[55] Ibid, p. 522.
[56] Ibid, p. 209.
[57] Ibid, p. 519.
[58] U.S. Department of Energy, Office of Civilian Radioactive Waste Management, "Why do scientists think a repository will work?" *Yucca Mountain Project Fact Sheets*, Washington, DC, August 1996.
[59] Jones, p. 261.
[60] Ibid, p. 325.
[61] DOE, 2002.
[62] General Electric Co. and KAPL, Inc., *Chart of the Nuclides, 15th Edition*, San Jose, CA, 1996.
[63] Malbrain, et al, "Analytical approximations for the long-term decay behavior of spent fuel and high-level waste," *Nuclear Technology*, Volume 57, May 1982. p. 292-305.
[64] DOE, 2002.
[65] Malbrain, 1982.
[66] DOE, 2002.
[67] Xu, Zhiwen, *Design Strategies for Optimizing High Burnup Fuel in Pressurized Water Reactors*, PhD Thesis, Massachusetts Institute of Technology, Cambridge, MA, January 2003.
[68] Lienhard, John IV and Linhard, John V, *A Heat Transfer Textbook*, Massachusetts Institute of Technology, Cambridge, MA, 2000. p. 64.
[69] Lienhard, p. 627.
[70] Ibid, p. 629.
[71] Ibid, p. 636.
[72] Mills, A.F. *Basic Heat and Mass Transfer*, Prentice Hill, Upper Saddle River, New Jersey, 1999, p. 920.
[73] Ibid, p. 924.
[74] Leinhard, p. 640-641. Calculated assuming 10% hydrogen gas and 90% nitrogen gas at 400 K. Thermal conductivities were 0.0326 W/m·K for nitrogen gas and 0.228 W/m·K for hydrogen gas, with k_{gas} calculated as (0.9 0.0326 + 0.1 0.228) W/m·K=0.054 W/mK.
[75] Kuo, 1991.
[76] Rollin, et al, "Determination of dissolution rates of spent fuel in carbonate solutions under different redox conditions with a flow-through experiment," *Journal of Nuclear Materials*, Vol. 297, 2001. p. 231-243.
[77] Loida, et al, "Anoxic corrosion of various high burnup spent fuel samples," *Journal of Nuclear Materials*, Vol. 238, 1996, p. 11-22.

[78] Ollila, et al, "Solubility and oxidation state of uranium under anoxic conditions (N_2 atmosphere)," *Radiochimica Acta*, Vol 74, 1996. p. 9-13.
[79] Province of British Columbia, *Variation in uranium and radioactivity levels in surface and ground water at selected sites in British Columbia*, B.C. Ministry of Energy, Mines, April 1980 - March 1981.
[80] Title 40, *Code of Federal Regulations*, Part 197.30, U.S. Government Printing Office, Washington, DC, July 2002. p. 64.
[81] Liu and Neretnieks, "The effect of hydrogen on oxidative dissolution of spent fuel," *Nuclear Technology*, Vol. 138, April 2002. p. 69-77.
[82] Kunze, et al, "Studies on the Immobilization of Technetium under Near Field Geochemical Conditions," *Radiochimica Acta*, Vol 74, 1996. p. 159-162.
[83] Allard, Bert and Rydberg, Jan, "Behavior of Plutonium in Natural Waters," *Plutonium Chemistry*, American Chemical Society, Washington, DC, 1983. p. 275-293.
[84] Gueguen, Yves and Palciauskas, Victor, *Introduction to the Physics of Rocks*, Princeton Universtiy Press, Princeton, NJ, 1994. p. 9.
[85] Clark, Brian, and Kleinberg, Robert, "Physics in Oil Exploration," *Physics Today*, Volume 55, Number 4. April 2002. p. 48-53.
[86] Liu, et al, "Diffusion of Tc-99 in granite," *Radiochemica Acta*, Volume 89, Issue 10, 2001. p. 639-642.
[87] Zapolskiy, Leonid and Man'ko, Ivan, Research Presentation, Cambridge, MA, July 21, 2004.
[88] DOE, 2002.
[89] General Electric Company, 1996.
[90] Kuo, 1991.
[91] http://ctdp.ensmp.fr/index.html